

Phase transition universality classes of classical, nonequilibrium systems

Géza Ódor

Budapest, February 7, 2020

Contents

1	Introduction	5
1.1	Critical exponents of equilibrium systems	6
1.2	Static percolation cluster exponents	7
1.3	Dynamical critical exponents	8
1.4	Critical exponents of spreading processes	9
1.4.1	Damage spreading exponents	11
2	Scaling at first order phase transitions	13
3	Out of equilibrium classes	15
3.1	Ising model classes	16
3.1.1	Correlated percolation clusters at T_C	17
3.1.2	Dynamical Ising classes	17
3.1.3	Competing dynamics added to spin-flip	19
3.1.4	Competing dynamics added to spin-exchange	22
3.1.5	Long-range correlations	23
3.1.6	Damage spreading behavior	24
3.2	Potts model classes	24
3.2.1	Correlated percolation at T_c	25
3.2.2	The vector Potts model	26
3.2.3	Dynamical Potts classes	26
3.2.4	Long-range correlations	27
3.3	XY model classes	27
3.3.1	Long-range correlations	29
3.4	O(N) symmetric model classes	29
3.4.1	Correlated percolation at T_c	30
4	Genuine nonequilibrium classes	31
4.1	Directed percolation classes	32
4.1.1	The Contact process	37

4.1.2	DP-class stochastic cellular automata	37
4.1.3	Branching and annihilating random walks with odd number of offsprings	40
4.1.4	DP with spatial boundary conditions	40
4.1.5	DP with mixed (parabolic) boundary condition scaling	43
4.1.6	Lévy flight anomalous diffusion in DP	44
4.1.7	Long-range correlated initial conditions in DP	45
4.1.8	Quench disordered DP systems	48
4.2	Dynamical percolation (DyP) classes	49
4.2.1	Isotropic percolation universality classes	50
4.2.2	DyP with spatial boundary conditions	51
4.2.3	Lévy flight anomalous diffusion in DyP	51
4.3	Voter model (VM) classes	52
4.3.1	The $2A \rightarrow \emptyset$ (ARW) and $2A \rightarrow A$ models	54
4.3.2	Compact DP (CDP) with spatial boundary conditions	54
4.3.3	CDP with parabolic boundary conditions	55
4.3.4	Lévy flight anomalous diffusion in ARW-s	56
4.4	Parity conserving (PC) classes	56
4.4.1	Grassberger's A and B model	57
4.4.2	Branching and annihilating random walks with even number of offsprings	58
4.4.3	The NEKIM model	61
4.4.4	The Generalized DK model	66
4.4.5	PC class surface catalytic models	67
4.4.6	NEKIM with long-range correlated initial conditions	70
4.4.7	GDK with spatial boundary conditions	70
4.5	Branching with $kA \rightarrow \emptyset$ annihilation	74
5	Multi-component system classes	75
5.1	The $A + B \rightarrow \emptyset$ classes	75
5.2	$AA \rightarrow \emptyset, BB \rightarrow \emptyset$ with hard-core repulsion	76
5.3	Unidirectionally coupled ARW classes	78
5.4	DP with coupled frozen field classes	79
5.4.1	The pair contact process model	81
5.4.2	The threshold transfer process (TTP)	83
5.5	DP with coupled diffusive field classes	84
5.5.1	The PCPD model	86
5.5.2	The annihilation-coagulation (AC) model	88
5.5.3	Cyclically coupled spreading with pair annihilation .	89
5.5.4	The parity conserving AF model	90
5.6	BARWe with coupled non-diffusive field class	91
5.7	DP with diffusive conserved slave field classes	91

5.8	DP with frozen conserved slave field classes	93
5.9	Coupled N-component DP classes	94
5.10	Coupled N-component BARW2 classes	95
5.10.1	Generalized contact processes with $n > 2$ absorbing state in 1d	96
5.10.2	The NEKIMA model	97
5.11	Hard-core 2-BARW2 classes in 1d	98
5.11.1	Hard-core 2-BARWo models in 1d	100
5.11.2	Coupled binary spreading processes	100
6	Interface growth model classes	103
6.1	The random deposition class	106
6.2	Edwards-Wilkinson (EW) classes	106
6.3	Quenched EW classes	107
6.4	Kardar-Parisi-Zhang (KPZ) classes	107
6.4.1	Multiplicative noise systems	108
6.5	Quenched KPZ classes	109
6.6	Other continuum growth classes	109
6.7	Unidirectionally coupled DP classes	110
6.7.1	Monomer adsorption-desorption at terraces models	112
6.7.2	Polynuclear growth models	113
6.8	Unidirectionally coupled PC classes	114
6.8.1	Dimer adsorption-desorption at terraces models	115
6.8.2	Parity conserving polynuclear growth	120
7	Summary	121
7.1	Frequently used abbreviations	124

Chapter 1

Introduction

Universality is an attractive feature in statistical physics because wide range of models can be classified purely in terms of their collective behavior into classes. This review aims to summarize the developments of the past few decades in the research of nonequilibrium phase transition universality classes in classical systems. While the theory of phase transitions is quite well understood in thermodynamic equilibrium its investigations in nonequilibrium situations is rather new. Nonequilibrium phase transitions appear in models of populations [1], epidemics [2, 3], catalysis [4], cooperative transport [5] and markets [6] for example. The simplest models are lattice Markov processes and interacting particle systems [2]. In these models in general there is no hermitian Hamiltonian but systems are defined by transition rates, which do not satisfy the detailed balance condition (the local time reversal symmetry is broken). Even so phase transitions, scaling and universality retain most of the fundamental concepts of equilibrium models. Dynamical extensions of static universality classes — established in equilibrium — appear in nonequilibrium models as well, but beyond that richer critical phenomena, with new classes have been explored so far [7, 8]. The basic ingredients affecting the universality classes are again the collective behavior of systems, symmetries, conservation laws and the spatial dimension – described by renormalization group theory – but also new factors have been identified recently [9]. Low dimensional systems are of primary interest because usually the fluctuation effects are relevant, hence mean-field type of description is not valid. The main purpose of this work is besides to give a general overview of the critical behavior of nonequilibrium phenomena to present the latest results that distinguish them from equilibrium ones. I shall not discuss critical behavior of quantum systems and neither show experimental realizations. I define a critical universality

class by the complete set of exponents at the phase transition. Therefore different dynamics split up the basic static classes of homogeneous systems.

In the first chapter I summarize the most important critical exponents and relations used in this work. In the second chapter I briefly address the question of scaling behavior at first order phase transitions. In chapter three I review dynamical extensions of basic static classes, show the effect of mixing dynamics and percolation behavior. The main body of this work is given in chapter four where genuine, dynamical universality classes specific to nonequilibrium systems are introduced. In chapter five I continue over-viewing such nonequilibrium classes but in coupled, multi-component systems. Most of known transitions in low dimensional systems are between active and absorbing states of reaction-diffusion type systems, but I shall briefly introduce related classes that appear in interface growth models in chapter six. Some of them are related to critical behavior of coupled, multi-component systems. Finally in chapter seven I summarize families of absorbing state system classes, mean-field classes and the most frequently used abbreviations. Naturally this review can't be complete and I apologize for the omitted references.

Acknowledgements:

I thank H. Hinrichsen, N. Menyhárd and M. A. Muñoz for their comments to the manuscript. Support from Hungarian research funds OTKA (No.25286), Bolyai (BO/00142/99) and IKTA (Project No.00111/2000) is acknowledged.

1.1 Critical exponents of equilibrium systems

In this section I briefly summarize the definition of well known critical exponents of homogenous equilibrium systems and show some scaling relations. The basic exponents are defined via the scaling laws:

$$c_H \propto \alpha_H^{-1} \left((|T - T_c|/T_c)^{-\alpha_H} - 1 \right), \quad (1.1)$$

$$m \propto (T_c - T)^\beta, \quad (1.2)$$

$$\chi \propto |T - T_c|^{-\gamma}, \quad (1.3)$$

$$m \propto H^{1/\delta_H}, \quad (1.4)$$

$$G_c^{(2)}(r) \propto r^{2-d-\eta_a}, \quad (1.5)$$

$$\xi \propto |T - T_c|^{-\nu_\perp}. \quad (1.6)$$

Here c_H denotes the specific heat, m the order parameter, χ the susceptibility and ξ the correlation length. The presence of another degree of

freedom besides the temperature T , like a (small) external field (labeled by H), leads to other interesting power laws when $H \rightarrow 0$. The d present in the expression of two-point correlation function $G_c^{(2)}(r)$ is the space dimension of the system.

Some laws are valid both to the right and to the left of the critical point; the values of the relative proportionality constants, or *amplitudes*, are in general different for the two branches of the functions, whereas the exponent is the same. However there are universal amplitude relations among them. We can see that there are altogether six basic exponents Nevertheless they are not independent of each other, but related by some simple scaling laws

$$\alpha_H + 2\beta + \gamma = 2, \quad \alpha_H + \beta(\delta_H + 1) = 2, \quad (2 - \eta_a)\nu_\perp = \gamma, \quad \nu_\perp d = 2 - \alpha_H, \quad (1.7)$$

so that there are only two independent exponents in equilibrium. One of the most interesting aspects of second order phase transitions is the so-called **universality**, i.e., the fact that systems which can be very different from each other share the same set of critical indices (exponents and some amplitude ratios). One can thus subdivide all systems into **classes**, each of them being identified by a set of critical indices.

1.2 Static percolation cluster exponents

Percolation [129, 132] is a geometrical phenomena that describes the occurrence of infinitely large connected clusters in lattice models. The definition of connected clusters is not unambiguous. It may mean the set of sites with variables in the same state, or connected by bonds or connected by bonds but with probability $b = 1 - \exp(-2J/kT)$. By changing the system control parameters ($p \rightarrow p_p$) (that usually is the temperature in equilibrium systems) the coherence length between sites may diverge as

$$\xi(p) \propto |p - p_p|^{-\nu_\perp}, \quad (1.8)$$

hence percolation at p_p is like standard critical phenomena exhibiting renormalizability and universality of critical exponents of physical quantities. At p_p the cluster size (s) distribution follows the scaling law:

$$n_s \propto s^{-\tau} f(|p - p_p|s^\sigma). \quad (1.9)$$

while the moments of this distribution exhibit singular behavior with the exponents

$$\sum_s s n_s(p) \propto |p - p_p|^{\beta_p}, \quad (1.10)$$

$$\sum_s s^2 n_s(p) \propto |p - p_p|^{-\gamma_p} \quad , \quad (1.11)$$

Further critical exponents and scaling relations among them are shown in [129]. In case of completely random displacement of (sites, bonds, etc) variables (with probability p) on lattices we find **random isotropic (ordinary) percolation** (see Sect.4.2.1). On the other hand percolating clusters may arise at critical, thermal transitions of models or by nonequilibrium processes. In these cases if the critical point (p_c) of the order parameter does not coincide with p_p at the percolation transition the order parameter coherence length is finite and do not influence the percolation properties and we find random percolation. Contrary if $p_p = p_c$ percolation is influenced by the order parameter behavior and we find different, **correlated percolation** universality, whose exponents may coincide with those of the order parameter.

According to the Fortuin-Kasteleyn construction [104] of clusters two nearest-neighbor spins of the same state belong to the same cluster with probability $b = 1 - \exp(-2J/kT)$. It was shown that using this prescription in case of Z_n and $O(n)$ and symmetric models [133, 134, 135, 136] the **thermal phase transition** and the order parameter exponents coincide with the percolation limit of such clusters. On the other hand in case of “pure-site clusters” ($b = 1$) different, universal cluster exponents are reported [135] in case of 2d models (see Sects. 3.1.1, 3.2.1, 3.4.1).

1.3 Dynamical critical exponents

Nonequilibrium systems were first introduced to study relaxation to equilibrium states [25] and phase ordering kinetics [26, 27] where power-law time dependences has been investigated away from the critical point (example domain growth by quenching to $T = 0$). Later the combination of different heat-baths, dynamics, external currents became popular investigation tools of fully nonequilibrium models. To describe dynamical behavior of a critical system additional exponents have been introduced. Example the relation of the divergences of the relaxation time τ and correlation length ξ is described by the dynamical exponent Z

$$\tau \propto \xi^Z \quad . \quad (1.12)$$

The systems out of equilibrium may show anisotropic scaling of two (and n) point functions

$$G(b\mathbf{r}, b^\zeta) = b^{-2x} G(\mathbf{r}, t) \quad (1.13)$$

where \mathbf{r} and t denote spatial and temporal coordinates, x is the scaling dimension and ζ is the anisotropy exponent. As the consequence the temporal (ν_{\parallel}) and spatial (ν_{\perp}) correlation length exponents may be different, described by $\zeta = Z$.

$$Z = \zeta = \frac{\nu_{\parallel}}{\nu_{\perp}} . \quad (1.14)$$

As we can see the *universality classes of static models are split by the dynamical exponents*.

For some years it was believed that dynamical critical phenomena are characterized by a set of three critical exponents, comprising two independent static exponents (other static exponents being related to these by scaling laws) and the dynamical exponent Z . Recently, it was discovered that there is another dynamical exponent, the ‘non-equilibrium’ or **short-time exponent** λ , needed to describe two-time correlations in a spin system ($\{s_i\}$) of size L relaxing to the critical state from a disordered initial condition [28, 29].

$$A(t, 0) = \frac{1}{L} \langle \sum_i s_i(0) s_i(t) \rangle \propto t^{-\lambda/Z} \quad (1.15)$$

More recently the **persistence exponents** θ_l and θ_g associated with the probability, $p(t)$, that the local or global order parameter has not changed sign in time t following a quench to the critical point were introduced by [30, 31]. In many systems of physical interest these exponents decay algebraically as

$$p(t) \propto t^{-\theta} \quad (1.16)$$

(see however example Sect. 5.1). It turned out that in systems where the scaling law

$$\theta_g Z = \lambda - d + 1 - \eta_a/2 \quad (1.17)$$

is satisfied the dynamics of the global order parameter is a Markov process. On contrary in systems with non-Markovian global order parameter the θ_g is in general a new, non-trivial critical exponent [31]. For example it was shown that while in the $d = 1$ Glauber Ising model the magnetization is Markovian and the scaling relation (1.17) is fulfilled, at the critical point of the $d = 1$ NEKIM Ising model this is not satisfied and the critical behavior there is characterized by a the exponent θ_g [32] (see discussion in Section 4.4.3).

1.4 Critical exponents of spreading processes

Here I define a basic set of critical exponents that occur in spreading processes and show the scaling relations among them. In such processes phase

transition may exist to **absorbing state(s)** where the density of spreading entity (particle, agent, epidemic etc.) disappears. So the order parameter is usually the density of active sites $\{s_i\}$:

$$\rho(t) = \left\langle \frac{1}{N} \sum_i s_i(t) \right\rangle, \quad (1.18)$$

which in the supercritical phase vanishes by varying the control parameter p as:

$$\rho^\infty \propto |p - p_c|^\beta, \quad (1.19)$$

The “dual” quantity is the ultimate survival probability P_∞ of an infinite cluster of active sites that scales in the active phase as

$$P_\infty \propto |p - p_c|^{\beta'} \quad (1.20)$$

with some critical exponent β' . In field theoretical description of such processes β is associated with the particle annihilation, β' with the particle creation operator and in case of time reversal symmetry (see Eq. (4.8)) they are equal. The critical long-time behavior of these quantities are described by

$$\rho(t) \propto t^{-\alpha} f(\Delta t^{1/\nu_{||}}), \quad P(t) \propto t^{-\delta} g(\Delta t^{1/\nu_{||}}), \quad (1.21)$$

where α and δ are the critical exponents for decay and survival, $\Delta = |p - p_c|$, f and g are *universal scaling functions*. The obvious scaling relations among them are

$$\alpha = \beta/\nu_{||}, \quad \delta = \beta'/\nu_{||}. \quad (1.22)$$

For finite, ($N = L^d$ sized) systems these quantities scale as

$$\rho(t) \propto t^{-\beta/\nu_{||}} f'(\Delta t^{1/\nu_{||}}, t^{d/Z}/N), \quad (1.23)$$

$$P(t) \propto t^{-\beta'/\nu_{||}} g'(\Delta t^{1/\nu_{||}}, t^{d/Z}/N). \quad (1.24)$$

For “relatively short times” or for initial conditions with a single active seed the the number of active sites $N(t)$ and its mean square of spreading from the origin $R^2(t)$ follow the “initial slip” scaling laws

$$N(t) \propto t^\eta, \quad (1.25)$$

$$R^2(t) \propto t^z, \quad (1.26)$$

where $z = 2/Z$ holds.

1.4.1 Damage spreading exponents

While damage spreading (DS) was first introduced in biology [33] it has become an interesting topic in physics as well [34, 35, 36]. The main question is if a damage introduced in a dynamical system survives or disappears. To investigate this the usual technique is to make replica(s) of the original system and let them evolving with the same dynamics and external noise. This method has been found to be very useful to measure accurately dynamical exponents of equilibrium systems [37]. It has turned out however, that DS properties do depend on the applied dynamics. An example is the case of the two-dimensional Ising model with heath-bath algorithm versus Glauber dynamics [38, 39, 40].

To avoid the dependences on dynamics Hinrichsen et al.[41] suggested a definition of "physical" family of DS dynamics according to which the active phase may be divided to a sub-phase within which DS occurs for every member of the family, another sub-phase where the damage heals for every member of the family, and a third possible sub-where DS is possible for some members and the damage disappears for other member. The family of possible DS dynamics is defined such that it is to be consistent with the physics of the single replicas (symmetries, interaction ranges etc.).

Usually the order parameter of the damage is the Hamming distance between replicas

$$D(t) = \left\langle \frac{1}{L} \sum_{i=1}^L |s(i) - s'(i)| \right\rangle \quad (1.27)$$

where $s(i)$ may denote now spin or kink variables. At continuous DS transitions D exhibits power-law singularities as physical quantities at the critical point. For example one can follow the faith of a single difference between two (or more) replicas and measure the spreading exponents:

$$D(t) \propto t^{\eta_d} , \quad (1.28)$$

Similarly the survival probability of damage variables behaves as:

$$P_D(t) \propto t^{-\delta_d} \quad (1.29)$$

and the average mean square distance of damage spreading from the center scales as:

$$R_D^2(t) \propto t^{z_d} . \quad (1.30)$$

Grassberger conjectured, that DS transitions should belong to DP class (see Sect.4.1) unless they coincide with other transition points and provided the probability for a locally damaged state to become healed is not zero [42]. This hypothesis has been confirmed by simulations of many different systems.

Chapter 2

Scaling at first order phase transitions

In nonequilibrium systems dynamical scaling of variables may occur even when the order parameter jumps at the transition. We call them first order transition although free energy is not defined, hence the original definition of first order transition could not be used. First order phase transitions have rarely been seen in low dimensions. This is due to the fact that in lower dimension the fluctuations are more relevant and may destabilize the ordered phase. Therefore fluctuation induced second ordered phase transitions appear. There is a hypothesis from Hinrichsen [10], that they do not exist in 1+1 dimensional systems without extra symmetries, conservation laws, special boundary conditions or long-range interactions (that can be generated by macroscopic currents or anomalous diffusion in nonequilibrium systems for instance). Examples for this are the Glauber and the NEKIM Ising spin systems (see sections 3.1,4.4.3) possessing Z_2 symmetry in one dimension [11, 12], where the introduction of a “temperature like” flip inside or an external field (h) cause discontinuous jump in the magnetization order parameter (m). Interestingly enough the correlation length diverges at the transition point: $\xi \propto p_T^{-\nu_\perp}$ and static

$$m \propto \xi^{-\beta_s/\nu_\perp} g(h\xi^{\Delta/\nu_\perp}) \quad (2.1)$$

as well as cluster critical exponents can be defined:

$$P_s(t, h) \propto t^{-\delta_s} \quad (2.2)$$

$$R_s^2(t, h) \propto t^{z_s} \quad (2.3)$$

$$|m(t, h) - m(0)| \propto t^{\eta_s} \quad (2.4)$$

$$\lim_{t \rightarrow \infty} P_s(t, h) \propto h^{\beta_s} \quad (2.5)$$

The following table summarizes the results obtained for these models. Other

	β_s	ν_{\perp}	β_s'	Δ	η_s	δ_s	z_s
Glauber	0	1/2	.99(2)	1/2	.0006(4)	.500(5)	1
NEKIM	.00(2)	.444	.45(1)	.49(1)	.288(4)	.287(3)	1.14

Table 2.1: Critical 1d Ising spin exponents at the Glauber and NEKIM transition points

examples for first order transition are known in driven diffusive systems [13], in the 1d asymmetric exclusion process [14], in bosonic annihilation-fission models (Sect.5.5) and DCF models for $D_A > D_B$ and $d > 1$ [237] (Sect.5.7). By simulations it is quite difficult to decide whether a transition is really discontinuous. The order parameter of weak first order transitions – where the jump is small – may look very similar to continuous transitions. Also the hysteresis in the order parameter that is considered to be the indication of a first order transition is a demanding task to measure. There are many examples where there were debates on the order of the transition (see example [15, 10, 16, 17, 18, 19]). In some cases the mean-field solution – that is valid above d_c or for long-range interaction/diffusion – results in first order transition [20, 21]. In two dimensions there are certain stochastic cellular automata models for which systematic cluster mean-field techniques combined with simulations made it possible to show first order transitions [22] firmly (see table below).

n	$y = 1$	$y = 2$		$y = 3$	
	p_c	p_c	$\rho(p_c)$	p_c	$\rho(p_c)$
1	0.111	0.354	0.216	0.534	0.372
2	0.113	0.326	0.240	0.455	0.400
4	0.131	0.388	0.244	0.647	0.410
simulation	0.163	0.404	0.245	0.661	0.418

Table 2.2: Convergence of the critical point estimates in various ($y = 1, 2, 3$) two dimensional SCA calculated by n-cluster (GMF) approximation. First order transitions are denoted by boldface numbers. Gap sizes ($\rho(p_c)$) of the order parameter are shown for $y = 2, 3$.

Chapter 3

Out of equilibrium classes

As the number of neighbouring interaction sites is decreasing by lowering the spatial dimensionality of a system with short-ranged interactions the relevance of fluctuations is increasing. In equilibrium models finite-range interactions cannot maintain long-range order in $d < 2$. This observation is known as the Landau-Peierls argument [23]. For systems with continuous symmetry according to the Mermin-Wagner theorem [24] the long-range order cannot exist even in $d = 2$. Hence we have universality classes of equilibrium models for $d \geq 2$ only. In this chapter I shall briefly discuss the most well known dynamical extensions of known static classes that may occur in nonequilibrium systems. The basic dynamical extensions were defined by Halperin and Hohenberg [25]. One of the main open questions to be answered is whether there exist a class of nonequilibrium systems with restricted dynamical rules for which the Landau-Peierls or Mermin-Wagner theorem can be applied.

Field theoretical investigations have revealed that **model A** systems (which do not conserve the order parameter) are **robust** against the introduction of various competing dynamics, which are *local* and *do not conserve the order parameter* [63]. Furthermore it was shown, that this robustness of the critical behavior persists if the competing dynamics breaks the discrete symmetry of the system [64] or it comes from reversible mode coupling to a non-critical conserved field [65].

On the other hand if a competing dynamics is coupled to **model B** systems (which conserve the order parameter) by external drive [66] or by local, anisotropic order-parameter conserving process [67, 68, 69] long-range interactions are generated in the steady state with angular dependence. The universality class will be the same as that of the kinetic version of the equilibrium Ising model with **dipolar long-range interactions**.

It is an important and new universal phenomena that scaling behavior can be observed far away from criticality as well. In quenches to zero temperature of **model A** systems the characteristic length in the late time regime grows with an universal power-law $\xi \propto t^{1/2}$, while in the case of **model B** systems this is $\xi \propto t^{1/3}$.

3.1 Ising model classes

The equilibrium Ising model was introduced by [48] as the simplest model for an uniaxial magnet and it is used in different settings for example binary fluids or alloys. It is defined in terms of spin variables $s_i = \pm 1$ attached to sites i of some lattice and the Hamiltonian is

$$H = -J \sum_{i,i'} s_i s_{i'} - B \sum_i s_i \quad (3.1)$$

where J is the coupling constant and B is the external field. In one and two dimensions it is solved exactly [49] and therefore it plays a fundamental test-ground for understanding the phase transitions. The Hamiltonian of this model exhibit a global, so called Z_2 (up-down) symmetry of the state variables. While in one dimension a first order phase transition occurs at $T = 0$ only (see section 2) in two dimensions there is a continuous phase transition where the system exhibits a conformal symmetry [50] as well. The critical dimension is $d_c = 4$. The following table (3.1) summarizes some of the known critical exponents of the Ising model. The quantum

exponent	$d = 2$	$d = 3$	$d = 4(\text{MF})$
α_H	$0(\log)$	$0.1097(6)$	0
β	$1/8$	$0.3265(7)$	$1/2$
γ	$7/4$	$1.3272(3)$	1
ν_{\perp}	1	$0.6301(2)$	$1/2$

Table 3.1: Static critical exponents of the Ising model

version of the Ising model, which in the simplest 1d case might take the form

$$H = -J \sum_i (t \sigma_i^x + \sigma_i^z \sigma_{i+1}^z + h \sigma_i^z), \quad (3.2)$$

– where $\sigma^{x,z}$ are Pauli matrices and t and h are couplings – for $T > 0$ has been shown to exhibit the same critical behavior as the classical one. For

$T = 0$ however the quantum effects become important and the quantum Ising chain can be associated with the two dimensional classical Ising model such that the transverse field t plays the role of the temperature. In general a mapping can be constructed between classical $d+1$ dimensional statistical systems and d dimensional quantum systems without changing the universal properties that has been heavily exploited [51, 52].

The effects of disorder and boundary conditions are not discussed here (for recent reviews see [53, 287]).

3.1.1 Correlated percolation clusters at T_C

If we generate clusters in such way that we join nearest neighbour spins of the same sign we can observe percolation at T_c in 2d. While the order parameter percolation exponents β_p and γ_p of this percolation (defined in section 4.2.1) were found to be different from the exponents of the magnetization (β, γ) the correlation length exponent is the same: $\nu = \nu_p$. These exponents are clearly different from those of the ordinary percolation classes (Table 4.4) or from Ising class exponents. For 2d models with Z_2 symmetry universal percolation exponents [135]:

$$\beta_p = 0.049(4), \quad \gamma_p = 1.908(16) \quad , \quad (3.3)$$

In case of Fortuin-Kasteleyn cluster construction [104] the percolation exponents of the Ising model at T_c coincide with those of the magnetization of the model.

3.1.2 Dynamical Ising classes

Kinetic Ising models such as the spin-flip Glauber Ising model [11] and the spin-exchange Kawasaki Ising model [54] were originally intended to study relaxational processes near equilibrium states. In order to assure the arrival to an equilibrium state the detailed balance condition for transition rates ($w_{i \rightarrow j}$) and probability distributions ($P(s)$) was required

$$w_{i \rightarrow j} P(s(i)) = w_{j \rightarrow i} P(s(j)) \quad . \quad (3.4)$$

Knowing that $P_{eq}(s) \propto \exp(-H(s)/(k_B T))$ this means a

$$\frac{w_{i \rightarrow j}}{w_{j \rightarrow i}} = \exp(-\Delta H(s)/(k_B T)) \quad (3.5)$$

condition that can be satisfied in many different way. Assuming **spin-flips** (that does not conserve the magnetization (**model A**)) Glauber formulated the most general form in a magnetic field (h)

$$w_i^h = w_i(1 - \tanh h s_i) \approx w_i(1 - h s_i) \quad (3.6)$$

$$w_i = \frac{\Gamma}{2}(1 + \tilde{\delta}s_{i-1}s_{i+1}) \left(1 - \frac{\gamma}{2}s_i(s_{i-1} + s_{i+1})\right) \quad (3.7)$$

where $\gamma = \tanh 2J/kT$, Γ and $\tilde{\delta}$ are further parameters. The $d = 1$ Ising model with Glauber kinetics is exactly solvable. In this case the critical temperature is at $T = 0$, the transition is of first order. We recall that $p_T = e^{-\frac{4J}{kT}}$ plays the role of $\frac{T-T_c}{T_c}$ in 1d and in the vicinity of $T = 0$ critical exponents can be defined as powers of p_T , thus e.g. that of the coherence length, ν_\perp , via $\xi \propto p_T^{-\nu_\perp}$ (see Section 2). In the presence of a magnetic field B , the magnetization is known exactly. At $T = 0$

$$m(T = 0, B) = \text{sgn}(B). \quad (3.8)$$

Moreover, for $\xi \gg 1$ and $B/kT \ll 1$ the exact solution reduces to

$$m \sim 2h\xi; \quad h = B/k_B T. \quad (3.9)$$

In scaling form one writes:

$$m \sim \xi^{-\frac{\beta_s}{\nu_\perp}} g(h\xi^{\frac{\Delta}{\nu_\perp}}) \quad (3.10)$$

where Δ is the static magnetic critical exponent. Comparison of eqs. (3.9) and (3.10) results in $\beta_s = 0$ and $\Delta = \nu_\perp$. These values are the ones well known for the 1-d Ising model. It is clear that the transition is discontinuous at $B = 0$ also when changing B from positive to negative values, see eq.(3.8) The order of limits are meant as: $B \rightarrow 0$ and then $T \rightarrow 0$. The $\delta = 0$, $\Gamma = 1$ case is usually referred to as the Glauber-Ising model. The dynamical exponents are

$$Z_{1d \text{ Glauber}} = 2, \quad \theta_{g,1d \text{ Glauber}} = 1/4 \quad (3.11)$$

Applying **spin-exchange** Kawasaki dynamics, that conserves the magnetization (**model B**)

$$w_i = \frac{1}{2\tau} \left[1 - \frac{\gamma_2}{2}(s_{i-1}s_i + s_{i+1}s_i + 2)\right] \quad (3.12)$$

where $\gamma_2 = \tanh(2J/k_B T)$, the dynamical exponent will be different. According to linear response theory [55] in one dimension at $T_c = 0$ critical point it is

$$Z_{1d \text{ Kaw}} = 5 \quad (3.13)$$

Note however, that in case of fast quenches to $T = 0$ coarsening with scaling exponent $1/3$ is reported [56]. Hence an other dynamic Ising universality class appears with the same static but different dynamical exponents.

Interestingly while the two dimensional equilibrium Ising model is solved the exact values of the dynamical exponents are not known. The Table 3.2 summarizes the known dynamical exponents of the Ising model in $d = 1, 2, 3, 4$. The $d = 4$ results are mean-field values. In Section 4.4.3 I

	$d = 1$		$d = 2$		$d = 3$	$d = 4$	
	A	B	A	B	A	A	B
Z	2	5[55]	2.165(10)[57]	2.325(10)[59]	2.032(4)[37]	2	4
λ	1		0.737(1)[57]	0.667(8)[59]	1.362(19)[60]	4	
θ_g	1/4		0.225(10)		0.41(2)[58]	1/2	

Table 3.2: Critical dynamical exponents in the Ising model. Columns denoted by (A) and (B) refer, model A and model B dynamics

shall discuss an other fully nonequilibrium critical point of the $d = 1$ Ising model with competing dynamics (NEKIM) where the dynamical exponents break the scaling relation (1.17) and therefore the magnetization is a non-Markovian process. For $d > 3$ there is no non-Markovian effect (hence θ is not independent) but for $d = 2, 3$ the situation is still not completely clear [57].

In one dimension the domain walls (kinks) between up and down regions can be considered as particles. The spin-flip dynamics can be mapped onto particle movement :



or the creation or annihilation of neighbouring particles.



Therefore the $T = 0$ Glauber dynamics is equivalent to the diffusion limited annihilation (ARW) mentioned already in Section. 2. Mapping the spin-exchange dynamics more complicated particle dynamics emerges, example:



one particle may give birth of two others or three particle may coagulate to one. Therefore these models are equivalent to branching and annihilating random walks to be discussed in Section 4.4.2.

3.1.3 Competing dynamics added to spin-flip

Competing dynamics in general break the detailed balance symmetry (3.4) and make the kinetic Ising model to relax to a nonequilibrium steady state

(if it exists). Generally these models become unsolvable, for an overview see [62]. Grinstein, Jayaprakash and Yu He [63] argued in 1985, that stochastic **spin-flip** models with two states per site and updating rules of a short-range nature with Z_2 symmetry should belong to the (kinetic) Ising model universality class. Their argument rests on the stability of the dynamic Ising fixed point in $d = 4 - \epsilon$ dimensions with respect to perturbations preserving both the spin inversion and the lattice symmetries. This hypothesis has received extensive confirmation from MC simulations [162]–[74], [79, 78, 81] as well as from analytic calculations [75, 76, 77]. The models investigated include Ising models with a competition of two (or three [79]) Glauber-like rates at different temperatures [75, 77, 72, 73], or a combination of spin-flip and spin-exchange dynamics [80], majority vote models [162, 81] and other types of transition rules with the restrictions mentioned above [74].

Note that in all of the above cases the ordered state is fluctuating, non-absorbing. By relaxation process this allows fluctuations in the bulk of a domain. It is also possible to generate (and in 1d it is the only choice) nonequilibrium two-state spin models (with short ranged interactions) where the ordered states are frozen (absorbing), hence by the relaxation to steady state fluctuations happen at the boundaries only. In this case non-Ising universality appears that is called the voter model (VM) universality class (see Sect.4.3).

In two dimensions **general Z_2 symmetric update rules** were investigated by [74, 82, 83, 84]. The essence of this following [82] is described below. Let us consider a two dimensional lattice of spins $s_i = \pm 1$, evolving with the following dynamical rule. At each evolution step, the spin to be updated flips with the heat bath rule: the probability that the spin s_i takes the value $+1$ is $P(s_i = 1) = p(h_i)$, where the local field h_i is the sum over neighbouring sites $\sum_j s_j$ and

$$p(h) = \frac{1}{2} (1 + \tanh[\beta(h)h]). \quad (3.17)$$

The functions $p(h)$ and $\beta(h)$ are defined over integral values of h . For a square lattice, h takes the values 4, 2, 0, -2 , -4 . We require that $p(-h) = 1 - p(h)$, in order to keep the up down symmetry, hence $\beta(-h) = \beta(h)$ and this fixes $p(0) = 1/2$. The dynamics therefore depends on two parameters

$$p_1 = p(2), \quad p_2 = p(4), \quad (3.18)$$

or equivalently on two effective temperatures

$$T_1 = \frac{1}{\beta(2)}, \quad T_2 = \frac{1}{\beta(4)}. \quad (3.19)$$

Defining the coordinate system

$$t_1 = \tanh \frac{2}{T_1}, \quad t_2 = \tanh \frac{2}{T_2} \quad (3.20)$$

with $0 \leq t_1, t_2 \leq 1$, yields

$$p_1 = \frac{1}{2}(1 + t_1), \quad p_2 = \frac{1}{2} \left(1 + \frac{2t_2}{1 + t_2^2} \right), \quad (3.21)$$

with $1/2 \leq p_1, p_2 \leq 1$. One can call T_1 and T_2 as two temperatures, respectively associated to *interfacial noise*, and to *bulk noise*. Each point in the parameter plane (p_1, p_2) , or alternatively in the temperature plane (t_1, t_2) , corresponds to a particular model. The class of models thus defined comprises as special cases the Ising model, the voter and anti-voter models [2], as well as the majority vote [2, 162] model (see Fig. 3.1). The $p_2 = 1$ line

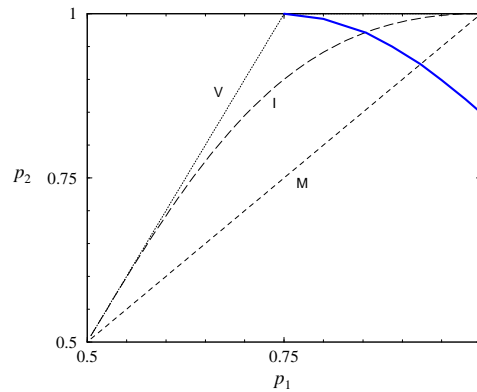


Figure 3.1: Phase diagram of 2d, Z_2 symmetric nonequilibrium spin models from [82]. Broken lines correspond to the noisy voter model (V), the Ising model (I) and the majority vote model (M). The low temperature phase is located in the upper right corner, above the transition line (full line).

corresponds to models with no bulk noise ($T_2 = 0$), hence the dynamics is only driven by interfacial noise, defined above. The $p_1 = 1$ line corresponds to models with no interfacial noise ($T_1 = 0$), hence the dynamics is only driven by bulk noise. (In both cases the effect due to the curvature of the interfaces is always present, as mentioned above.) For these last models,

the local spin aligns in the direction of the majority of its neighbors with probability one, if the local field $h = 2$, i.e. if there is no consensus amongst the neighbors. If there is consensus amongst them, i.e. if $h = 4$, the local spin aligns with its neighbors with a probability $p_2 < 1$.

The simulations [74] revealed that the transition line between the low and high temperature regions is Ising type except for the endpoint ($p_1 = 1, p_2 = 0.75$), that is first-order and corresponds to the voter model class. The local persistence exponent was also found to be constant along the line $\theta_l \sim 0.22$ [82] in agreement with that of the A-model (see Table 3.2) except for the VM point. The dynamics of this class of models may be described formally in terms of reaction diffusion processes for a set of coalescing, annihilating, and branching random walkers [82]. There are simulation results of other models exhibiting absorbing state ordered state indicating VM critical behavior [85, 199].

It is important that nontrivial, nonequilibrium phase transition may occur even in one dimension if spin-exchange is added to spin-flip dynamics, the details will be discussed in Section 4.4.3.

3.1.4 Competing dynamics added to spin-exchange

As mentioned in Section 3 the **model-B** systems are more sensible to competing dynamics. *Local and anisotropic* order parameter conserving processes generate critical behavior that coincides with that of the kinetic dipolar-interaction Ising model. In two dimensions both simulations and field theory [92] predicts the critical exponents The critical dimension is

β	γ	η_a	ν_{\perp}
0.33(2)	1.16(6)	0.13(4)	0.62(3)

Table 3.3: Critical exponents of the $d = 2$ randomly driven lattice gas

$d_c = 3$. It is shown that the Langevin equation (and therefore the critical behavior) of the anisotropic diffusive system coincides with that of the randomly driven lattice gas system (RDLG) as well. Other systems in this universality class are the two-temperature model [93] and the ALGA model [94] and the infinitely fast driven lattice gas model [95]. In the RDLG model particle current does not exist but an anisotropy only, therefore Achacbar et al. argue [95] that the particle current is not a relevant feature for this class. This gives possibility to understand why some set of simulations of driven lattice systems [96] leads to different critical behavior than the

canonical coarse-grained representative of this class (DDS) in which an explicit particle current $j\hat{\mathbf{x}}$ is added to the continuous model-B Ising model Hamiltonian

$$\frac{\partial\phi(\mathbf{r},t)}{\partial t} = -\nabla \left[\eta \frac{\delta H}{\delta\phi} + j\hat{\mathbf{x}} \right] + \nabla\zeta \quad (3.22)$$

[7] (here η is a parameter, ζ is a Gaussian noise) In the DDS model one obtains mean-field exponents for $2 \geq d \geq 5$ (with weak logarithmic corrections at $d = 2$) with $\beta = 1/2$ exactly. To resolve contradictions between simulation results [96, 97] Zia et al. [98] raises the possibility of the existence of an other, extraordinary, “stringy” ordered phase in Ising type driven lattice gases that may be stable in *square* systems.

3.1.5 Long-range correlations

If the Glauber Ising model (with non-conserving dynamics) changed into a nonequilibrium one in such a way that one couples a **nonlocal dynamics** [99] to its long-range isotropic interactions will be generated and the mean-field critical behavior should emerge. For example if the nonlocal dynamics is a random Levy flight with spin exchange probability distribution

$$P(r) \propto \frac{1}{r^{d+\sigma}} \quad (3.23)$$

effective long range interactions of the form $V_{eff} \propto r^{-d-\sigma}$ are generated and the critical exponents can be changed continuously as the function σ and d [101]. Similar conclusions for other nonequilibrium classes will be discussed later (Sect.4.1.6).

The effect of power-law correlated initial conditions $\langle\phi(0)\phi(r)\rangle \sim r^{-(d-\sigma)}$ in case of a **quench to the ordered phase of systems with non-conserved order parameter** has been investigated by Bray et. al. [100]. Such systems are characterized by coarsening domains that grow with time as $t^{1/2}$. An important example is the (2+1)-dimensional Glauber-Ising model quenched to zero temperature. It was observed that long-range correlations are relevant only if σ exceeds a critical value σ_c . Furthermore, it was shown that the relevant regime is characterized by a continuously changing exponent in the autocorrelation function $A(t) = [\phi(r,t)\phi(r,0)] \sim t^{-(d-\sigma)/4}$, whereas the usual short-range scaling exponents could be recovered below the threshold. The results were found to be in agreement with the simulation results for the two-dimensional Ising model quenched from $T = T_c$ to $T = 0$.

3.1.6 Damage spreading behavior

The dynamics dependent DS critical behavior of different Ising models are in agreement with Grassberger's conjecture [42]. Dynamical simulations with heath-bath algorithm in 2 and 3 dimensions [37, 43, 44] have found that $T_d = T_c$ and the DS dynamical exponent coincides with that of the Z -s of the replicas, so the DS exhibits the corresponding Ising class universality. For Glauber dynamics in 2d $T_d < T_c$ and DP class DS exponents were found [40]. With Kawasaki dynamics on the other hand damage always spreads in 2d [45]. With Swendsen-Wang dynamics in 2d $T_d > T_c$ and DP class DS behavior was observed [46].

In 1d it is possible to design dynamics either with PC class or DP class DS behavior depending on the DS transition coincides or not with the critical point [47, 253]. In the PC class DS case the damage variables follow BARW-2 dynamics (see Sects.4.4.2 and 4.4.3) and Z_2 symmetric absorbing phases occur.

3.2 Potts model classes

The generalization of the two-state equilibrium Ising model was introduced by Potts [102] for an overview see [103]. In the q -state Potts model the state variables can take q different values $s_i \in (0, 1, 2, \dots, q)$ and the Hamiltonian is

$$H = -J \sum_{\langle i, i' \rangle} \delta(s_i - s_{i'}) \quad (3.24)$$

a sum of Kronecker delta function of states over nearest neighbors. This has a global symmetry described by the permutation group of q elements S_q . The Ising model is recovered in the $q = 2$ case (discussed in Section 3.1). The q -states Potts model exhibits a disordered high-temperature phase and an ordered low-temperature phase. The transition is first-order, mean-field-like for q -s above the $q_c(d)$ curve (shown on Figure 3.2) (and for $q > 2$ for high dimension). The $q = 1$ case can be shown [104] to be equivalent to the isotropic percolation (see Section 4.2.1) that is known to exhibit continuous phase transition with $d_c = 6$. The problem of finding the effective resistance between two node points of a network of linear resistors was solved by Kirchhoff in 1847. Fortuin and Kasteleyn [104] showed that Kirchhoff's solution can be expressed as a $q = 0$ limit of the Potts partition function. Further mappings were discovered between the spin glass [105] and the $q = 1/2$ Potts model and the two dimensional $q = 3, 4$ cases to vertex models (see [106]). From this figure we can see that for $q > 2$ Potts models with continuous transitions happen in two dimensions only. Fortu-

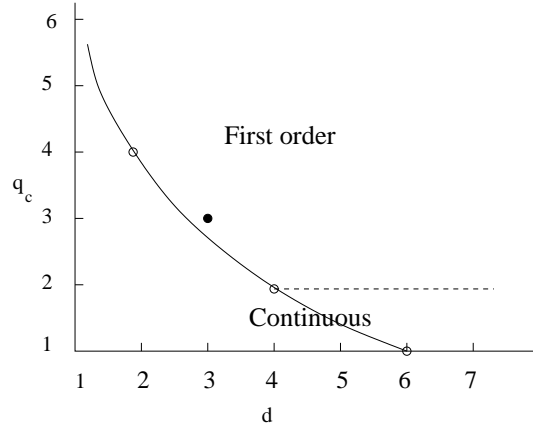


Figure 3.2: Schematic plot from [103] for $q_c(d)$ (solid line). Open symbols correspond to continuous phase transition, filled symbol to a known first order transition. Below the dashed line the transition is continuous too.

nately these models are exactly solvable (see [106]) and exhibit conformal symmetry and topological Yang-Baxter invariance. The static exponents in two dimensions are known exactly (Table 3.4)

exponent	$q = 0$	$q = 1$	$q = 2$	$q = 3$	$q = 4$
α_H	$-\infty$	$-2/3$	$0(\log)$	$1/3$	$2/3$
β	$1/6$	$5/36$	$1/8$	$1/9$	$1/12$
γ	∞	$43/18$	$7/4$	$13/9$	$7/6$
ν_{\perp}	∞	$4/3$	1	$5/6$	$2/3$

Table 3.4: Static exponents of the q states Potts model in two dimension

3.2.1 Correlated percolation at T_c

In 2d models with Z_3 symmetry the critical point coincides with the percolation of site connected clusters and the following percolation exponents are reported [135]:

$$\beta_p = 0.075(14), \quad \gamma_p = 1.53(21) . \quad (3.25)$$

In case of Fortuin-Kasteleyn cluster construction [104] the percolation exponents of q state Potts model at T_c coincide with those of the magnetization

of the model.

3.2.2 The vector Potts model

A variant of the q -state Potts model is the vector Potts model (or clock model), which exhibits a Z_q cyclic symmetry (a subgroup of S_q) with variables $\Theta = (2\pi/q)r, r = 0, \dots, q-1$ and Hamiltonian

$$H = -J \sum_{i,i'} \cos(\Theta_i - \Theta_{i'}) . \quad (3.26)$$

Note that for $q = 2, 3$ it is equivalent to the ordinary Potts model. In two dimensions for $q \leq 4$ it exhibits second order phase transition but for $q > 4$ it has several distinct critical points. These separate a high temperature disordered phase from an intermediate phase with a conventional second-order transition and the intermediate phase from a low-temperature vortex phase with an XY type transition (see Section 3.3).

3.2.3 Dynamical Potts classes

The **model-A** dynamical exponents are determined in two dimensions for $q = 3, 4$ by short-time Monte Carlo simulations [107] (Table 3.5). The exponents were found to be the same for heat-bath and Metropolis algorithms. For the zero temperature **local persistence** exponent in one dimension

exponent	$q = 3$	$q = 4$
Z	2.198(2)	2.290(3)
λ	0.836(2)	
θ_g	0.350(8)	

Table 3.5: Known dynamical exponents of the q states Potts model in two dimensions

exact formulas have been determined. For sequential dynamics [108]

$$\theta_{l,s} = -\frac{1}{8} + \frac{2}{\pi^2} \left[\cos^{-1} \left(\frac{2-q}{\sqrt{2q}} \right) \right]^2 \quad (3.27)$$

while for parallel dynamics $\theta_{l,p} = 2\theta_{l,s}$ [109]. In a deterministic coarsening it is again different (see [110, 111]). As we can see *the dynamical universality class characterized by the $\xi \propto t^{1/2}$ characteristic length growth is split as reflected by the persistence exponent.*

Similarly to the Ising case in nonequilibrium systems the role of Potts model symmetry has been shown to be the relevant factor for determining the universal behavior [113, 114, 115] of transitions to **fluctuating ordered states**. On the other hand in case of nonequilibrium transitions to **absorbing states** a simulation study [85] suggests first order transition for all $q > 2$ state Potts models in $d > 1$ dimensions. The $q = 2, d = 2$ case corresponds to the Voter model class (Sect. 4.3) and in 1d either PC class transition ($q = 2$) or N-BARW2 class transition ($q = 3$) (Sect.5.10).

The **DS transition** of a $q = 3, d = 2$ Potts model with heath-bath dynamics was found to belong to the DP class (Sect.4.1) because $T_d > T_c$ [116].

3.2.4 Long-range correlations

The effect of long-range interaction has also been investigated in case of the one dimensional $q = 3$ Potts model [112] with Hamiltonian

$$H = - \sum_{i < j} \frac{J}{|i - j|^{1+\sigma}} \delta(s_i, s_j) \quad (3.28)$$

and for $\sigma < \sigma_c \sim 0.65$ a crossover from second order to first order (mean-field) transition was located by simulations. Similarly to the Ising model here we can expect to see this crossover if we generate the long-range interactions by the addition of an additional Levy type of Kawasaki dynamics.

3.3 XY model classes

The classical XY model is defined by the same Hamiltonian as the clock model

$$H = -J \sum_{i, i'} \cos(\Theta_i - \Theta_{i'}) \quad (3.29)$$

but the state variables are continuous $\Theta_i \in [0, 2\pi]$ and therefore it can be considered as the $q \rightarrow \infty$ limit of the vector Potts model. This model has a global $U(1)$ symmetry. The critical behavior is similar to the vortex transition of the clock model. Alternatively the XY model can be defined as a special $N = 2$ case of $O(N)$ symmetric models such that the spin vectors are two dimensional \mathbf{S}_i with absolute value $\mathbf{S}_i^2 = 1$

$$H = -J \sum_{\langle i, i' \rangle} \mathbf{S}_i \mathbf{S}_{i'} \quad (3.30)$$

In this continuous model in **two dimensions** no local order parameter can take zero value according to the Mermin-Wagner theorem [24]. The appearance of free vortices (that are non-local) cause an unusual transition mechanism that implies that most of the thermodynamic quantities do not show power-law singularities. The singular behavior of the correlation length (ξ) and the susceptibility (χ) is described by the forms for $T > T_c$

$$\xi \propto \exp\left(C(T - T_c)^{-1/2}\right) \quad , \quad \chi \propto \xi^{2-\eta_a} \quad , \quad (3.31)$$

where C is a non-universal positive constant. Conventional critical exponents can not be defined but one can define scaling dimensions. At T_c the two-point correlation function has the following long-distance behavior

$$G(r) \propto r^{-1/4}(\ln r)^{1/8} \quad (3.32)$$

implying $\eta_a = 1/4$, and in the entire low-temperature phase

$$G(r) \propto r^{-\eta_a(T)} \quad (3.33)$$

such that the exponent η_a is a continuous function of the temperature, i.e the model has a line of critical points starting from T_c to $T = 0$. This is the so called Kosterlitz-Thouless critical behavior [117] and corresponds to the conformal field theory with $c = 1$ [118]. This kind of transition can experimentally observed in many effectively two-dimensional systems with $O(2)$ symmetry, such as thin films of superfluid helium and describes roughening transitions of SOS models at crystal interfaces. In **three dimensions**

α_H	β	γ	ν_\perp	η_a
-0.011(4)	0.347(1)	1.317(2)	0.670(1)	0.035(2)

Table 3.6: Static exponents of the XY model in three dimensions

the critical exponents of the $O(N)$ ($N = 0, 1, 2, 3, 4$) symmetric field theory have been determined by perturbative expansions up to seven loop order [119]. The Table 3.6 summarizes these results for the XY case (for a more detailed overview see [121]).

The dynamical exponents for **model A** have been determined by short-time dynamical simulations and logarithmic correction to scaling was found [122]. The Table 3.7 summarizes the known dynamical exponents

Z	λ	η
2.04(1)	0.730(1)	0.250(2)

Table 3.7: Dynamical exponents of the XY model in two dimensions

3.3.1 Long-range correlations

For **model B** Bassler and Rácz [123] studied the validity of the Mermin-Wagner theorem by transforming the two dimensional XY model to a non-equilibrium one with two-temperature dynamics. They found that the Mermin-Wagner theorem does not apply for this case because dipole type of long-range correlations are generated and the universality class of the phase transition of the model will coincide with that of the two temperature driven Ising model (see Table 3.3).

3.4 $O(N)$ symmetric model classes

As already mentioned in the previous section the $O(N)$ symmetric models are defined on spin vectors \mathbf{S}_i of unit length $\mathbf{S}_i^2 = 1$ with the Hamiltonian

$$H = -J \sum_{\langle i, i' \rangle} \mathbf{S}_i \mathbf{S}_{i'} \quad . \quad (3.34)$$

The most well known of them is the classical Heisenberg model that corresponds to $N = 3$ being the simplest model of isotropic ferromagnets. The $N = 4$ case corresponds to the Higgs sector of the Standard Model at finite temperature, the $N = 0$ case to polymers and the $N = 1$ and $N = 2$ cases to Ising and XY models respectively. The critical dimension is $d_c = 4$ and by the Mermin-Wagner theorem we can not find finite temperature phase transition in the short range equilibrium models for $N > 2$ below $d = 3$. Static critical exponents have been calculated by $\epsilon = 4 - d$ RG expansions up to five loops [124], by Exact RG methods (see [125] and the references therein), simulations [126] and series expansions in 3D (see [119] and the references there). In Table 3.8 I show the latest estimates from [119] in three dimensions for $N = 0, 3, 4$. The $N \rightarrow \infty$ limit is the exactly solvable spherical model [120]. For a detailed discussion of the static critical behavior of the $O(N)$ models see [121].

The dynamical exponents for **model A** are known exactly for the ($N \rightarrow \infty$) spherical model [28, 31] case. For other cases $\epsilon = 4 - d$ expansions up to two loop order exist [31, 127]. For a discussion about the combination of different dynamics see the general introduction Section 3 and [128].

N	α_H	β	γ	ν_{\perp}	η_a
0	0.235(3)	0.3024(1)	1.597(2)	0.588(1)	0.028(2)
3	-0.12(1)	0.366(2)	1.395(5)	0.707(3)	0.035(2)
4	-0.22(2)	0.383(4)	1.45(1)	0.741(6)	0.035(4)

Table 3.8: Static exponents of the O(N) model in three dimensions

N	Z	λ	θ_g
∞	2	5/2	1/4
3	2.032(4)	2.789(6)	0.38

Table 3.9: Known dynamical exponents of model A O(n) model in three dimensions

3.4.1 Correlated percolation at T_c

In three dimensions $O(2)$, $O(3)$ and $O(4)$ symmetric models with Fortuin-Kasteleyn cluster construction [104] the percolation points and percolation exponents coincide with the corresponding T_c -s and magnetization exponent values [136].

Chapter 4

Genuine nonequilibrium classes

In this chapter I introduce such “genuine nonequilibrium” dynamical classes where even the static exponents do not appear in equilibrium models. These are reaction-diffusion type of systems with such order-disorder transitions where the ordered state may exhibit only small fluctuations, hence they trap a system falling in it (absorbing state). Such phase transitions may occur in low dimensions too unlike those of the equilibrium models [7]. As it was already shown in Section 3.1.2 reaction-diffusion particle systems may be mapped onto spin-flip systems stochastic cellular automata or interface growth models (see Sect. 6). The mapping however may lead to nonlocal systems that does not bear real physical relevance.

For a long time mainly such phase transitions were known where the absorbing state is completely frozen. A few universality classes of this kind were known [8],[9], the most prominent and the first one that was discovered is that of the directed percolation (DP) [188]. An early hypothesis [189] was confirmed by all examples up to now. This **DP hypothesis** claims that **in one component systems exhibiting continuous phase transitions to single absorbing state (without extra symmetry and inhomogeneity or disorder) short ranged interactions can generate DP class transition only**. Despite the robustness of this class experimental observation is still lacking [8, 190] probably owing to the sensitivity to disorder that can not be avoided in real materials. Besides DP a few more universality classes have been established in the last decade.

A major problem of these models is that they are usually far from the critical dimension and critical fluctuations prohibit mean-field (MF) like

behavior. Further complication is that bosonic field theoretical methods can not describe particle exclusion that may obviously happen in 1d. The success of the application of bosonic field theory in many cases is the consequence of the asymptotically low density of particles near the critical point. However in multi-component systems, where the exchange between different types is non-trivial, bosonic field theoretical descriptions may fail. In case of the binary production (BP) models (Sect. 5.5) bosonic RG predicts diverging density in the active phase contrary to the lattice model version of hard-core particles [224, 225, 226, 227, 228, 230]. Fermionic field theories on the other hand have the disadvantage that they are non-local and results exist for very simple reaction-diffusion systems only [241, 242, 283]. Other techniques like independent interval approximation [243], empty interval method [244] or density matrix renormalization (DMRG) are currently under development to be able to solve problems of critical reaction-diffusion models.

4.1 Directed percolation classes

The directed percolation (DP) introduced by [245] is an anisotropic percolation with a preferred direction t . This means that this problem should be $d \geq 2$ dimensional. If there is an object (bond, site etc.) at (x_i, y_j, \dots, t_k) it must have a nearest neighboring object at t_{k-1} unless $t_k = 0$ (see Figure 4.1). If we consider the preferred direction as time this means that

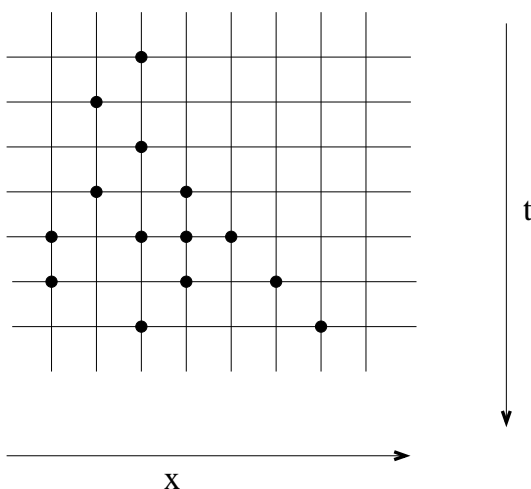


Figure 4.1: Directed site percolation in $d = 1 + 1$ dimensions

we have a spreading process of agent A that can not have spontaneous source: $\emptyset \not\rightarrow A$. This results in the possibility of a completely frozen, so called *absorbing state* from which the system can not escape if it has fallen into it. As the consequence these kinds of models may have phase transitions in $d = 1$ spatial dimension already. By increasing the probability p of the branching rate of the agent we can have a phase transition between the absorbing state and an active steady state with finite density of A -s. If the transition is continuous it is very likely that it belongs to a robust universality (DP) class. For a long time all examples of such absorbing phase transitions were found to belong to the DP class and a conjecture was set up by [189]. This claims that in one component systems exhibiting continuous phase transitions to single absorbing state (without extra symmetry, inhomogeneity or disorder) short ranged interactions can generate DP class transition only. This hypothesis was confirmed by all examples up to know and DP class exponents were found in some systems with multiple absorbing states too. For example in systems with infinitely many frozen absorbing states [333, 246, 247] the static exponents were found to coincide with those of DP. Also by models without any special symmetry of absorbing states DP behavior was reported [248, 251, 253]. So although the necessary conditions for DP behavior seem to be confirmed the determination of sufficient conditions is an open problem. There are many introductory works available now to DP [188, 7, 8, 9] therefore I shall not go very deeply into the discussions of details of various representations.

In the reaction-diffusion language the DP process is built up from the following processes



The static **mean-field** equation for the coarse-grained particle density $\rho(t)$ is

$$\frac{d\rho}{dt} = (\sigma - \gamma)\rho - (\lambda + \sigma)\rho^2 \quad . \quad (4.2)$$

This has the stationary stable solution

$$\rho(\infty) = \begin{cases} \frac{\sigma - \gamma}{\lambda + \sigma} & \text{for : } \sigma > \gamma \\ 0 & \text{for : } \sigma \leq \gamma \end{cases} \quad (4.3)$$

exhibiting a continuous transition at $\sigma = \gamma$. A small variation of σ or γ near the critical point implies a linear change of ρ therefore the order parameter exponent in the mean-field approximation is $\beta = 1$. Near the critical point the $O(\rho)$ term is the dominant one hence the density approaches the stationary value exponentially. For $\sigma = \gamma$ the remaining $O(\rho^2)$ term causes power-law decay $\rho \propto t^{-1}$ indicating $\alpha = 1$. To get information about other

critical exponent	$d = 1$ [263]	$d = 2$ [264]	$d = 3$ [265]	$d = 4 - \epsilon$ [266, 189]
$\beta = \beta'$	0.276486(8)	0.584(4)	0.81(1)	$1 - \epsilon/6 - 0.01128 \epsilon^2$
ν_{\perp}	1.096854(4)	0.734(4)	0.581(5)	$1/2 + \epsilon/16 + 0.02110 \epsilon^2$
ν_{\parallel}	1.733847(6)	1.295(6)	1.105(5)	$1 + \epsilon/12 + 0.02238 \epsilon^2$
$Z = 2/z$	1.580745(10)	1.76(3)	1.90(1)	$2 - \epsilon/12 - 0.02921 \epsilon^2$
$\delta = \alpha$	0.159464(6)	0.451	0.73	$1 - \epsilon/4 - 0.01283 \epsilon^2$
η	0.313686(8)	0.230	0.12	$\epsilon/12 + 0.03751 \epsilon^2$
$\gamma_p = \gamma + \nu_{\parallel}$	2.277730(5)	1.60	1.25	$1 + \epsilon/6 + 0.06683 \epsilon^2$
$\gamma_t = \nu_{\parallel} - \beta$	1.457361(14)	0.71(1)	0.29(15)	$\epsilon/4 + 0.033664 \epsilon^2$

Table 4.1: Estimates for the critical exponents of directed percolation.

scaling exponents we have to take into account the diffusion term $D\nabla^2$ describing local density fluctuations. Using rescaling invariance two more independent exponents can be determined: $\nu_{\perp} = 1/2$ and $Z = 2$ if $d > 4$. Therefore the upper critical dimension of directed percolation is $d_c = 4$.

Below the critical dimension the standard, bosonic field theoretical approach [189] is the RG analysis of the Langevin equation

$$\frac{\partial \rho(x, t)}{\partial t} = D\nabla^2 \rho(x, t) + (\sigma - \gamma)\rho(x, t) - (\lambda + \sigma)\rho^2(x, t) + \sqrt{\rho(x, t)}\eta(x, t) \quad (4.4)$$

is necessary, where $\eta(x, t)$ is the Gaussian noise field, defined by the correlations

$$\langle \eta(x, t) \rangle = 0 \quad (4.5)$$

$$\langle \eta(x, t)\eta(x', t') \rangle = \Gamma \delta^d(x - x')\delta(t - t') \quad (4.6)$$

The noise term is proportional $\sqrt{\rho(x, t)}$ ensuring that in the absorbing state ($\rho(x, t) = 0$) it vanishes. The square-root behavior stems from the definition of $\rho(x, t)$ as a coarse-grained density of active sites averaged over some mesoscopic box size. Note that DP universality occurs in many other processes like in the BARWo (see Section 4.1.3) or in cases with higher order terms like $\rho^3(x, t)$ or $\nabla^4 \rho(x, t)$ which are irrelevant under the RG transformation. This stochastic process can through standard techniques [254] be transformed into a Lagrangian formulation with the action

$$S = \int d^d x dt \left[\frac{D}{2} \psi^2 \phi + \psi (\partial_t \phi - \nabla^2 \phi - r\phi + u\phi^2) \right] \quad (4.7)$$

where ϕ is the density field and ψ is the response field (appearing in response functions) and the action is invariant under the following time-reversal sym-

metry

$$\phi(x, t) \rightarrow -\psi(x, -t) \quad , \quad \psi(x, t) \rightarrow -\phi(x, t) \quad . \quad (4.8)$$

This symmetry yields [257, 258] the scaling relations

$$\beta = \beta' \quad (4.9)$$

$$4\delta + 2\eta = dz \quad (4.10)$$

This field theory was found to be equivalent [255] to the Reggeon field theory [256] that is a model of scattering elementary particles at high energies and low-momentum transfers.

Perturbative $\epsilon = 4 - d$ renormalization group analysis [266, 189] up to two-loop order resulted in estimates for the critical exponents shown in the Table 4.1. The best results obtained by approximative techniques for DP like improved mean-field [259], coherent anomaly method [260], Monte Carlo simulations [257, 267, 268, 269], series expansions [270, 263], DMRG [280] are also shown in Table 4.1.

The **local persistence** probability may be defined as the probability ($p_l(t)$) that a particular site never becomes active up to time t . Numerical simulations [261] for this in the 1+1 d Domany-Kinzel SCA (see Sect.4.1.2) found power-law with exponent

$$\theta_l = 1.50(1) \quad (4.11)$$

The **global persistence** probability defined as the probability ($p_g(t)$) of the global order parameter does not change sign up to time t . The simulations of [261] in 1+1 d claim $\theta_g \geq \theta_l$. This agrees with field theoretical $\epsilon = 4 - d$ expansions [262] that predict $\theta_g = 2$ for $d \geq 4$ and for $d < 4$:

$$\theta_g = 2 - \frac{5\epsilon}{24} + O(\epsilon^2) \quad . \quad (4.12)$$

Crossover from isotropic to directed percolation was investigated by perturbative RG [281] up to one loop order. They found that while for $d > 6$ the isotropic, for $d > 5$ the directed Gaussian fixed point becomes stable. For $d < 5$ the asymptotic behavior is governed by the DP fixed point. On the other hand in $d = 2$ exact calculations and simulations [282] found that the isotropic percolation (IP) is stable with respect to DP if we control the crossover by a spontaneous particle birth parameter. It is still an open question what happens for $2 < d < 5$. **Crossovers to mean-field behavior** generated by long-range interactions 4.1.7 and to compact directed percolation 4.3 will be discussed later.

It was conjectured [284] that in 1d fermionic (single occupancy) and bosonic (multiple occupancy) models may have different critical behavior.

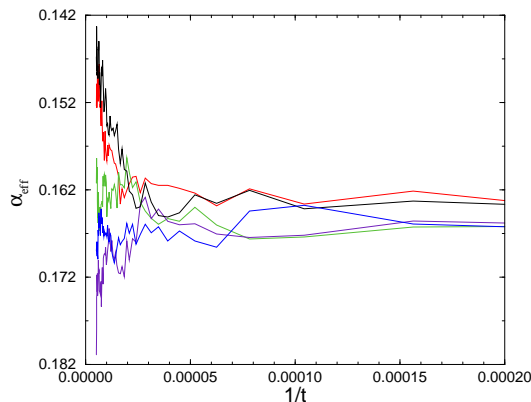


Figure 4.2: Local slopes of the density decay in a bosonic BARW1 model (Sect. 4.1.3). Different curves correspond to $\lambda = 0.12883, 0.12882, 0.12881, 0.1288, 0.12879$ (from bottom to top) [285].

An attempt for fermionic field theoretical solution of DP in 1+1 d was shown in [242, 283] but run into severe convergence problems and has not resulted in precise quantitative estimates for critical exponents. Although the bosonic field theory is expected to be valid owing to the asymptotically low density at criticality it has never been proven rigorously. Since only bosonic field theory exists that gives rather inaccurate critical exponent estimates, in [285] simulations of a a BARW1 process (4.20) with unrestricted site occupancy were performed to investigate the density ($\rho(t)$) decay of a DP process from random initial state. Figure 4.2 shows the local slopes of density decay defined as

$$\alpha_{eff} = -\frac{d \log \rho(t)}{d \log t} \quad (4.13)$$

around the critical point for several annihilation rates (λ). The critical point is estimated at $\lambda_c = 0.12882(1)$ (corresponding to straight line) with the extrapolated decay exponent $\alpha = 0.165(5)$ that agrees well with fermionic model simulation and series expansion results $0.1595(1)$ [270].

Models exhibiting DP transitions have been reviewed in great detail in [7] and in [9]. In the next subsections I recall only three important examples.

4.1.1 The Contact process

The contact process (CP) is one of the earliest and simplest lattice model for DP with **asynchronous** update introduced by Harris [271] to model epidemic spreading without immunization. Its dynamics is defined by nearest-neighbor processes that occur spontaneously due to specific rates (rather than probabilities). In numerical simulations models of this type are usually realized by random sequential updates. In one dimension this means that a pair of sites $\{s_i, s_{i+1}\}$ is chosen at random and an update is attempted according to specific transition rates $w(s_{i,t+dt}, s_{i+1,t+dt} | s_{i,t}, s_{i+1,t})$. Each

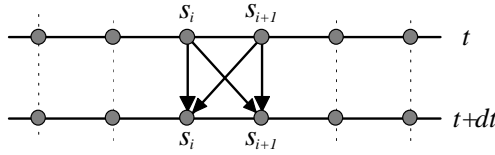


Figure 4.3: Update in the contact process [199].

attempt to update a pair of sites increases the time t by $dt = 1/N$, where N is the total number of sites. One time step (sweep) therefore consists of N such attempts. The contact process is defined by the rates

$$w(A, I | A, A) = w(I, A | A, A) = \lambda, \quad (4.14)$$

$$w(I, I | A, I) = w(I, I | I, A) = \mu, \quad (4.15)$$

$$w(A, A | A, I) = w(A, A | I, A) = 1, \quad (4.16)$$

where $\lambda > 0$ and $\mu > 0$ are two parameters (all other rates are zero). Equation (4.14) describes the creation of inactive (dry) spots within active (wet) islands. Equations (4.15) and (4.16) describe the shrinkage and growth of active islands. In order to fix the time scale, we chose the rate in Eq. (4.16) to be equal to one. The active phase is restricted to the region $\mu < 1$ where wet islands are likely to grow. In one dimension series expansions and numerical simulations determined the critical point and critical exponents precisely [269, 270, 272]. In two dimensions Dickman et al have determined order parameter moments and cumulant ratios [272].

4.1.2 DP-class stochastic cellular automata

There are many stochastic cellular automata (SCA) that exhibit DP transition [273] perhaps the first and simplest one is the (1+1)-dimensional Domany-Kinzel (DK) model [205]. In this model the state at a given time t

is specified by binary variables $\{s_i\}$, which can have the values Ac (active) and I (inactive). At odd (even) times, odd- (even-) indexed sites are updated according to specific conditional probabilities. This defines a cellular automaton with **parallel** updates (discrete time evolution) acting on two independent triangular sub-lattices: The conditional probabilities in the

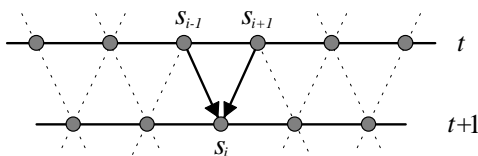


Figure 4.4: Update in the Domany-Kinzel model [199].

Domany-Kinzel model $P(s_{i,t+1} | s_{i-1,t}, s_{i+1,t})$ are given by

$$P(I | I, I) = 1, \quad (4.17)$$

$$P(Ac | Ac, Ac) = p_2, \quad (4.18)$$

$$P(Ac | I, Ac) = P(Ac | Ac, I) = p_1, \quad (4.19)$$

and $P(I | s_{i-1}, s_{i+1}) + P(Ac | s_{i-1}, s_{i+1}) = 1$, where $0 \leq p_1 \leq 1$ and $0 \leq p_2 \leq 1$ are two parameters. Equation (4.17) ensures that the configuration \dots, I, I, I, \dots is the absorbing state. The process in Eq. (4.18) describes the creation of inactive spots within active islands with probability $1 - p_2$. The random walk of boundaries between active and inactive domains is realized by the processes in Eq. (4.19). A DP transitions can be observed only if $p > \frac{1}{2}$ when active islands are biased to grow. [274]. The phase diagram of the 1d DK model is shown on Fig. 4.5. It comprises an active and an inactive phase, separated by a phase transition line (solid line) belonging to DP class. The dashed lines corresponds to *directed bond percolation* ($p_2 = p(2 - p_1)$) and *directed site percolation* ($p_1 = p_2$) models. At the special symmetry endpoint ($p_1 = \frac{1}{2}, p_2 = 1$) compact domain growth occurs (CDP) and the transition becomes first order (see Section 4.3). The transition on the $p_2 = 0$ axis corresponds to the transition of the stochastic version of Wolfram's rule-18 cellular automaton [274]. This range-1 SCA generates 1 at time t only when right or left neighbour was 1 at $t - 1$:

$$\begin{array}{rcc} t-1: & 100 & 001 \\ t: & 1 & 1 \end{array}$$

with probability p_1 [273]. The critical point was determined by precise simulations ($p_1^* = 0.80948(1)$) [275]. At $t \rightarrow \infty$ the steady state can be

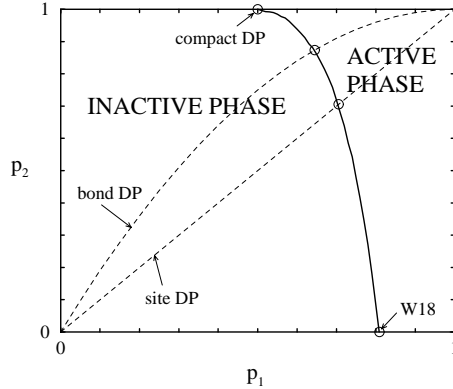


Figure 4.5: Phase diagram of the 1d Domany-Kinzel SCA [199].

built up from 00 and 01 blocks [277]. This permits to map this model onto the even simpler rule-6/16 SCA with new variables $01 \rightarrow 1$ and $00 \rightarrow 0$:

$$\begin{array}{rcccc}
 \tau-1: & 0 & 0 & 0 & 1 & 1 & 0 & 1 & 1 \\
 \tau: & & 0 & & 1 & & 1 & & 0
 \end{array}$$

By solving GMF approximations and applying Padé approximations [276] or CAM method [260] very precise order parameter exponent estimates were found: $\beta = 0.2796(2)$.

The **DS phase structure** of the 1d DK model was explored by [41] and DP class transitions were found.

Another SCA example I mention is the family of **range-4 SCA** with an acceptance rule

$$s(t+1, j) = \begin{cases} X & \text{if } y \leq \sum_{j-4}^{j+4} s(t, j) \leq 6 \\ 0 & \text{otherwise} \end{cases} ,$$

where $X \in \{0, 1\}$ is a two valued random variable such that $Prob(X = 1) = p$ [22]. The $y = 3$ case was introduced and investigated by [278] in $d = 1, 2, 3$. First simulations in one dimension [278] suggested a counter-example to the DP conjecture. More precise spreading simulations of this model [279] and GMF + CAM calculations and simulations of the $y < 6$ family in one and two dimensions have proven that this does not happen for any case [22]. The transitions are either belong to DP class or first order.

4.1.3 Branching and annihilating random walks with odd number of offsprings

Branching and annihilating random walks (BARW) introduced by [191] are defined by the following reaction-diffusion processes



As one can see for $k = 2$ and $m = 1$ (BARW1) this differs from the DP process (4.1) that spontaneous annihilation of particles is not allowed. The $2A \rightarrow A$ and $2A \rightarrow \emptyset$ reactions dominating in the inactive phase are shown to be equivalent [325] (see Sect.4.3.1). The action of the BARW process was set up by [193]

$$S = \int d^d x dt [\psi(\partial_t - D\nabla^2)\phi - \lambda(1 - \psi^k)\phi^k + \sigma(1 - \psi^m)\psi\phi] \quad (4.21)$$

The bosonic RG analysis of BARW systems [193] have shown that for $k = 2$ all the lower branching reactions with $m = 2, m = 4, \dots$ are generated via fluctuations involving combinations of branching and annihilation processes and as the consequence for **odd** m the $A \rightarrow \emptyset$ appears too. Therefore in the BARW1 case (and in general in the odd m BARW (BARWo) cases) the field theoretical solution will be the same as that of the DP process with the same universal behavior. This was confirmed by simulations (see example [286]).

For even m (BARWe) the spontaneous decay $A \rightarrow \emptyset$ is not generated, hence there is an absorbing state with lonely wandering particle and the parity of the number of particles is conserved. This conservation results in a non-DP critical behavior that will be discussed in Sect.4.4.2.

4.1.4 DP with spatial boundary conditions

For a review of critical behavior at surfaces of *equilibrium* models see Iglói *et al.* [287]). Cardy [288] suggested that surface critical phenomena may be described by introducing an additional *surface exponent* for the order parameter field which is generally independent of the other bulk exponents. In nonequilibrium statistical physics one can introduce spatial, temporal (see Sect.4.1.7) or mixed (see Sect.4.1.5) boundary conditions.

In DP an absorbing wall may be introduced by cutting all bonds (**IBC**) crossing a given $(d-1)$ -dimensional hyperplane in space. In case of reflecting boundary condition (**RBC**) where the wall acts like a mirror so that the sites within the wall are always a mirror image of those next to the wall. A third type of boundary condition is the active boundary condition (**ABC**) where the sites within the wall are forced to be active.

The density at the wall is found to scale as

$$\rho_s^{stat} \sim (p - p_c)^{\beta_1} \quad (4.22)$$

with a surface critical exponent $\beta_1 > \beta$. Owing to the time reversal symmetry of DP (4.8) only one extra exponent is needed to describe surface effects, hence the cluster survival exponent is the same

$$\beta'_1 = \beta_1 \quad . \quad (4.23)$$

The mean lifetime of finite clusters at the wall is defined as

$$\langle t \rangle \sim |\Delta|^{-\tau_1} \quad (4.24)$$

where $\Delta_s = (p - p_c)$, and is related to β_1 by the scaling relation

$$\tau_1 = \nu_{||} - \beta_1 \quad (4.25)$$

The average size of finite clusters grown from seeds on the wall is

$$\langle s \rangle \sim |\Delta|^{-\gamma_1}, \quad (4.26)$$

Series expansions [289] and numerical simulations [290] in 1+1 dimensions indicate that the presence of the wall alters several exponents. However, the scaling properties of the correlation lengths (as given by $\nu_{||}$ and ν_{\perp}) are *not* altered.

The field theory for DP in a semi-infinite geometry was first analyzed by Janssen et al. [291]. They showed that the appropriate action for DP with a wall at $x_{\perp} = 0$ is given by $S = S_{\text{bulk}} + S_{\text{surface}}$, where

$$S_{\text{surface}} = \int d^{d-1}x \int dt \Delta_s \psi_s \phi_s, \quad (4.27)$$

with the definitions $\phi_s = \phi(\mathbf{x}_{||}, x_{\perp} = 0, t)$ and $\psi_s = \psi(\mathbf{x}_{||}, x_{\perp} = 0, t)$. The surface term S_{surface} corresponds to the most relevant interaction consistent with the symmetries of the problem and which also respects the absorbing state condition. The appropriate surface exponents were computed to first order in $\epsilon = 4 - d$ using renormalization group techniques:

$$\beta_1 = \frac{3}{2} - \frac{7\epsilon}{48} + O(\epsilon^2). \quad (4.28)$$

They also showed that the corresponding hyperscaling relation is

$$\nu_{||} + d\nu_{\perp} = \beta_1 + \beta + \gamma_1 \quad (4.29)$$

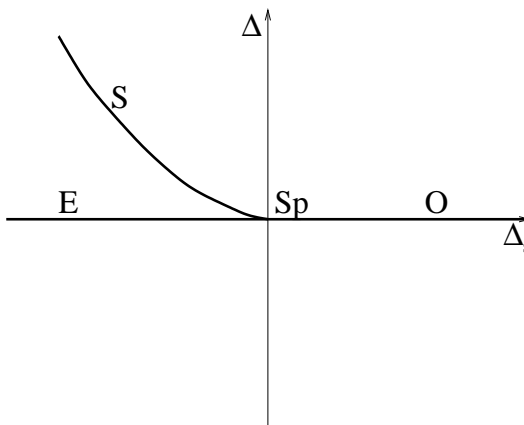


Figure 4.6: Schematic mean field phase diagram for boundary DP [250]. The transitions are labeled by O=ordinary, E=extraordinary, S=surface, and Sp=special.

relating β_1 to

$$\gamma_1 = \frac{1}{2} + \frac{7\epsilon}{48} + O(\epsilon^2). \quad (4.30)$$

The schematic phase diagram for boundary DP is shown on Fig. 4.6, where Δ and Δ_s represent, respectively, the deviations of the bulk and surface from criticality. For $\Delta > 0$ and for Δ_s sufficiently negative the boundary orders even while the bulk is disordered, i.e. the *surface transition*. For $\Delta_s < 0$ and $\Delta \rightarrow 0$, the bulk orders in the presence of an already ordered boundary, i.e. an *extraordinary transition* for the boundary. Finally at $\Delta = \Delta_s = 0$, where all the critical lines meet, and where both the bulk and isolated surface are critical, we find a multi-critical point, i.e. the *special transition*.

For $\Delta_s > 0$ and as $\Delta \rightarrow 0$ there is an *ordinary transition*, since the bulk orders in a situation where the boundary, if isolated, would be disordered. At the ordinary transition, one finds just **one extra independent exponent** associated with the boundary: this can be taken to be the surface density exponent $\beta_{1,\text{dens}}$. In 1d the IBC and RBC cases belong to the same universality class [249] that was identified as the ordinary transition. There are numerical data for the exponents of the extraordinary and special transitions (however see [291] for an RG analysis).

The best exponent estimates currently available were summarized in

[250]. Some of them are shown in Table 4.2. In $d = 1$ the best results are from series expansions [289, 292]; in all other cases are from Monte-Carlo data [290, 293, 249, 294] The exponent τ_1 has been conjectured to

	$d = 1$	$d = 2$	Mean Field
β_1	0.733 71(2)	1.07(5)	3/2
$\delta_1 = \alpha_1$	0.423 17(2)	0.82(4)	3/2
τ_1	1.000 14(2)	0.26(2)	0
γ_1	1.820 51(1)	1.05(2)	1/2

Table 4.2: Critical exponents for DP in $d = 1$ and $d = 2$ for the ordinary transition at the boundary.

equal unity, [289] although this has now been challenged by the estimate $\tau_1 = 1.00014(2)$ [292].

It has been known for some time that the presence of an **edge** introduces new exponents, independent of those associated with the bulk or with a surface (see [288]). For an investigation showing numerical estimates in 2d and mean-field values see [293]. Table 4.1.4 summarizes results for the ordinary edge exponents. A closely related application is the study of spreading processes in narrow channels [295].

Angle (α)	$\pi/2$	$3\pi/4$	π	$5\pi/4$
β_2^O ($d = 2$)	1.6(1)	1.23(7)	1.07(5)	0.98(5)
β_2^O (MF)	2	5/3	3/2	7/5

Table 4.3: Numerical estimates for the ordinary β_2^O exponents for edge DP together with the mean field values. Note that $\beta_2^O(\pi) = \beta_1^O$

4.1.5 DP with mixed (parabolic) boundary condition scaling

Kaiser and Turban [296] investigated the 1+d d DP process confined in parabola-shaped geometry. Assuming an absorbing boundary of the form $x = \pm Ct^\sigma$ they proposed a general scaling theory. It is based on the observation that the width C of the parabola C scales as $C \rightarrow \Lambda^{Z\sigma-1}C$ under rescaling

$$x \rightarrow \Lambda x, \quad t \rightarrow \Lambda^Z t, \quad \Delta \rightarrow \Lambda^{-1/\nu_\perp} \Delta, \quad \rho \rightarrow \Lambda^{-\beta/\nu_\perp} \rho, \quad (4.31)$$

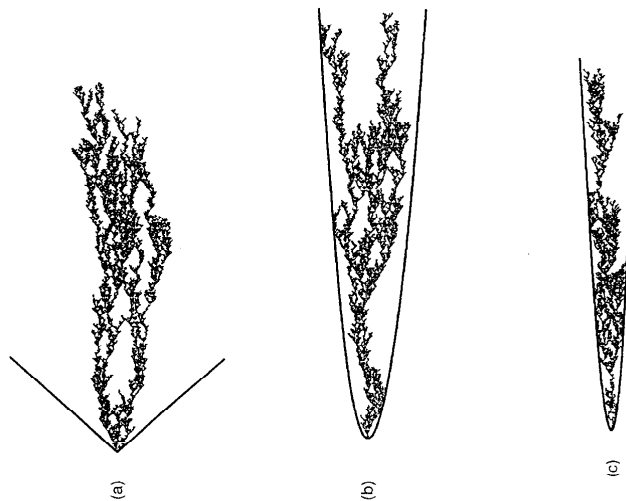


Figure 4.7: 1+1 d directed site percolation process confined by parabola [296]. (a) $\sigma < 1/Z$, (b) $\sigma = 1/Z$, (c) $\sigma > 1/Z$.

where $\Delta = |p - p_c|$ and Z is the dynamical exponent of DP. By referring to conformal mapping of the parabola to straight lines and showing it in the mean-field approximation they claim that the boundary is a relevant perturbation for $\sigma > 1/Z$ irrelevant for $\sigma < 1/Z$ and marginal for $\sigma = 1/Z$. The marginal case results in C dependent non-universal power-law decay, while for the relevant case stretched exponential functions have been obtained. The above authors have given support to these claims by numerical simulations.

4.1.6 Lévy flight anomalous diffusion in DP

The effect of Lévy flight anomalous diffusion has already mentioned in Sections 3.1.5, 3.2.4 in case of equilibrium models. In non-equilibrium models first following a suggestion of Mollison [3], Grassberger [137] introduced a variation of the epidemic processes with infection probability distributions $P(R)$, which decays with the distance R as a power-law like

$$P(R) \propto \frac{1}{R^{d+\sigma}} \quad (4.32)$$

and claimed that the critical exponents should depend continuously on σ . This was confirmed by estimating β based on CAM calculations [138]. This

was extended for GEP processes (see Sect.4.2). The effective action of the DP model is

$$S[\bar{\psi}, \psi] = \int d^d x dt \left[\bar{\psi}(\partial_t - \tau - D_N \nabla^2 - D_A \nabla^\sigma) \psi + \frac{g}{2}(\bar{\psi}\psi^2 - \bar{\psi}^2\psi) \right]. \quad (4.33)$$

Field theoretical RG method up to first order in $\epsilon = 2\sigma - d$ expansion [139] gives:

$$\begin{aligned} \beta &= 1 - \frac{2\epsilon}{7\sigma} + O(\epsilon^2), \\ \nu_\perp &= \frac{1}{\sigma} + \frac{2\epsilon}{7\sigma^2} + O(\epsilon^2), \\ \nu_\parallel &= 1 + \frac{\epsilon}{7\sigma} + O(\epsilon^2), \\ Z = \frac{\nu_\parallel}{\nu_\perp} &= \sigma - \epsilon/7 + O(\epsilon^2). \end{aligned} \quad (4.34)$$

Moreover, it was shown that the hyperscaling relation

$$\eta + 2\delta = d/Z \quad (\delta = \beta/\nu_\parallel), \quad (4.35)$$

for the so-called critical initial slip exponent η and the relation

$$\nu_\parallel - \nu_\perp(\sigma - d) - 2\beta = 0. \quad (4.36)$$

hold exactly for arbitrary values of σ . Numerical simulations on 1+1 d bond percolation confirmed these results except in the neighborhood of $\sigma = 2$ [140] (see Fig.4.8).

4.1.7 Long-range correlated initial conditions in DP

It is well known that initial conditions influence the temporal evolution of nonequilibrium systems. The “memory” of systems for the initial state usually depends on the dynamical rules. For example, stochastic processes with a finite temporal correlation length relax to their stationary state in an exponentially short time. An interesting situation emerges when a system undergoes a nonequilibrium phase transition where the temporal correlation length diverges. This raises the question whether it is possible construct initial states that affect the *entire* temporal evolution of such systems.

Monte-Carlo simulations of critical models with absorbing states usually employ two different types of initial conditions. On the one hand *uncorrelated random initial conditions* (Poisson distributions) are used to study the

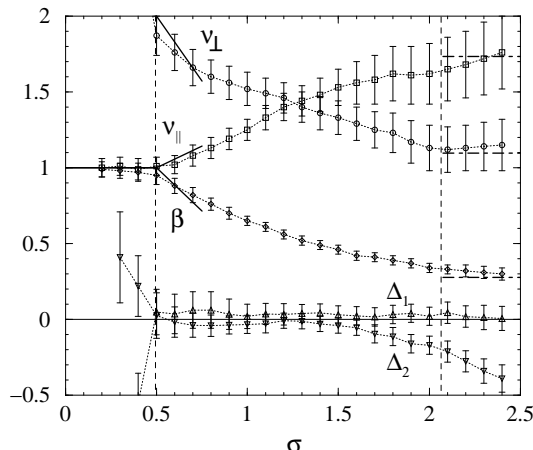


Figure 4.8: Estimates for the exponent β and the derived exponents ν_{\perp} and ν_{\parallel} in comparison with the field-theoretic results (solid lines) and the DP exponents (dot-dashed lines) [140]. The quantities Δ_1 and Δ_2 represent deviations from the scaling relations (4.35) and (4.36), respectively.

relaxation of an initial state with a finite particle density towards the absorbing state. In this case the particle density $\rho(t)$ *decreases* on the infinite lattice asymptotically as

$$\rho(t) \sim t^{-\beta/\nu_{\parallel}}. \quad (4.37)$$

On the other hand, in spreading simulations [257], each run starts with a *single particle* as a localized active seed from where a cluster originates (this is a long-range correlated state). Although many of these clusters survive for only a short time, the number of particles $n(t)$ averaged over many independent runs *increases* as

$$\langle n(t) \rangle \sim t^{+\eta}, \quad (4.38)$$

These two cases seem to represent extremal situations where the average particle number either decreases or increases.

A *crossover* between these two extremal cases takes place in a critical spreading process that starts from a random initial condition at very low density. Here the particles are initially separated by empty intervals of a certain typical size wherefore the average particle number first increases according to Eq. (4.38). Later, when the growing clusters begin to interact with each other, the system crosses over to the algebraic decay of Eq. (4.37)

– a phenomenon which is referred to as the “critical initial slip” of nonequilibrium systems [28].

In [144, 344] it was investigated whether it is possible to interpolate *continuously* between the two extremal cases in cases of 1+1 dimensional DP and PC processes. It was shown that one can in fact generate certain initial states in a way that the particle density on the infinite lattice varies as

$$\rho(t) \sim t^\kappa \quad (4.39)$$

with a continuously adjustable exponent κ in the range

$$-\beta/\nu_{\parallel} \leq \kappa \leq +\eta. \quad (4.40)$$

To this end artificial initial configurations with algebraic long-range correlations of the form

$$C(r) = \langle s_i s_{i+r} \rangle \sim r^{-(d-\sigma)}, \quad (4.41)$$

were constructed, where $\langle \rangle$ denotes the average over many independent realizations, d the spatial dimension, and $s_i = 0, 1$ inactive and active sites. The exponent σ is a free parameter and can be varied continuously between 0 and 1. This initial condition can be taken into account by adding the term

$$S_{ic} = \mu \int d^d x \psi(x, 0) \phi_0(x) \quad (4.42)$$

to the action, where $\phi_0(x)$ represents the initial particle distribution. The long-range correlations limit $\sigma \rightarrow d$ corresponds to a constant particle density and thus we expect Eq. (4.37) to hold ($\phi_0(x) = \text{const.}$ is irrelevant under rescaling). On the other hand, the short-range limit $\sigma \rightarrow 0$ represents an initial state where active sites are separated by infinitely large intervals ($\phi_0(x) = \delta^d(x)$) so that the particle density should increase according to Eq. (4.38). In between we expect $\rho(t)$ to vary algebraically according to Eq. (4.39) with an exponent κ depending continuously on σ .

In case of the 1+1 d **Domany-Kinzel SCA** (see Sect. 4.1.2) field-theoretical renormalization group calculation and simulations proved [144] the exact functional dependence

$$\kappa(\sigma) = \begin{cases} \eta & \text{for } \sigma < \sigma_c \\ \frac{1}{z}(d - \sigma - \beta/\nu_{\perp}) & \text{for } \sigma > \sigma_c \end{cases} \quad (4.43)$$

with the critical threshold $\sigma_c = \beta/\nu_{\perp}$.

4.1.8 Quench disordered DP systems

Perhaps the lack of experimental observation of the robust DP class lies in the fact that even weak disorder changes the critical behavior of such models.

First Noest showed [146] using Harris criterion [145] that **spatially quenched disorder** (frozen in space) changes the critical behavior of DP systems for $d < 4$. Janssen [147] studied the problem by field theory taking into account the disorder in the action by adding the term

$$S \rightarrow S + \gamma \int d^d x \left[\int dt \psi \phi \right]^2 . \quad (4.44)$$

This additional term causes **marginal perturbation** and the stable fixed point is shifted to an unphysical region, leading to runaway solutions of the flow equations in the physical region of interest. This means that spatially quenched disorder changes the critical behavior of DP. This conclusion is supported by the simulation results of Moreira and Dickman [148] who reported logarithmic spreading behavior in two-dimensional contact process at criticality. In the sub-critical region they found Griffiths phase in which the time dependence is governed by non-universal power-laws, while in the active phase the relaxation of $P(t)$ is algebraic.

In 1+1 dimension Noest predicted [146] generic scale invariance. Webman et al. [149] reported glassy phase with non-universal exponents in a 1+1 d DP process with quenched disorder. Cafiero *et al.* [150] showed that DP with spatially quenched randomness in the large time limit can be mapped onto a non-Markovian spreading process with memory, in agreement with previous results. They showed that the time reversal symmetry of the DP process (4.8) is not broken therefore

$$\delta = \delta' \quad (4.45)$$

and derived the scaling law for the inactive phase

$$\eta = dZ/2 \quad (4.46)$$

and for the absorbing phase

$$\eta + \delta = dZ/2 \quad (4.47)$$

They confirmed these and found continuously changing exponents by simulations. An RG study by Hooyberghs et al. [151] showed that in case of strong enough disorder the critical behavior is controlled by an infinite randomness fixed point (IRFP), the static exponents of which in 1d are

$$\beta = (3 - \sqrt{5})/2 \quad , \quad \nu_{\perp} = 2 \quad (4.48)$$

and $\xi^{1/2} \propto \ln \tau$. For disorder strengths outside the attractive region of the IRFP disorder dependent critical exponents are detected.

The **temporally quenched disorder** can be taken into the action by adding the term:

$$S \rightarrow S + \gamma \int dt \left[\int d^d x \psi \phi \right]^2 . \quad (4.49)$$

This is a **relevant** perturbation for the DP processes. Jensen [152] investigated the 1+1 d directed bond percolation (see Sect. 4.1.2) with temporal disorder via series expansions and Monte Carlo simulations. The temporal disorder was introduced by allowing time slices to become fully deterministic ($p_1 = p_2 = 1$), with probability α . He found α dependent, continuously changing critical point and critical exponent values between those of the the 1+1 d DP class and those of the deterministic percolation. This latter class is defined by the exponents:

$$\beta = 0, \quad \delta = 0, \quad \eta = 1, \quad Z = 1, \quad \nu_{||} = 2, \quad \nu_{\perp} = 2 . \quad (4.50)$$

For small disorder parameter values violation of the Harris criterion is reported.

If **quenched disorder takes place in both space and time** the corresponding term to action is

$$S \rightarrow S + \gamma \int dt d^d x [\psi \phi]^2 . \quad (4.51)$$

and becomes an **irrelevant** perturbation to the Reggeon field theory. This has the same properties as the intrinsic noise in the system and can be considered as being annealed.

4.2 Dynamical percolation (DyP) classes

If we allow memory in the unary DP spreading process (Sect.4.1) such that the infected sites may have a different re-infection probability (p) than the virgin ones (q) we obtain different percolation behavior [297]. The model in which the re-infection probability is zero is called the General Epidemic Model (GEP) [298]. In this case the epidemic stops in finite systems but an infinite epidemic is possible in the form of a solitary wave of activity. When starting from a single seed this leads to annual growth patterns. The transition between survival and extinction is a critical phenomenon called dynamical percolation [299]. Clusters generated at criticality are the ordinary percolation clusters of the lattice in question. Field theoretical

treatment was given by [300, 301, 302, 304]. The action of the model is

$$S = \int d^d x dt \left[\frac{D}{2} \psi^2 \phi - \psi \left(\partial_t \phi - \nabla^2 \phi - r \phi + w \phi \int_0^t ds \phi(s) \right) \right] \quad (4.52)$$

Is is invariant under the symmetry transformation

$$\phi(x, t) \leftrightarrow -\partial_t \psi(x, t) \quad (4.53)$$

that results in the hyperscaling relation [258]:

$$\eta + 2\delta + 1 = \frac{dz}{2} \quad (4.54)$$

Like in case of the DP class the $\beta = \beta'$ and the $\delta = \alpha$ relations hold again. The dynamical critical exponents as well as spreading and avalanche exponents are summarized in [312]. The dynamical exponents are $Z = 1.1295$ for $d = 2$, $Z = 1.336$ for $d = 3$ and $Z = 2$ for $d = 6$. Dynamical percolation was observed in forest fire models [313, 1] and in some Lotka-Volterra type lattice prey-predator models [314] as well.

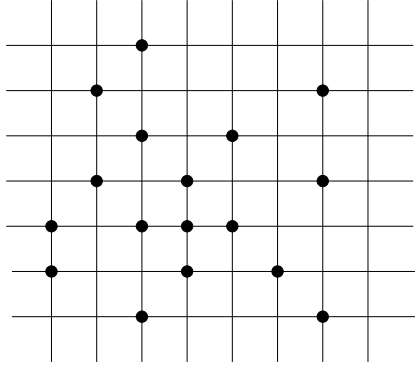
4.2.1 Isotropic percolation universality classes

Isotropic, ordinary percolation [129, 132] is a geometrical phenomena that describes the occurrence of infinitely large connected clusters by **completely random** displacement of some variables (sites, bonds, etc) (with probability p) on lattices (see Fig.4.9).

The dynamical percolation process is known to generate such percolating clusters (see Sect.4.2). At the transition point moments of the s cluster size distribution $n_s(p)$ show singular behavior. The ordinary percolation corresponds to the $q = 1$ limit of the Potts model. That means its generating functions can be expressed in terms of the free energy of the $q \rightarrow 1$ Potts model. In the low-temperature dilute Ising model the occupation probability (p) driven continuous magnetization transition can be described by percolation. As the consequence the critical exponents of the magnetization can be related to the cluster-size exponents. For example the susceptibility obeys simple homogeneity form with $p - p_c$ replacing $T - T_c$

$$\chi \propto |p - p_c|^{-\gamma} \quad (4.55)$$

The Table 4.4 summarizes the known critical exponents of the ordinary percolation. The exponents are from the overview [130]. Field theoretical treatment [131] provided an upper critical dimension $d_c = 6$. The $d = 1$ case is special : $p_c = 1$ and the order parameter jumps ($\beta = 0$). Furthermore here some exponents exhibit non-universal behavior by increasing the interaction length unless the we redefine the scaling variable (see [129]).

Figure 4.9: Isotropic site percolation in $d = 2$ dimensions

d	$\beta = \beta'$	γ_p	ν_{\perp}	σ	τ
1	0	1	1	1	2
2	5/36	43/18	4/3	36/91	187/91
3	0.418(1)	1.793(4)	0.8765(17)	0.452(1)	2.189(1)
4	0.64	1.44	0.68	0.48	2.31
5	0.84	1.18	0.57	0.49	2.41
6	1	1	1/2	1/2	3/2

Table 4.4: Critical exponents of the ordinary percolation

4.2.2 DyP with spatial boundary conditions

There are very few numerical results exists for surface critical exponents of dynamical percolation. The GEP process in 3d was investigated numerically by Grassberger [315]. The surface and edge exponents (for angle $\pi/2$) were determined in case of IBC. Different measurements (density and cluster simulations) result in single surface $\beta_1 = 0.848(6)$ and single edge $\beta_e = 1.36(1)$.

4.2.3 Lévy flight anomalous diffusion in DyP

The renormalization group analysis of the GEP with anomalous diffusion [139] resulted in the following $\epsilon = 3\sigma - d$ expansion results for the critical initial slip exponent:

$$\eta = \frac{3\bar{\epsilon}}{16\sigma} + O(\bar{\epsilon}^2), \quad (4.56)$$

for the order parameter (density of removed (immune) individuals) exponent:

$$\beta = 1 - \frac{\tilde{\varepsilon}}{4\sigma} + O(\tilde{\varepsilon}^2), \quad (4.57)$$

for the spatial correlation exponent

$$\nu_{\perp} = \frac{1}{\sigma} + \frac{\tilde{\varepsilon}}{4\sigma^2} + O(\tilde{\varepsilon}^2), \quad (4.58)$$

and for the temporal correlation length exponent

$$\nu_{\parallel} = 1 + \frac{\tilde{\varepsilon}}{16\sigma} + O(\tilde{\varepsilon}^2). \quad (4.59)$$

4.3 Voter model (VM) classes

The voter model [2, 317] defined by the following spin-flip dynamics. A site is selected randomly that takes the “opinion” (or spin) of one of its nearest neighbors (with probability p). This ensures that the model has two homogeneous absorbing states (all spin up or down) and invariant under Z_2 symmetry. The general feature of these models that dynamics takes place only at the boundaries. The action describing this was proposed in [316, 325].

$$S = \int d^d x dt \left[\frac{D}{2} \phi(1-\phi)\psi^2 - \psi(\partial_t \phi - \lambda \nabla^2 \phi) \right] \quad (4.60)$$

is invariant under the transformation

$$\phi \leftrightarrow 1 - \phi, \quad \psi \leftrightarrow -\psi \quad . \quad (4.61)$$

This results in the “hyperscaling” [258]

$$\delta + \eta = dz/2 \quad (4.62)$$

that is valid for all first order transitions ($\beta = 0$) with $d \leq 2$, hence $d_c = 2$ is the upper critical dimension. It is also valid for all **compact growth processes** (where “compact” means that the density in surviving colonies remains finite as $t \rightarrow \infty$).

In **one dimension** at the upper terminal point of the DK SCA (Fig.4.5 $p_1 = \frac{1}{2}$, $p_2 = 1$) an extra Z_2 symmetry takes place between 1-s and 0-s, still the scaling behavior is not DP class like but corresponds to the inactive phase (fixed point) of PC class (Sect. 4.4) models. As the consequence *compact domains* of 0-s and 1-s grow such as the domain walls follow annihilating random walks (ARW) (see Sect.4.3.1) and belong to the 1d VM

class. In 1d the compact directed percolation (CDP) is also equivalent to the $T = 0$ Galuber Ising model (see Sections 2,3.1). By applying non-zero temperature (corresponding to spin flips in domains) or symmetry breaking (like changing p_2 or external magnetic field) a first order transition takes place ($\beta = 0$).

In **two (and higher) dimensions** the $p = 1$ situation corresponds to the $p_1 = 3/4$, $p_2 = 1$ point in the phase diagram of Z_2 symmetric models (see Fig.3.1). This model has a “duality” with coalescing random walks: going backward in time, the successive ancestors of a given spin follow the trail of a simple random walk (RW); comparing the values of several spins shows that their associated RW-s necessarily merge upon encounter [2]. This correspondence allows to solve many aspects of the kinetics. In particular, the calculation of the density of interfaces $\rho_m(t)$ (i.e. the fraction of $+-$ n.n. pairs) starting from random initial conditions of magnetization m , is ultimately given by the probability that a RW initially at unit distance from the origin, has not yet reached it at time t . Therefore, owing to the recurrence properties of RW-s, the VM shows coarsening for $d \leq 2$ (i.e. $\rho_m(t) \rightarrow 0$ when $t \rightarrow \infty$). For the the ‘marginal’ case $d = 2$ one finds the slow logarithmic decay [318, 319]:

$$\rho_m(t) = (1 - m^2) \left[\frac{2\pi D}{\ln t} + \mathcal{O}\left(\frac{1}{\ln^2 t}\right) \right], \quad (4.63)$$

with D is being the diffusion constant of the underlying random walk ($D = 1/4$ for the standard case of n.n., square lattice walks, when each spin is updated on average once per unit of time).

Simulating general, Z_2 symmetric spin-flip rules in 2d Drnic et al. [83] conjectured that all critical Z_2 -symmetric rules without bulk noise form a co-dimension-1 ‘voter-like’ manifold separating order from disorder, characterized by the logarithmic decay of both ρ and m . The critical exponents for this class are summarized in Table 4.5. Furthermore ref. [83] found that

d	β	β'	γ	ν_{\parallel}	ν_{\perp}	Z	δ	η
1	0.0	1	2	2	1	2	1/2	0
2	0.0	1	1	1	1/2	2	1	0

Table 4.5: Critical exponents of VM classes

this Z_2 symmetry is not a necessary condition, the VM behavior can also be observed in systems without bulk fluctuations, where the total magnetization is conserved. Field theoretical understanding of these results are still lacking.

4.3.1 The $2A \rightarrow \emptyset$ (ARW) and $2A \rightarrow A$ models

As it was mentioned in Sect. 4.3 in 1d annihilating random walks and VM are equivalent. In higher dimensions it is not the case (see Sect. 4.5). This simplest reaction-diffusion model (ARW) – in which identical particles follow random walk and annihilate on contact of a pair – is adequately described by mean-field-type equations in $d_c > 2$ dimensions

$$\rho(t) \propto t^{-1} \quad (4.64)$$

but in lower dimensions fluctuations become relevant. Omitting boundary and initial condition terms, the field theoretical action is

$$S = \int d^d x dt [\psi(\partial_t \phi - D\nabla^2 \phi) - \lambda(1 - \psi^2)\phi^2] \quad (4.65)$$

where, D denotes the diffusion coefficient, λ is the annihilation rate.

For $d = d_c = 2$ the leading order decay of ARW was found exactly by RG field theory [322]:

$$\rho(t) = \frac{1}{8\pi D} \ln(t)/t + O(1/t) \quad (4.66)$$

For $d = 1$ [323, 324] predicted that the particle density decays as

$$\rho(t) = A_2(Dt)^{-1/2} \quad (4.67)$$

This was confirmed by ϵ expansions and the universal amplitude A_2 is

$$\frac{1}{4\pi} + \frac{2 \ln 8\pi - 5}{16\pi} + O(1) \quad (4.68)$$

The ARW was also shown to be equivalent with the $A + A \rightarrow A$ process by Peliti [325] and renormalization group approach provided universal decay amplitudes to all orders in epsilon expansion. It was also shown [205] that the motion of kinks in the compact version of directed percolation (CDP) [204] and the Glauber-Ising model [11] at the $T = 0$ transition point are also described exactly by (4.67).

4.3.2 Compact DP (CDP) with spatial boundary conditions

By introducing a wall in CDP, the survival probability is altered and one obtains surface critical exponents just as for DP. With **IBC**, the cluster is free to approach and leave the wall, but not cross. For $d = 1$, this gives rise to $\beta'_1 = 2$.

On the other hand, for **ABC**, the cluster is stuck to the wall and therefore described by a single random walker for $d = 1$. By reflection in the wall, this may be viewed as *symmetric* compact DP which has the same β' as normal compact DP, giving $\beta'_1 = 1$ [206, 207].

4.3.3 CDP with parabolic boundary conditions

Cluster simulations in 1+1 d and MF approximations [329, 330] for CDP confined by repulsive parabolic boundary condition of the form $x = \pm Ct^\sigma$ found C dependent δ and η exponents (see Fig.4.10) similarly to the DP case (see Sect. 4.1.5) in case of marginal condition: $\sigma = 1/2$. In the

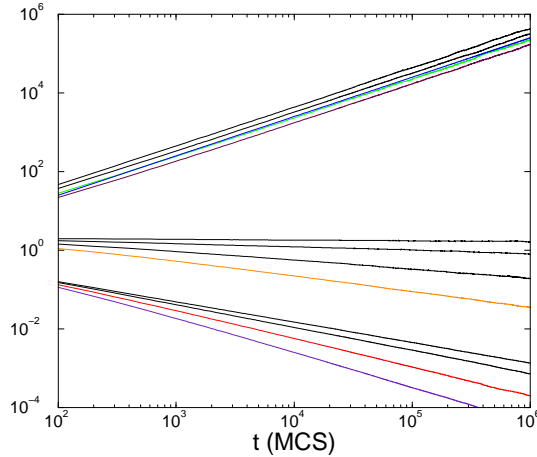


Figure 4.10: Parabola boundary confinement cluster simulations for CDP [329]. Middle curves: number of active sites ($C = 2, 1.5, 1.2, 1$ top to bottom); Lower curves: survival probability ($C = 2, 1.5, 1.2, 1$ top to bottom); Upper curves: $R^2(t)$ ($C = 2, 1.5, 1.2, 1$ top to bottom).

mean-field approximations [329] similar results were obtained as in case of DP ([296]). Analytical results can be obtained only in limiting cases. For narrow systems (small C) one obtains the following asymptotic behaviour for the connectedness function to the origin:

$$P(t, x) \sim t^{-\pi^2/8C^2} \cos\left(\frac{\pi x}{2C\sqrt{t}}\right). \quad (4.69)$$

Analytical solution was found for a related problem [330]. For a one-dimensional lattice random walk with an absorbing boundary at the origin and a movable partial reflector (with probability r) δ varies continuously between 1/2 and 1 as r varies between 0 and 1.

4.3.4 Lévy flight anomalous diffusion in ARW-s

Particles performing simple random walks subject to the reactions $A+B \rightarrow \emptyset$ (Sect.4.3.1) and $A+A \rightarrow \emptyset$ (Sect.5.1) in the presence of a quenched velocity field were investigated in [141]. The effect of the quenched velocity field is then to enhance diffusion in such a way that the effective action of the velocity field is reproduced if Lévy flights are substituted for the simple random walk motion. In the above mentioned reactions the time decay of the particle density is algebraic with an exponent related to that of the step length distribution of the Lévy flights defined in Eq. (4.32). These results have been confirmed by several renormalization group calculations [142, 143].

The anomalous $A+A \rightarrow \emptyset$ process was investigated by field theory [140]. The action of the model is

$$S[\bar{\psi}, \psi] = \int d^d x dt \left\{ \bar{\psi}(\partial_t - D_N \nabla^2 - D_A \nabla^\sigma) \psi + 2\lambda \bar{\psi} \psi^2 + \lambda \bar{\psi}^2 \psi^2 - n_0 \bar{\psi} \delta(t) \right\}, \quad (4.70)$$

where n_0 is the initial (homogeneous) density at $t = 0$. The density decay for $\sigma < 2$ as :

$$n(t) \sim \begin{cases} t^{-d/\sigma} & \text{for } d < \sigma, \\ t^{-1} \ln t & \text{for } d = d_c = \sigma, \\ t^{-1} & \text{for } d > \sigma. \end{cases} \quad (4.71)$$

The results of the simulations of the corresponding 1+1 d lattice model [140] are shown on Fig. 4.11. It was also shown in [140] that Lévy flight **annihilation and coagulation processes** ($A+A \rightarrow A$) are in the same universality class.

4.4 Parity conserving (PC) classes

This class appears among 1+1 d single component reaction-diffusion models. Although it is usually named parity conserving class (PC) examples have proved that the parity conservation itself is not enough condition for the PC class behavior. For example in [336] a 1d stochastic cellular automaton with a global parity conservation was shown to exhibit DP class

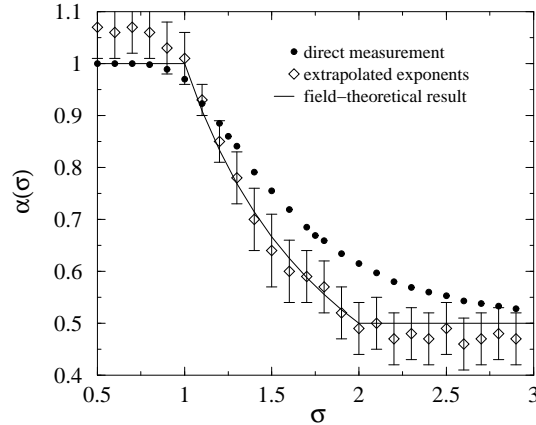


Figure 4.11: The anomalous annihilation process: the graph from [140] shows direct estimates and extrapolations for the decay exponent α , as a function of σ . The solid line represents the exact result (neglecting log corrections at $\sigma = 1$).

transition. Binary spreading process (see Sect.5.5) in one [337] and two dimensions [338] were also found to be insensitive whether parity conservation is present or not. Multi-component BARW models in 1d (see Sect.5.10) generate different robust classes again, where the parity conservation is irrelevant. [193, 340, 203]. Up to now it is known that the BARW2 dynamics in **single-component, single-absorbing** state systems (without inhomogeneities, long-range interactions and other symmetries) provides enough condition for PC class [193]. In **single-component, multi-absorbing** state systems the Z_2 symmetry ensures necessary but not enough condition. By defining the domain walls (kinks) in these systems as particles of a reaction-diffusion system the BARW2 dynamics (Sect.4.4.2) is a necessary condition too. Some studies have shown [341, 196, 342] that an external field that destroys the Z_2 symmetry of absorbing states (but preserves the the BARW2 dynamics) leaves DP instead of PC class transition in the system. Some other names for this class are also used, like directed Ising (DI) class, or BARW class (see sections below).

4.4.1 Grassberger's A and B model

The first models where non-DP class transition can be found were two 1d stochastic cellular automata designed by Grassberger [194]. The “**B**”

model defined by the following rules (I show the configurations at $t - 1$ and the probability of getting '1' at time t):

$$\begin{array}{rcccccccc} \text{t-1:} & 100 & 001 & 101 & 110 & 011 & 111 & 000 & 010 \\ \text{t:} & 1 & 1 & 1 & p & p & 0 & 0 & 0 \end{array}$$

The time evolution pattern for $p = 0$ is a regular chess-board in $1 + 1$ dimensions (rule-50 with double degeneration according to Wolfram's classification of CA [274]). In the $p = 1$ limit we get the deterministic Rule-122, which is known to be chaotic. If we consider the '00' and '11' pairs as the 'particles' or 'kinks' they obey parity conservation. For $p < p_c (= 0.539(1))$ the kinks disappear with an ARW mechanism (Sect. 4.3.1), the corresponding absorbing state is a Z_2 symmetric doublet. For $p > p_c$ they survive with a finite concentration. At $p = 0.539(1)$ a continuous transition takes place in terms of the kink density order parameter with PC class exponents.

The **DS transition** of this model happens at $p_d > p_c$, in the active phase where the symmetry of replicas is broken. In accordance with this a DP class DS behavior was observed [253].

The "**A**" **model** is similarly defined by the transitions:

$$\begin{array}{rcccccccc} \text{t-1:} & 100 & 001 & 101 & 110 & 011 & 111 & 000 & 010 \\ \text{t:} & 1 & 1 & 0 & 1-p & 1-p & 0 & 0 & 1 \end{array}$$

For $p = 0$ it is the Rule-94, class 1 CA, while the $p = 1$ limit is the chaotic Rule-22 deterministic CA. The time evolution pattern in $1 + 1$ dimension, for small p evolves towards a stripe-like ordered steady state (with double degeneration), while for $p > p_c(0.1245(5))$ the kinks (the '00' and '11' pairs) survive. In the absorbing state the system oscillates between the states:

$$\begin{array}{r} \text{t-1:} & 1010101010101010101010101010101 \\ \text{t:} & 0101010101010101010101010101010 \end{array}$$

The critical exponents estimated by simulations for these models [349] were $\delta = 0.283 \pm 0.16$, $\beta = 0.94 \pm 0.06$, $\nu_{||} = 3.3(2)$. Note that in the fully synchronous version of these SCA the occurrence of BARW2 kink dynamics is not obvious.

The **DS transition** of this model coincides with p_c and the DS scaling behavior is PC class type [253].

4.4.2 Branching and annihilating random walks with even number of offsprings

BARW models – introduced in Sect. 4.1.3 – with $k = 2$ and even number (m) of offsprings (BARWe) conserve the particle number mod 2 [350, 351,

352, 353, 354, 192]. That means that there are two distinct sectors of this model, an odd and an even parity one. In the even sector the particles finally can die out ($\delta \neq 0, \eta = 0$) while in the odd one at least one particle always remain alive ($\delta = 0, \eta \neq 0$). BARW2 systems may also appear in multi-component models exhibiting Z_2 symmetric absorbing states in terms of the kinks between ordered domains. Such systems are the NEKIM (Sect. 4.4.3) and GDK models (Sect. 4.4.4) for example. It was conjectured [344] that in all models with Z_2 symmetric absorbing states an underlying BARWe process is a necessary condition for transitions with PC criticality. Sometimes it is not so easy to find the underlying BARWe process and can be seen on the coarse grained level only (see example the GDK model where the kinks are spatially extended objects) that might have lead some studies to the conjecture that the Z_2 symmetry is a sufficient condition for the PC class [343]. However the example of CDP (see Sect.4.3) shows that this can not be true. The field theory of BARWe models have been investigated by Cardy and Täuber [193]. For this case the action

$$S = \int d^d x dt [\psi(\partial_t - D\nabla^2)\phi - \lambda(1 - \psi^2)\phi^2 + \sigma(1 - \psi^2)\psi\phi] \quad (4.72)$$

is invariant under the simultaneous transformation of fields

$$\psi \leftrightarrow -\psi, \quad \phi \leftrightarrow -\phi \quad (4.73)$$

Owing to the non-recurrence of random walks in $d \geq 2$ the system is in the active phase for $\sigma > 0$ and mean-field type transition occurs with $\beta = 1$. However the survival probability of a particle cluster is finite for any $\sigma > 0$ implying $\beta' = 0$. Hence unlike the DP case $\beta \neq \beta'$ for $d \geq 2$. At $d = 2$ random walks are barely recurrent and logarithmic corrections can be found. In this case the generalized hyperscaling law [247] is valid among the exponents

$$2 \left(1 + \frac{\beta}{\beta'}\right) \delta' + 2\eta' = dz. \quad (4.74)$$

In $d = 1$ however $\beta = \beta'$ holds owing to an exact duality mapping [345] and the hyperscaling is the same that of the DP (eq. 4.10).

The RG analysis of BARWe for $d < 2$ run into difficulties. These stem from, the presence of an other critical dimension $d'_c = 4/3$ (above which the branching reaction is relevant at $\sigma = 0$, and irrelevant there for $d < d'_c$) hence the $d = 1$ dimension cannot be accessed by controlled expansions from $d_c = 2$. The truncated one-loop expansions [193] for $d = 1$ resulted in

$$\beta = 4/7, \quad \nu_{||} = 3/7, \quad \nu_{\perp} = 7/17, \quad Z = 2 \quad (4.75)$$

d	β	β'	γ	δ	Z	$\nu_{ }$	η
1	0.92(3)	0.92(3)	0.00(5)	0.285(2)	1.75	3.25(10)	0.000(1)
2	1	0	1	0	2	1	-1/2

Table 4.6: Critical exponents of BARWe.

which are quite far from the numerical values determined by Jensen's simulations [192] (Table 4.6). Here cluster exponent values δ and η corresponding to even number of initial particles are shown. In case of odd number of initial particles they swap values.

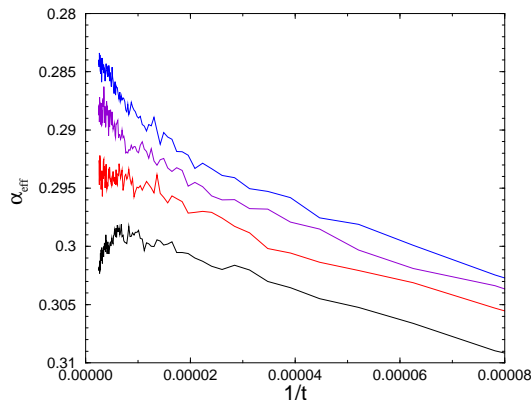


Figure 4.12: Local slopes (4.13) of the density decay in a bosonic BARW2 model. Different curves correspond to $\sigma = 0.466, 0.468, 0.469, 0.47$ (from bottom to top) [285].

It was conjectured [284] that in 1d fermionic (single occupancy) and bosonic (multiple occupancy) models may have different critical behavior. Since only bosonic field theory exists that gives rather inaccurate critical exponent estimates in [285] bosonic simulations were performed to investigate the density decay of BARW2 from random initial state. Figure 4.12 shows the local slopes of density decay (α_{eff} (4.13)) around the critical point for several branching rates (σ). The critical point is estimated at $\sigma_c = 0.04685(5)$, with the corresponding decay exponent $\alpha = 0.290(3)$. This value agrees with that of the PC class again $0.285(2)$ [192].

If there is no explicit diffusion of particles besides the $AA \rightarrow \emptyset$, $A \rightarrow 3A$ (DBAP) process following the Subury's naming [346]) an implicit diffusion

can still be generated. By spatially asymmetric branching: $A\emptyset\emptyset \rightarrow AAA$, $\emptyset\emptyset A \rightarrow AAA$ this diffusion may happen by two lattice steps only: $A\emptyset\emptyset \rightarrow AAA \rightarrow \emptyset\emptyset A$. As the consequence the decay process slows down, a single particle can't join a domain, hence the domain sizes exhibit a parity conservation. This results in additional new sectors (besides the existing two BARW2 sectors) that depend on the initial conditions. For example in case of random initial distribution $\delta \sim 0.13(1)$ was measured by simulations [347]. Similar sector decomposition has been observed in diffusion of k -mer models (see for example M. Barma and co-workers [348]).

4.4.3 The NEKIM model

Nonequilibrium kinetic Ising models, in which the steady state is produced by kinetic processes in connection with heat baths at different temperatures have been widely investigated [355, 72, 356, 357] and results have shown that different phase transitions even in 1d are possible under nonequilibrium conditions (for a review see Rácz Z. in [62]). In short ranged interaction models any non-zero temperature spin-flip dynamics cause disordered steady state. A class of general nonequilibrium kinetic Ising models (NEKIM) with combined spin flip dynamics at $T = 0$ and Kawasaki spin exchange dynamics at $T = \infty$ has been proposed by Menyhárd [195] in which, for a range of parameters of the model, a PC-type transition takes place.

A general form of the Glauber spin-flip transition rate in one-dimension for spin s_i sitting at site i is [11] ($s_i = \pm 1$):

$$W_i = \frac{\Gamma}{2}(1 + \tilde{\delta}s_{i-1}s_{i+1}) \left(1 - \frac{\tilde{\gamma}}{2}s_i(s_{i-1} + s_{i+1})\right) \quad (4.76)$$

where $\tilde{\gamma} = \tanh 2J/kT$, with J denoting the coupling constant in the ferromagnetic Ising Hamiltonian, Γ and $\tilde{\delta}$ are further parameters which can, in general, also depend on temperature. The Glauber model is a special case corresponding to $\tilde{\delta} = 0$, $\Gamma = 1$. There are three independent rates:

$$\begin{aligned} w_{same} &= \frac{\Gamma}{2}(1 + \tilde{\delta})(1 - \tilde{\gamma}) \\ w_{oppo} &= \frac{\Gamma}{2}(1 + \tilde{\delta})(1 + \tilde{\gamma}) \\ w_{indif} &= \frac{\Gamma}{2}(1 - \tilde{\delta}), \end{aligned} \quad (4.77)$$

where the suffices *same* etc. indicate the three possible neighborhoods of a given spin ($\uparrow\uparrow\uparrow$, $\downarrow\uparrow\downarrow$ and $\uparrow\uparrow\downarrow$, respectively). In the following $T = 0$ will be

taken, thus $\tilde{\gamma} = 1$, $w_{same} = 0$ and Γ , $\tilde{\delta}$ are constants to be varied.

The Kawasaki spin-exchange transition rate of neighbouring spins is:

$$w_{ii+1}(s_i, s_{i+1}) = \frac{p_{ex}}{2}(1 - s_i s_{i+1}) \left[1 - \frac{\tilde{\gamma}}{2}(s_{i-1} s_i + s_{i+1} s_{i+2}) \right]. \quad (4.78)$$

At $T = \infty$ ($\tilde{\gamma} = 0$) the above exchange is simply an unconditional nearest neighbor exchange:

$$w_{ii+1} = \frac{1}{2} p_{ex} [1 - s_i s_{i+1}] \quad (4.79)$$

where p_{ex} is the probability of spin exchange.

The transition probabilities in eqs.(4.76) and (4.79) are responsible for basic elementary processes of kinks. Kinks separating two ferromagnetically ordered domains can carry out random walks with probability

$$p_{rw} \propto 2w_{indif} = \Gamma(1 - \tilde{\delta}) \quad (4.80)$$

while two kinks getting into neighbouring positions will annihilate with probability

$$p_{an} \propto w_{oppo} = \Gamma(1 + \tilde{\delta}) \quad (4.81)$$

(w_{same} is responsible for creation of kink pairs inside of ordered domains at $T \neq 0$). In case of the spin exchanges, which act only at domain boundaries, the process of main importance here is that a kink can produce two offsprings by the next time step with probability

$$p_{k \rightarrow 3k} \propto p_{ex}. \quad (4.82)$$

The abovementioned three processes compete, and it depends on the values of the parameters Γ , $\tilde{\delta}$ and p_{ex} what the result of this competition will be. It is important to realize that the process $K \rightarrow 3K$ can develop into propagating offspring production only if $p_{rw} > p_{an}$, i.e. the new kinks are able to travel on the average some lattice points away from their place of birth and can thus avoid immediate annihilation. It is seen from the above definitions that $\tilde{\delta} < 0$ is necessary for this to happen. In the opposite case the only effect of the $K \rightarrow 3K$ process on the usual Ising kinetics is to soften domain walls. In the NEKIM model investigations the normalization condition $p_{rw} + p_{an} + p_{k \rightarrow 3k} = 1$ was set.

The phase diagram determined by simulations and GMF calculations [21, 344] is shown on Fig. 4.13. The line of phase transitions separates two kinds of steady states reachable by the system for large times: in the Ising phase, supposing that an even number of kinks are present in the initial

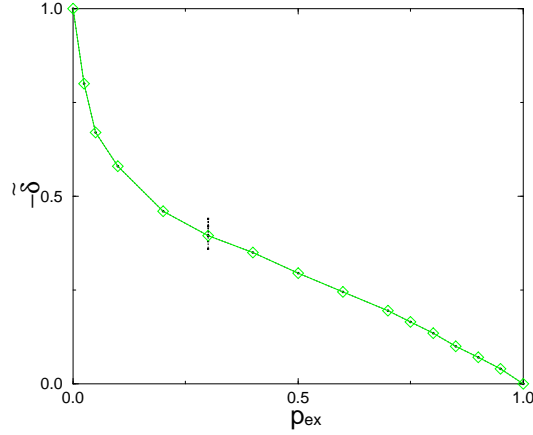


Figure 4.13: Phase diagram of the two-parameter model. The transversal dotted line indicates the critical point that was investigated in more detail [344].

states, the system orders in one of the possible ferromagnetic states of all spins up or all spins down, while the active phase is disordered from the point of view of the underlying spins. The cause of disorder is the steadily growing number of kinks with time. While the low-level, $N = 1, 2$ GMF solutions exhibit first order transitions for $N > 2$ this becomes continuous. The GMF approximations (up to $N = 6$) with CAM extrapolation found $\beta \simeq 1$ [21]. Recent high precision Monte Carlo simulations [344] resulted in critical exponents $\beta = 0.95(2)$ (see Fig. 4.14) and $\delta = 0.280(5)$ at the dotted line of the phase diagram.

Mussawisade et al. [345] have shown that exact duality mapping exist in the phase diagram of the NEKIM:

$$\begin{aligned} p'_{an} &= p_{an}, \\ p'_{rw} &= p_{an} + 2p_{ex}, \\ 2p'_{ex} &= p_{rw} - p_{an}. \end{aligned} \tag{4.83}$$

The regions mapped onto each other have, of course, the same physical properties. In particular, the line $p_{ex} = 0$ maps onto the line $p_{rw} = p_{an}$ and the fast-diffusion limit to the limit $p_{ex} \rightarrow \infty$. There is a self-dual line

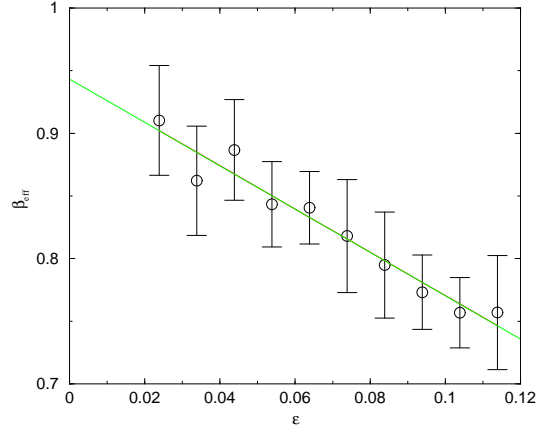


Figure 4.14: $\beta_{eff} = \frac{d \log n_{\infty}}{d \log \epsilon}$ (circles) near the critical point ($\epsilon = |\tilde{\delta} - \tilde{\delta}'|$) and linear extrapolation (dashed line) to the asymptotic value ($\beta = 0.95(2)$). Simulations were performed on a 1d NEKIM ring of size $L = 24000$ [344].

at

$$\tilde{\delta} = \frac{-2p_{ex}}{1 - p_{ex}} \quad . \quad (4.84)$$

By various static and dynamical simulations spin and kink density critical exponents have been determined in [251] and as the consequence of the generalized hyperscaling law for the structure factor

$$S(0, t) = L[\langle M^2 \rangle - \langle M \rangle^2] \propto t^x, \quad (4.85)$$

and kink density

$$n(t) = \frac{1}{L} \langle \sum_i \frac{1}{2} (1 - s_i s_{i+1}) \rangle \propto t^{-y} \quad (4.86)$$

the exponent relation

$$2y = x \quad (4.87)$$

is established. Spins-clusters at the PC point grow by compact domains as in the Glauber point albeit with different exponents [12]. The spin-cluster critical exponents in magnetic field were summarized in Table (2). The global persistence (θ_g) and time autocorrelation exponents (λ) were determined both at the Glauber an at the PC critical points [32] and are shown in Table (4.7). While at the Glauber point the scaling law (1.17) is

	β_s	γ_s	$\nu_{\perp,s}$	Z	θ_g	λ_s
Glauber-Ising	0	1/2	1/2	2	1/4	1
PC	.00(1)	.444(2)	.444(2)	1.75(1)	.67(1)	1.50(2)

Table 4.7: Simulation data for static and dynamic critical spin exponents for NEKIM.

satisfied by these exponents it is not the case at PC criticality, therefore the magnetization is non-Markovian process here.

By applying an external magnetic field h that breaks the Z_2 symmetry the transition type of the model changes to DP type (see Table 4.8). [251]

h	0.0	0.01	0.05	0.08	0.1	DP
β	1.0	0.281	0.270	0.258	0.285	0.2767(4)
γ		0.674	0.428	0.622	0.551	0.5438(13)

Table 4.8: CAM estimates for the kink density and its fluctuation exponents.

A generalization is the probabilistic cellular automaton version of NEKIM, which consists in keeping the spin-flip rates given in eqs.(4.77) and prescribing *synchronous updating*. In this case the $K \rightarrow 3K$ branching is generated without the need of additional, explicit spin-exchange process and for certain values of parameter-pairs $(\Gamma, \tilde{\delta})$ with $\tilde{\delta} < 0$ PC-type transition takes place. The phase boundary of NEKIM-CA in the $(\Gamma, -\tilde{\delta})$ plane is similar to that on Fig. 4.13 except for the highest value of $\Gamma = 1$, $\tilde{\delta}_c = 0$ can not be reached, the limiting value is $\tilde{\delta}_c = -.065$.

An other possible variant of NEKIM was introduced in [344] in which the Kawasaki rate eq.(4.78) is considered at some finite temperature, instead of $T = \infty$, but keeping $T = 0$ in the Glauber-part of the rule. As lowering the temperature of the spin exchange process acts against kink production, the result is that the active phase part of the phase diagram shrinks. For more details see ([252]).

The **DS transition** of this model was found to coincide with the critical point and the scaling behavior of spin and kink damages is the same as that of the corresponding NEKIM variables [253].

4.4.4 The Generalized DK model

A generalization of the Domany-Kinzel stochastic cellular automaton [205] (see Section 4.1.2) was introduced by Hinrichsen (GDK) [199]. This model has $n + 1$ states per site: one active state Ac and n different inactive states I_1, I_2, \dots, I_n . The conditional updating probabilities are given by ($k, l = 1, \dots, n; k \neq l$)

$$P(I_k | I_k, I_k) = 1, \quad (4.88)$$

$$P(Ac | Ac, Ac) = 1 - n P(I_k | Ac, Ac) = q, \quad (4.89)$$

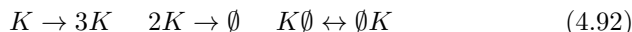
$$P(Ac | I_k, Ac) = P(A | A, I_k) = p_k, \quad (4.90)$$

$$P(I_k | I_k, Ac) = P(I_k | Ac, I_k) = 1 - p_k,$$

$$P(Ac | I_k, I_l) = 1, \quad (4.91)$$

and the symmetric case $p_1, \dots, p_n = p$ was explored. Equations (4.88)–(4.90) are straightforward generalizations of Eqs. (4.17)–(4.19). The only different process is the creation of active sites between two inactive domains of different colors in Eq. (4.91). For simplicity the probability of this process was chosen to be equal to one.

For $n = 1$ the model defined above reduces to the original Domany-Kinzel model. For $n = 2$ it has two Z_2 symmetrical absorbing states. The phase diagram of this model (Fig. 4.15) is very similar to that of the DK model (Fig. 4.5) except the transition line is PC type. If we call the regions separating inactive domains I_1 and I_2 as domain walls (denoted by K), they follow BARW2 process



but for $1 > q > 0$ the size of active regions, hence the domain walls stays finite. Therefore a the observation of the BARW2 process is not so obvious and can be done on coarse grained level only (except at point “C” where active sites really look like kinks of the NEKIM model). The symmetrical endpoint “A” ($q = 1, p = \frac{1}{2}$) again shows different scaling behavior (here three types of compact domains grow in competition, the boundaries perform annihilating random walks with exclusion (see. Section 5.2). Series expansions for the transition point and for the order parameter critical exponent resulted in $\beta = 1.00(5)$ [200] that is slightly higher than the most precise simulation results [344] but agrees with the GMF+CAM estimates [21].

Models with $n > 3$ symmetric absorbing states in 1d do not show phase transitions (they are always active). In terms of domain walls as particles they are related with $N > 1$ component N-BARW2 processes that exhibit

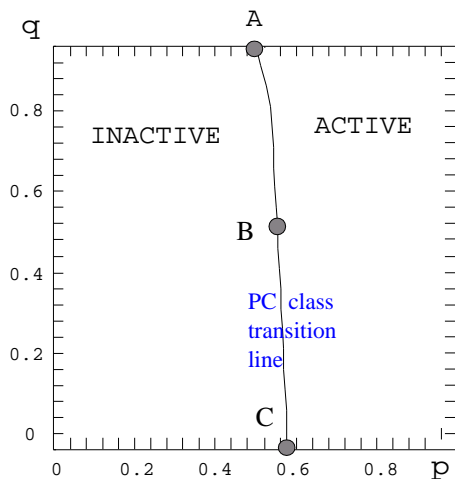


Figure 4.15: The phase diagram of the $n = 2$ GDK model [199].

phase transition for zero branching rate only (see Sect.5.10) [193, 203]. Similarly to the NEKIM model the application of external symmetry breaking field changes the PC class transition into a DP class one [199].

GDK type models – exhibiting n symmetric absorbing states – can be generalized to higher dimensions. In two dimensions Hinrichsen’s spreading simulations for the $n = 2$ case found mean-field like behavior with $\delta = 1$, $\eta = 0$ and $z = 1$ and conjectured that $1 < d_c < 2$. A similar model exhibiting Potts-like dynamics with Z_n symmetric absorbing states in 2d reported similar spreading exponents but a first order transition ($\beta = \alpha = 0$) [85]. In three dimensions the same model seems to exhibit mean-field like transition with $\beta = 1$. The verification of these findings would require further research.

4.4.5 PC class surface catalytic models

In this subsection I shall discuss some 1d surface catalytic-type reaction-diffusion models exhibiting PC class transition. Strictly speaking they are multi-component models, but I show that the symmetries among species enables to describe the domain-wall dynamics by simple BARW2 process.

The two-species monomer-monomer (MM) model was first introduced by [86]. Two monomers, called A and B , adsorb at the vacant sites of a one-dimensional lattice with probabilities p and q , respectively, where $p + q = 1$. The adsorption of a monomer at a vacant site is affected by monomers

present on neighboring sites. If either neighboring site is occupied by the same species as that trying to adsorb, the adsorption probability is reduced by a factor $r < 1$, mimicking the effect of a nearest-neighbor repulsive interaction. Unlike monomers on adjacent sites react immediately and leave the lattice, leading to a process limited only by adsorption. The basic reactions are



The phase diagram, displayed in Fig. 4.16 with p plotted *vs.* r , shows a reactive steady state (R) containing vacancies bordered by two equivalent saturated phases (labeled A and B). The transitions from the reactive

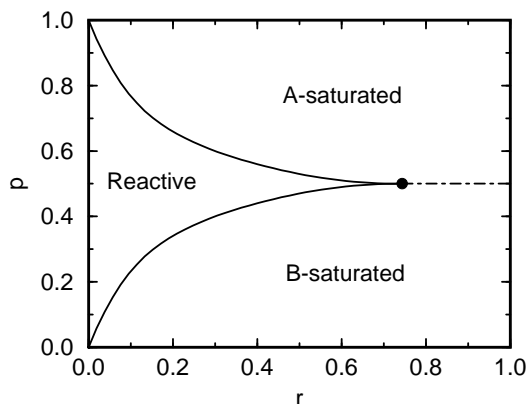


Figure 4.16: Phase diagram of the MM from [88].

phase to either of the saturated phases are continuous, while the transition between the saturated phases is first-order discontinuous. The two saturated phases meet the reactive phase at a *bi-critical* point at a critical value of $r = r_c$. In the case of $r = 1$, the reactive region no longer exists and the only transition line is the first-order discontinuous line between the saturated phases. Considering the density of vacancies between unlike species as the order parameter (that can also be called a species “C”) the model is the so called “three species monomer-monomer model”. Simulations and cluster mean-field approximations were applied to investigate the phase transitions of these models [198, 87, 88, 89]. As Fig.4.17 shows if we call the extended objects filled with vacancies between different species as domain-walls (C) we can observe $C \rightarrow 3C$ and $2C \rightarrow \emptyset$ BARW2 processes in terms of them. These C parity conserving processes arise as the combination of the elementary reaction steps (4.93). The reactions always take

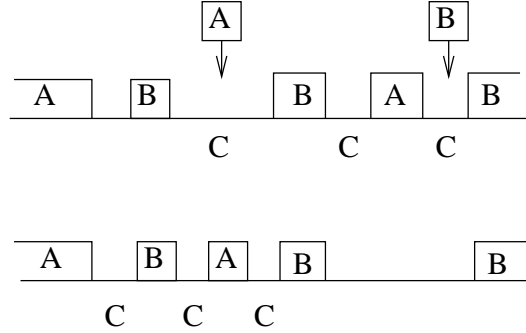


Figure 4.17: Domain-wall dynamics in the interacting monomer-monomer model. Left part: branching; right part: annihilation

place at domain boundaries, hence the Z_2 symmetric A and B saturated phases are absorbing.

The interacting monomer-dimer model (IMD) [197] is a generalization of the simple monomer-dimer model [4], in which particles of the same species have nearest-neighbor repulsive interactions. This is parameterized by specifying that a monomer (A) can adsorb at a nearest-neighbor site of an already-adsorbed monomer (restricted vacancy) at a rate $r_A k_A$ with $0 \leq r_A \leq 1$, where k_A is an adsorption rate of a monomer at a free vacant site with no adjacent monomer-occupied sites. Similarly, a dimer (B_2) can adsorb at a pair of restricted vacancies (B in nearest-neighbor sites) at a rate $r_B k_B$ with $0 \leq r_B \leq 1$, where k_B is an adsorption rate of a dimer at a pair of free vacancies. There are no nearest-neighbor restrictions in adsorbing particles of different species and the $AB \rightarrow \emptyset$ desorption reaction happens with probability 1. The case $r_A = r_B = 1$ corresponds to the ordinary noninteracting monomer-dimer model which exhibits a first-order phase transition between two saturated phases in one dimension. In the other limiting case $r_A = r_B = 0$, there exists no fully saturated phase of monomers or dimers. However, this does not mean that this model has no absorbing states any more. In fact, there are two equivalent (Z_2 symmetric) absorbing states in this model. These states comprise of only the monomers at the odd- or even-numbered lattice sites. There needs a pair of adjacent vacancies for a dimer to adsorb, so a state with alternating sites occupied by monomers can be identified with an absorbing state. The PC class phase transition of the $r_A = r_B = 0$ infinite repulsive case has been investigated in [197, 90, 248, 91, 342]. As one can see the basic reactions are similar to those of the MM model (eq. (4.93)) but the order parameter here is the density of dimers (K) that may appear between ordered domains of alternating

sequences: '0A0..A0A.' and 'A0A..0A0', where monomers are on even or odd sites only. The recognition of an underlying BARW2 process (4.92) is not so easy in this case, still considering regions between odd and even filled ordered domains one can identify domain wall random-walk, annihilation and branching processes through the reactions with dimers as one can see on the examples below. The introduction of Z_2 symmetry-breaking field, that makes the system prefer one absorbing state to the other was shown to change that transition type from PC to DP [248].

t	A 0 A 0 A 0 A 0 A 0 A 0 A 0 A 0 A 0 A	K
t+1	A 0 A 0 A 0 A 0 A B B A 0 A 0 A 0 A	K
t+2	A 0 A 0 A 0 A 0 0 0 B A 0 A 0 A 0 A	K K K
t	A 0 A 0 A 0 A 0 A 0 0 0 A 0 A 0 A 0	K K
t+1	A 0 A 0 A 0 A 0 A 0 A 0 A 0 A 0 A 0	

4.4.6 NEKIM with long-range correlated initial conditions

In case of the NEKIM model (see Sect. 4.4.3) simulations [252, 344] found that the density of kinks $\rho_k(t)$ change as

$$\rho_k(t) \propto t^{\kappa(\sigma)} \quad (4.94)$$

by starting the system with long-range correlated kink distributions of the form (4.41) and $\kappa(\sigma)$ changes linearly between the two extremes $\beta/\nu_{||} = \pm 0.285$ shown on Fig. 4.18. This behavior is similar to the DP case (Sect. 4.1.7) but here one can observe a symmetry:

$$\sigma \leftrightarrow 1 - \sigma, \quad \kappa \leftrightarrow -\kappa \quad (4.95)$$

that is probably related to the duality symmetry of the NEKIM model (4.83).

4.4.7 GDK with spatial boundary conditions

The surface critical behavior of the PC class GDK model (Sect. 4.4.4) has been explored by [249, 294, 250]. The basic idea is that on the surface one may include not only the usual BARW2 reactions (4.92) but potentially also a parity symmetry breaking $A \rightarrow \emptyset$ reaction. Depending on whether or not the $A \rightarrow \emptyset$ reaction is actually present, we may then expect different boundary universality classes according to whether the symmetry of the bulk is broken or respected at the surface. Since the time reversal symmetry

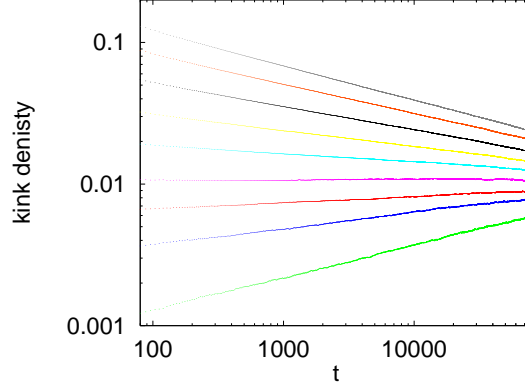


Figure 4.18: $\log(\rho_k(t))$ versus $\log(t)$ in NEKIM simulations for $\sigma = 0, 0.1, 0.2, \dots, 1$ initial conditions (from bottom to top curves) [344].

(4.8) is broken for BARW2 processes two independent exponents ($\beta_{1,\text{seed}}, \beta_{1,\text{dens}}$) characterize the surface critical behavior.

The surface phase diagram for the mean field theory of BARW (valid for $d > d_c = 2$) is shown in Fig. 4.19. Here σ_m, σ_{m_s} are the rates for the branching processes $A \rightarrow (m+1)A$ in the bulk and at the surface, respectively, and μ_s is the rate for the surface spontaneous annihilation reaction $A \rightarrow \emptyset$. Otherwise, the labeling is the same as that for the DP phase diagram (see Figure 4.6). The $\mu_s > 0$ corresponds to the parity symmetry breaking RBC.

For $\mu_s = 0$ (IBC) parity conserving case the surface action is of the form

$$S_s = \int d^{d-1}x_{\parallel} \int_0^{\tau} dt \left(\sum_{l=1}^{m/2} \sigma_{2l_s} (1 - \psi_s^{2l}) \psi_s \phi_s \right), \quad (4.96)$$

where $\psi_s = \psi(\mathbf{x}_{\parallel}, x_{\perp} = 0, t)$ and $\phi_s = \phi(\mathbf{x}_{\parallel}, x_{\perp} = 0, t)$. In $d = 1$ the boundary and bulk transitions inaccessible to controlled perturbative expansions, but scaling analysis shows that surface branching is *irrelevant* leading to the Sp* and Sp special transitions. For $\mu_s > 0$ (RBC) parity symmetry breaking case the surface action is

$$S_2 = \int d^{d-1}x_{\parallel} \int_0^{\tau} dt \left(\sum_{l=1}^m \sigma_{l_s} (1 - \psi_s^l) \psi_s \phi_s + \mu_s (\psi_s - 1) \phi_s \right). \quad (4.97)$$

and RG procedure shows that the stable fixed point corresponds to the ordinary transition. Therefore in 1d the phase diagram looks very differ-

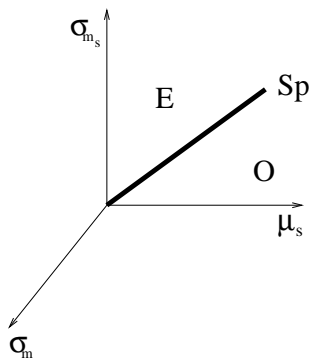


Figure 4.19: Schematic mean field boundary phase diagram for BARW from [250]. See text for an explanation of the labeling.

ently from the mean-field case (Fig. 4.20). One can differentiate two cases corresponding to (a) the annihilation fixed point of the bulk and (b) the PC critical point of the bulk. As one can see in both cases the ordinary transition (O, O^*) corresponds to $\mu_s > 0$, RBC and the special transitions (Sp, Sp^*) to $\mu_s = 0$, IBC. The ABC condition obviously behaves as if there existed a surface reaction equivalent to $\emptyset \rightarrow A$, and thus it belongs to the normal transition universality class. By scaling considerations the following scaling relations can be derived:

$$\tau_1 = \nu_{||} - \beta_{1,\text{dens}} \quad , \quad (4.98)$$

$$\nu_{||} + d\nu_{\perp} = \beta_{1,\text{seed}} + \beta_{\text{dens}} + \gamma_1. \quad (4.99)$$

In [294] Howard et al showed that on the self-dual line of the 1d BARWe model (see Sect. 4.4.3 and [345]) the scaling relations between exponents of ordinary and special transitions

$$\beta_{1,\text{seed}}^O = \beta_{1,\text{dens}}^{\text{Sp}} \quad (4.100)$$

and

$$\beta_{1,\text{seed}}^{\text{Sp}} = \beta_{1,\text{dens}}^O. \quad (4.101)$$

hold. Relying on universality they claim that they should be valid elsewhere close to the transition line. Numerical simulations support this hypothesis as shown on Table 4.9.

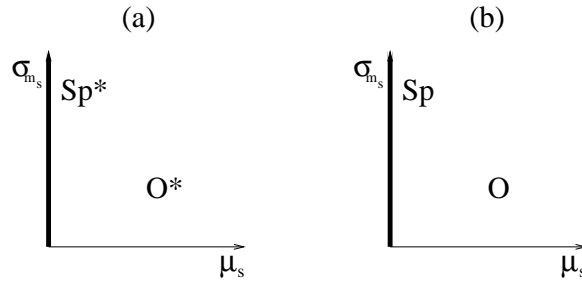


Figure 4.20: Schematic surface phase diagrams for BARW in $d = 1$ for (a) $\sigma_m < \sigma_{m,\text{critical}}$, and (b) $\sigma_m = \sigma_{m,\text{critical}}$ [250]. See text for an explanation of the labeling.

	$d = 1$ (IBC)	$d = 1$ (RBC)	$d = 2$ (O)	$d = 2$ (Sp)
$\beta_{1,\text{seed}}$	2.06(2)	1.37(2)	0	0
$\beta_{1,\text{dens}}$	1.34(2)	2.04(2)	3/2	1
τ_1	1.16(4)	1.85(4)	1	1
γ_1	2.08(4)	2.77(4)	1/2	1/2

Table 4.9: Critical boundary exponents of the PC class in $d = 1, 2$ for ordinary and special cases.

4.5 Branching with $kA \rightarrow \emptyset$ annihilation

In Sect. 4.3.1 the $2A \rightarrow \emptyset$ model and with the addition of branching in Sects. 4.1.3 and 4.4.2 the BARWo and BARWe classes were already discussed. More generally m -branching and $kA \rightarrow \emptyset$ annihilation type of models exhibiting field theoretical action:

$$S = \int d^d x dt [\psi(\partial_t - D\nabla^2)\phi - \lambda(1 - \psi^k)\phi^k + \sigma(1 - \psi^m)\psi\phi] \quad (4.102)$$

were found to exhibit an upper critical dimension at $d_c = 2/(k-1)$ [322, 193] with the mean-field exponents

$$\alpha = \beta = 1/(k-1), \quad Z = 2, \quad \nu_\perp = 1/2. \quad (4.103)$$

At d_c (which falls below physical dimensions for $k > 3$) the decay has logarithmic corrections:

$$\rho(t) = A_k (\ln(t))^{1/(k-1)}. \quad (4.104)$$

So for the $AAA \rightarrow \emptyset$ process in one dimension this gives the decay behavior [322]:

$$\rho(t) = \left(\frac{1}{4\pi\sqrt{3}D}\right)^{\frac{1}{2}} (\ln(t)/t)^{\frac{1}{2}} + O(t^{\frac{1}{2}}), \quad (4.105)$$

which is the dominant behavior of the 1d bosonic PCPD model at the transition point (see Sect.5.5).

Chapter 5

Multi-component system classes

First I recall some well known results (see refs. in [321]) for multi-component reaction-diffusion systems without particle creation. From the viewpoint of phase transitions these describe the behavior in the inactive phase or in case of some N-BARW models right at the critical point. Then I show the effect of particle exclusions in 1d. Later universal behavior of more complex, coupled multi-component systems are discussed. This field is quite new and some of the results are still under debate.

5.1 The $A + B \rightarrow \emptyset$ classes

The simplest two-component reaction-diffusion model involves two types of particles undergoing diffusive random walks and reacting upon contact to form an inert particle. The action of this model is:

$$S = \int d^d x dt [\psi_A (\partial_t - D_A \nabla^2) \phi_A + \psi_B (\partial_t - D_B \nabla^2) \phi_B - \lambda (1 - \psi_A \psi_B) \phi_A \phi_B] - \rho(0) (\psi_A(0) + \psi_B(0)) \quad (5.1)$$

where D_A and D_B denotes the diffusion constants of species A and B . In $d_c = 4 > d$ dimensions and for homogeneous, initially equal density of A and B particles (ρ_0) the density decays asymptotically as [326, 327]

$$\rho_A(t) = \rho_B(t) \propto C \sqrt{\Delta} t^{-d/4}, \quad (5.2)$$

where $\Delta = \rho(0) - C' \rho^{d/2}(0) + \dots$, C is a universal C' is a non-universal constant. This slow decay behavior is due to the fact that in the course of

the reaction, local fluctuations in the initial distribution of reactants lead to the formation of clusters of like particles that do not react and they will be asymptotically segregated for $d < 4$. The asymptotically dominant process is the diffusive decay of the fluctuations of the initial conditions. Since this is a short ranged process the system has a long-time memory – appearing in the amplitude dependence – for the initial density $\rho(0)$. For $d \leq 2$ controlled RG calculation is not possible, but the result (5.2) gives the leading order term in $\epsilon = 2 - d$ expansion. For $D_A \neq D_B$ case the RG study [327] found new amplitude but the same exponents.

The **persistence** behavior in 1d with equal initial density of particles ($\rho_0 = \rho_A(0) + \rho_B(0)$) and homogeneous initial conditions was studied by [328]. The probability $p(t)$, that an annihilation process has not occurred at a given site (“type I persistence”) has the asymptotic form

$$p(t) \sim \text{const.} + t^{-\theta_I} . \quad (5.3)$$

For a density of particles $\rho \gg 1$, θ_I is identical to that governing the persistence properties of the one-dimensional diffusion equation, where $\theta_I \approx 0.1207$. In the case of an initially low density, $\rho_0 \ll 1$, $\theta_I \approx 1/4$ was found asymptotically. The probability that a site remains unvisited by any random walker (“type II persistence”) was found to decay with a stretched exponential form

$$p(t) \sim \exp(-\text{const.} \times \rho_0^{1/2} t^{1/4}) \quad (5.4)$$

provided $\rho_0 \ll 1$.

5.2 $AA \rightarrow \emptyset, BB \rightarrow \emptyset$ with hard-core repulsion

At the symmetric “A” point of the GDK model (see Sect. 4.4.4) compact domains of $I1$ and $I2$ grow separated by $A = Ac - I1$ and $B = Ac - I2$ kinks that can not penetrate each other. In particle language this system is a reaction-diffusion model of two types $A + A \rightarrow \emptyset, B + B \rightarrow \emptyset$ with exclusion $AB \not\leftrightarrow BA$ and special **pairwise initial conditions** (because the domains are bounded by kinks of the same type):

$$\dots A \dots A \dots B \dots B \dots B \dots B \dots A \dots A \dots$$

In the case of homogeneous, pairwise initial conditions simulations [329] showed a density decay of kinks $\rho \propto t^{-\alpha}$ characterized by a power-law with an exponent larger than $\alpha = 0.5$. The $\alpha = 1/2$ would have been expected in case of two copies of ARW systems that do not exclude each other. Furthermore the deviation of α from 0.5 showed an initial density dependence. Ref. [329] provided a possible explanation based on permutation symmetry

between types, according to which hard-core interactions cause **marginal perturbation** resulting in non-universal scaling. This is in analogy with the CDP confined by parabolic boundary conditions (see Sect.4.3.3) by assuming that the AB, BA pairs exert a parabolic space-time confinement on the coarsening domains. Non-universal scaling can also be observed at surface critical phenomena. Similarly here AB, BA pairs produce 'multi surfaces' in the bulk. However simulations and independent interval approximations on a similar model predict a logarithmic correction of the form : $\rho \sim t^{-1/2}/\ln(t)$ [332]. Note that both kinds of behavior may occur in case of marginal perturbations. Cluster simulations [329] again show initial density ($\rho_{I1}(0)$) dependent survival probability of $I2$ -s in the sea of $I1$ -s:

$$P_{I2}(t) \propto t^{-\delta(\rho_{I1}(0))} . \quad (5.5)$$

(see local slopes defined as $\delta_{eff} = -\frac{d \log P(t)}{d \log t}$ on Fig.5.1)

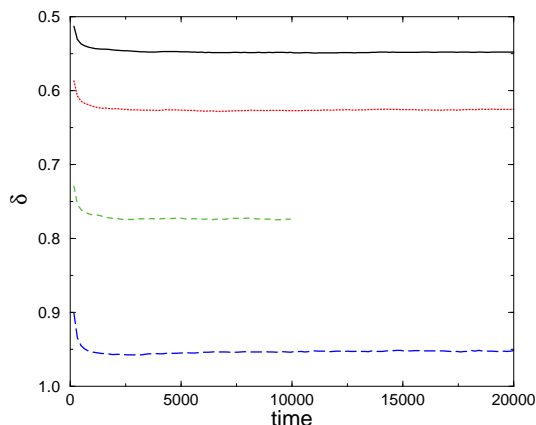


Figure 5.1: Local slopes of the $I2$ cluster survival probability in the GDK model at point “A”. The initial state contains uniformly distributed $I1$ -s with initial densities: $\rho_0(I1) = 0.1$ (solid line), 0.25 (dotted line), 0.5 (dashed line), 0.75 (long-dashed line) [329].

This reaction-diffusion model with homogeneous, **random initial distribution** of A -s and B -s however shows a much slower density decay. An exact duality mapping [331] helps to understand the coarsening behavior. Consider the leftmost particle, which may be either A or B , and arbitrarily

relabel it as a particle of species X . For the second particle, we relabel it as Y if it is the same species as the initial particle; otherwise we relabel the second particle as X . We continue to relabel each subsequent particle according to this prescription until all particles are relabeled from $\{A, B\}$ to $\{X, Y\}$. For example, the string

$$AABABBBBA \dots$$

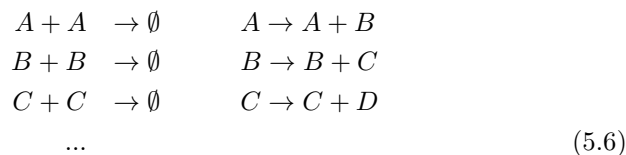
translates to

$$XYYYXXYY \dots$$

The diffusion of the original A and B particles at equal rates translates into diffusion of the X and Y particles. Furthermore, the parallel single-species reactions, $A + A \rightarrow \emptyset$ and $B + B \rightarrow \emptyset$, translate directly to two-species annihilation $X + Y \rightarrow \emptyset$ (see Sect. 5.1) in the dual system. The interesting point is that in the $X + Y \rightarrow \emptyset$ model blockades do not exist, because XY pairs annihilate, and there is no blockade between XX and YY pairs. Therefore the density decay should be proportional to $t^{-1/4}$. Simulations confirmed this for the $A + A \rightarrow \emptyset, B + B \rightarrow \emptyset$ [201] model, nevertheless corrections to scaling were also observed. The pairwise initial condition transforms in the dual system to domains of $\dots XYXY \dots$ where reactions occur separated by YY and XX pairs that do not allow X and Y particles to escape each other.

5.3 Unidirectionally coupled ARW classes

Unidirectionally coupled ARW (Sect.4.3.1) system was introduced and analyzed with RG and simulations by Goldschmidt et al.[365]:



This kind of coupling was chosen because $A \rightarrow B$ would constitute a spontaneous death process of A particles leading to exponential density decay. On the other hand quadratic coupling of the form $A + A \rightarrow B + B$ leads to asymptotically decoupled systems [223]. The mean-field theory is described by the rate equation for the density $\rho_i(x, t)$ at level i :

$$\frac{\partial \rho_i(x, t)}{\partial t} = D \nabla^2 \rho_i(x, t) - 2\lambda_i \rho_i(x, t)^2 + \sigma_{i, i-1} \rho_{i-1}(x, t), \tag{5.7}$$

which relates the long time behavior of level i to level $i - 1$:

$$n_i(t) \propto n_{i-1}^{1/2}. \quad (5.8)$$

By inserting into this the exact solution for ARW (Sect.4.3.1) one gets:

$$\rho_i(t) \sim \begin{cases} t^{-d/2^i} & \text{for } d < 2, \\ (t^{-1} \ln t)^{1/2^{i-1}} & \text{for } d = d_c = 2, \\ t^{-1/2^{i-1}} & \text{for } d > 2, \end{cases} \quad (5.9)$$

The action of a two-component system with fields a, \hat{a} , b , \hat{b} for equal annihilation rates (λ) looks as

$$S = \int d^d x \int dt \left[\hat{a}(\partial_t - D\nabla^2)a - \lambda(1 - \hat{a}^2)a^2 + \hat{b}(\partial_t - D\nabla^2)b - \lambda(1 - \hat{b}^2)b^2 + \sigma(1 - \hat{b})\hat{a}a \right]. \quad (5.10)$$

The RG solution is plagued by IR-divergent diagrams similarly to UCDP (see Sect.6.7) that can be interpreted as eventual *non-universal* crossover to the decoupled regime. Simulation results – exhibiting finite particle numbers and coupling strengths – really show the breakdown of scaling (5.9), but the asymptotic behavior could not be determined. Therefore the results (5.9) are valid for an intermediate time region.

5.4 DP with coupled frozen field classes

Several variants of models with infinitely many absorbing states containing frozen particle configurations have been introduced. The common behavior of these models that non-diffusive (slave) particles are coupled to a DP-like (order parameter) process. The conditions of DP hypothesis [189] (Sect. 4) are not satisfied still continuous transitions with, DP class exponents in case of homogeneous, uncorrelated initial conditions were found. On the other hand in case of cluster simulations – that involves correlated initial conditions for the order parameter particles – initial density dependent scaling exponents (η and δ) arise. These cluster exponents take the DP class values only if the initial density of slave particles agrees with the “natural density” that occurs in the steady state. The first such models introduced by Jensen and Dickman [333] were the so called pair contact process (PCP) (see Sect. 5.4.1) and dimer the reaction model. In these models there is only one component defined explicitly but the rules for pairs (following DP process) as the order parameter and the faith of lonely

frozen particles makes them different. In the threshold transfer process (TTP) [247] (Sect.5.4.2) there are two types: the '2'-s making up the order parameter and sites where $\emptyset \xrightarrow{r} 1 \xrightarrow{1-r} \emptyset$ fluctuations stabilize the density of '1'-s to r .

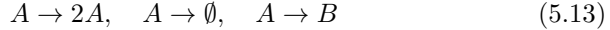
For the PCP model defined by the simple processes (5.16) a set of coupled Langevin equations were set up [304, 303] for the fields $n_1(\mathbf{x}, t)$ and $n_2(\mathbf{x}, t)$ (order parameter):

$$\begin{aligned}\frac{\partial n_2}{\partial t} &= [r_2 + D_2 \nabla^2 - u_2 n_2 - w_2 n_1] n_2 + \sqrt{n_2} \eta_2 \\ \frac{\partial n_1}{\partial t} &= [r_1 + D_1 \nabla^2 - u_1 n_2 - w_1 n_1] + \sqrt{n_2} \eta_1\end{aligned}\quad (5.11)$$

where D_i, r_i, u_i , and w_i are constants and $\eta_1(\mathbf{x}, t)$ and $\eta_2(\mathbf{x}, t)$ are Gaussian white noises. Owing to the multiple absorbing states and the lack of the time reversal symmetry (4.8) a generalized hyperscaling law (4.74) has been derived by Mendes et al. [247]. As discussed in [304] this set of equations can be simplified by dropping the D_1, u_1 , and noise terms in the n_1 equation, and then solving that equation for n_1 in terms of n_2 . Substituting in the n_2 equation, one obtains

$$\begin{aligned}\frac{\partial n_2(\mathbf{x}, t)}{\partial t} &= D_2 \nabla^2 n_2(\mathbf{x}, t) + m_2 n_2(\mathbf{x}, t) - u_2 n_2^2(\mathbf{x}, t) + \\ &+ w_2 (r_1/w_1 - n_1(\mathbf{x}, 0)) n_2(\mathbf{x}, t) e^{-w_1 \int_0^t n_2(\mathbf{x}, s) ds} + \sqrt{n_2(\mathbf{x}, t)} \eta_2(\mathbf{x}, t),\end{aligned}\quad (5.12)$$

where $n_1(\mathbf{x}, 0)$ is the initial condition of the n_1 field, and $m_2 = r_2 - w_2 r_1 / w_1$. The ‘‘natural density’’ [333], n_1^{nat} , then corresponds to the uniform density, $n_1(t=0) = r_1/w_1$, for which the coefficient of the exponential term vanishes, and we get back the Langevin equation of RFT (4.4). This derivation provides a simple explanation for the numerical observation of DP exponents in case of natural initial conditions. However it does not take into account the long-time memory and DP-like fluctuations of passive particles (with power-law time and p dependences [305]). Therefore, some of the terms omitted by this derivation (as for instance the term proportional to n_2^2 in the equation for n_1) cannot be safely eliminated [306] and this simplified theory does not generate critical fluctuations for its background field. To overcome these problems a more rigorous field theoretical analysis involving path integral representation of a two-component variant of this class (with 'A' activity and 'B' slave):



has been done [307] and provided some evidence that the homogeneous state critical properties of the activity field are DP like irrespectively of the

criticality of the slave field. For this model Muñoz et al. [307] could also prove the numerical result [305] that the slave field decays as

$$\rho_B(t) - \rho_B^{nat} \propto t^{-\alpha_{DP}} . \quad (5.14)$$

However this treatment has still not provided theoretical proof for the initial density dependent spreading exponents observed in simulations [333, 247, 305]. Furthermore the situation is much more complicated when approaching criticality from the **inactive phase**. In particular, the scaling behavior of n_A in this case seems to be unrelated to n_B (this is similar to the diffusive slave field case [338] Sect. 5.5.4). In this case it is more difficult to analyze the field theory and dynamical percolation type of terms are generated that can be observed in 2d by simulations and by mean-field analysis [304].

In **two dimensions** the critical point of spreading (p_s) moves (as the function of initial conditions) and do not necessarily coincide with the bulk critical point (p_c). The spreading behavior depends on the coefficient of the exponential, non-Markovian term of (5.12). For positive coefficient the p_s falls in the inactive phase of the bulk and the spreading follows **dynamical percolation** (see Sect. 4.2). For negative coefficient the p_s falls in the active phase of the bulk and spreading exponents are **non-universal** (like in 1d) but satisfy the hyper-scaling (4.74).

Simulations and GMF analysis [306, 307] in 1d showed that the steady state density of slave particles approaches the natural value in the inactive phase also by a power-law

$$|\rho_1^{nat} - \rho_1| \propto |p - p_c|^{\beta_1} , \quad (5.15)$$

with $\beta_1 \sim 0.9$ for PCPD and $\beta_1 = 1$ for TTP models. This difference might be the consequence that in TTP models the slave field fluctuates and relaxes to r quickly while in PCP case it is frozen. Due to this fact one might expect initial condition dependence here again.

5.4.1 The pair contact process model

Up to now I discussed spreading processes with unary particle production. Here I introduce a family of systems with **binary** particle production (i.e for a new particle production two particles need to collide). The PCP model **in one dimension** is defined on the lattice by the following processes:



such that reactions take place at nearest-neighbor (NN) sites and we allow single particle occupancy at most. The order parameter is the density of NN pairs ρ_2 . The PCP exhibits an active phase for $p < p_c$; for $p \geq p_c$ the system eventually falls into an absorbing configuration devoid of NN pairs, (but that contains a density ρ_1 of isolated particles). The best estimate for the critical parameter is $p_c = 0.077090(5)$ [308]. Static and dynamic exponents corresponding to initially uncorrelated homogeneous state agree well with those of 1+1 d DP (4.1). Spreading exponents that involve averaging over all runs hence involving the survival probability are non-universal (see Fig. 5.2 [305]). The anomalous critical spreading of PCP can be traced to a long

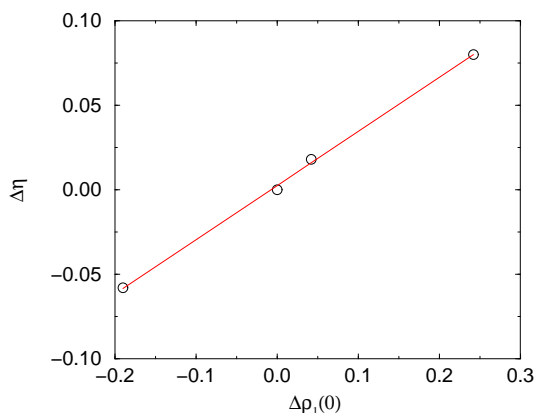


Figure 5.2: Initial concentration dependence of the exponent η for PCP model [305]. Linear regression gives a slope $0.320(7)$ between $\eta - \eta_{DP}$ and $\rho_1(0) - \rho_1^{nat}$

memory in the dynamics of the order parameter ρ_2 , arising from a coupling to an auxiliary field (the local particle density ρ), that remains frozen in regions where $\rho=0$. In [305] a slight variation of the spreading critical point (as the function of $\rho_1(0)$) was observed too (similarly to the 2d case) but more detailed simulations [309] suggest that instead of that corrections to scaling effects appear here. The ρ_1 was shown to exhibit anomalous scaling eq. (5.15) with $\rho_1^{nat} = 0.242(1)$ with DP exponent for $p < p_c$ [305] and $\beta_1 = 0.9(1)$ for $p > p_c$ [306].

The **DS transition** point and the DS exponents of this model were found to coincide with the critical point and the critical exponents of PCP [305].

The effect of **external particle source** that creates isolated particles, hence do not couple to the order parameter was investigated by simula-

tions and GMF+CAM approximations [310]. While the critical point p_c shows a singular dependence on the source intensity, the critical exponents appear to be unaffected by the presence of the source, except possibly for a small change in β .

The properties of the **two dimensional** PCP in case of homogeneous, uncorrelated initial conditions was investigated by simulations [311]. In this case all six NN of a pair was considered for reactions (5.16). The critical point is located at $p_c = 0.2005(2)$. By determining α , β/ν_\perp , Z exponents and order parameter ratios 2+1 d DP class universality (4.1) was confirmed. The spreading exponents are expected to behave as described in Sect. 5.4.

5.4.2 The threshold transfer process (TTP)

In the 1d TTP model [247], each site may be vacant, single or doubly (active) occupied, and this can be described by a 3-state variable $\sigma_i = 0, 1, 2$. In each time step, a site is chosen at random. In the absence of active sites, the dynamics is indeed trivial: if $\sigma_i(t) = 0$ (or 1), then $\sigma_i(t+1) = 1(0)$ with probability r (or $1-r$). The system relaxes exponentially to a steady state where a fraction r of sites have $\sigma_i = 1$ and the others are vacant. If $\sigma_i(t) = 2$ (active), then $\sigma_i(t+1) = 0$, $\sigma_{i-1}(t+1) = \sigma_{i-1}(t)+1$, $\sigma_{i+1}(t+1) = \sigma_{i+1}(t) + 1$ if $\sigma_{i+1}(t)$ and $\sigma_{i-1}(t)$ both < 2 and $\sigma_i(t+1) = 1$ if only one of the nearest neighbors of site i ($j = i-1$ or $i+1$) has $\sigma_j(t) < 2$, in which case $\sigma_j(t+1) = \sigma_j(t) + 1$. As can be easily seen, the number of active sites either decreases or remains the same in all processes other than $(1, 2, 1) \rightarrow (2, 0, 2)$; the frequency of these processes depends on the concentration of '1'-s, which is controlled by the parameter r . Any configuration consisting of only '0'-s or '1'-s is absorbing in what concerns the active sites. The absorbing states in the model are fluctuating - in the respective sector of phase space, ergodicity is not broken. It was shown in [305] that the dynamics of '1'-s is strongly affected by the presence of active sites. At the critical point, the concentration of '1'-s relaxes to its steady state value (equal to r_c) by a power-law (5.14), with 1+1 dimensional DP exponent. The steady state value of ρ_1 was also shown to exhibit anomalous scaling as (5.15), with $\rho_1^{nat} = r_c = 0.6894(3)$ [247]. In the supercritical region [305] this exponent is DP like (see Fig.5.3), while in the passive phase $\beta_1 = 1$ [306]. The order-parameter (ρ_2) exponents belong DP class (4.1) except for δ and η that are non-universal. They depend on $\rho_1(0)$ linearly and satisfy the hyperscaling law (4.74).

The **DS transition** and DS exponents of this model were found to coincide with the critical point and critical exponents of the TTP model [305].

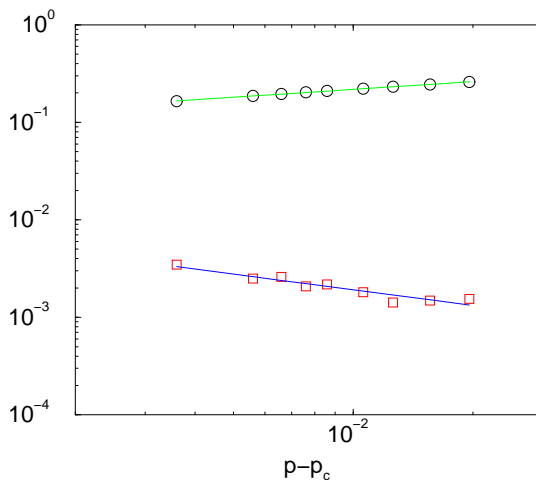
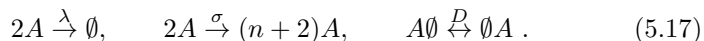


Figure 5.3: Log-log plot of $\rho_1(r) - \rho_1(r_c)$ (\circ) and respective fluctuation (\square) v.s. $p - p_c$ above the critical point of the TTP model. Least-square regression results in $\beta = 0.27(2)$ and $\gamma = 0.53(6)$ [305].

5.5 DP with coupled diffusive field classes

The prominent representatives of these classes are binary particle production systems with diffusive slave field. The critical behavior of such systems are still under investigations. The annihilation-fission (AF) process is defined as



The corresponding action for bosonic particles was derived from master equation by Howard and Täuber [223]

$$S = \int d^d x dt [\psi(\partial_t - D\nabla^2)\phi - \lambda(1 - \psi^2)\phi^2 + \sigma(1 - \psi^n)\psi^2\phi^2]. \quad (5.18)$$

Usually bosonic field theories well describe the critical behavior of fermionic particles (with maximum one particle/site occupation). This is due to the fact that at absorbing phase transitions the occupation number vanishes. In this case however the active phase of bosonic and fermionic models differ significantly: in the bosonic model the particle density diverges, in the fermionic model there is a steady state with finite density. As the consequence the bosonic field theory can not describe the active phase and the critical behavior of the fermionic particle system.

As one can see this model lacks terms proportional to the field ϕ . Although the field theory of **bosonic AF** has turned out to be non-renormalizable Howard and Tauber [223] concluded that critical behavior cannot be in DP class. In fact the upper critical behavior is $d_c = 2$ that is different from that of DP and PC classes [338]. In the Langevin formulation

$$\frac{\partial \rho(x, t)}{\partial t} = D \nabla^2 \rho(x, t) + (n\sigma - 2\lambda) \rho^2(x, t) + \rho(x, t) \eta(x, t) \quad (5.19)$$

the noise is complex:

$$\langle \eta(x, t) \rangle = 0 \quad (5.20)$$

$$\langle \eta(x, t) \eta(x', t') \rangle = [n(n+3)\sigma - 2\lambda] \delta^d(x - x') (t - t'), \quad (5.21)$$

that is again a new feature (it is real in case of DP and purely imaginary in case of CDP and PC classes).

Eq.(5.19) without noise gives the **MF behavior of the bosonic model**: for $n\sigma > 2\lambda$ the density diverges, while for $n\sigma < 2\lambda$ it decays with a power-law with $\alpha_b^{MF} = 1$. The MF behavior of the **inactive phase** of the bosonic model has been found to describe the inactive phase of a 2d fermionic AF system too [338]. Here the pair density decay follows $\rho_2(t) \propto t^{-2}$ [338] in agreement with the MF approximation. Contrary to this for $\lambda \leq \lambda_c$ ρ and ρ_2 seem to be coupled up to a logarithmic ratio $\rho(T)/\rho_2(t) \propto \ln(t)$. This behavior could not be described by the mean-field approximations.

The critical behavior of the **1d bosonic model** in the inactive phase was conjectured to be dominated by the $3A \rightarrow \emptyset$ process that has upper critical dimension $d_c = 1$, so in 1d the particle density decays with $\alpha = 1/2$ and logarithmic corrections (see Sect. 4.5). This was confirmed by simulations of the 1d AF model [285].

The field theoretical description of the **fermionic AF** process run into even more serious difficulties [339] than that of the bosonic model and predicted an upper an critical dimension $d_c = 1$ that contradicts simulation results [338]. For the fermionic AF system **mean-field** approximations [225, 338] give a continuous transition with exponents

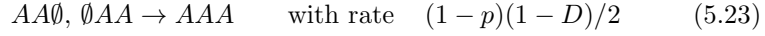
$$\beta = 1, \quad \beta' = 0, \quad Z = 2, \quad \nu_{||} = 2, \quad \nu_{\perp} = 1, \quad \alpha = 1/2, \quad \eta = 0. \quad (5.22)$$

These MF exponents are distinct from those of other well known classes (DP, PC, VM ...). They were confirmed to – with logarithmic corrections indicating $d_c = 2$ – in a 2d fermionic AF model [338]. An explanation for the new type of critical behavior based on symmetry arguments are still missing but numerical simulations suggest [224, 228] that the behavior of this system can be described (at least for strong diffusion) by coupled sub-systems:

single particles performing annihilating random walk coupled to pairs (B) following DP process: $B \rightarrow 2B, B \rightarrow \emptyset$. The model has two non-symmetric absorbing states: one is completely empty, in the other a single particle walks randomly. Owing to this fluctuating absorbing state this model does not oppose the conditions of the DP hypothesis. It was conjectured by Henkel and Hinrichsen [229] that this kind of phase transition appears in models where (i) solitary particles diffuse, (ii) particle creation requires two particles and (iii) particle removal requires at least two particles to meet. The exploration of other conditions that affect these classes are still under investigation.

5.5.1 The PCPD model

A PCPD like model was introduced in an early work by Grassberger [222]. His preliminary simulations in 1d showed non-DP type transition, but the model has been forgotten for a long time. The PCPD model introduced by Carlon et al [225] is controlled by two parameters, namely the probability of pair annihilation p and the probability of particle diffusion D . The dynamical rules are



The *mean-field* approximation gives a continuous transition at $p = 1/3$. For $p \leq p_c(D)$ the particle and pair densities exhibit singular behavior:

$$\rho(\infty) \propto (p_c - p)^\beta \quad \rho_2(\infty) \propto (p_c - p)^{\beta_2} \quad (5.26)$$

while at $p = p_c(D)$ they decay as:

$$\rho(t) \propto t^{-\alpha} , \quad \rho_2(t) \propto t^{-\alpha_2} , \quad (5.27)$$

with the exponents:

$$\alpha = 1/2, \quad \alpha_2 = 1, \quad \beta = 1, \quad \beta_2 = 2 . \quad (5.28)$$

According to *pair mean-field* approximations the phase diagram can be separated into two regions (see Fig.5.4). While for high values of D (greater than approximately 0.3) the pair approximation gives the same $p_c(D)$ and exponents as the simple MF, for low D -s the transition line breaks and the exponents are different

$$\alpha = 1, \quad \alpha_2 = 1, \quad \beta = 1, \quad \beta_2 = 1 . \quad (5.29)$$

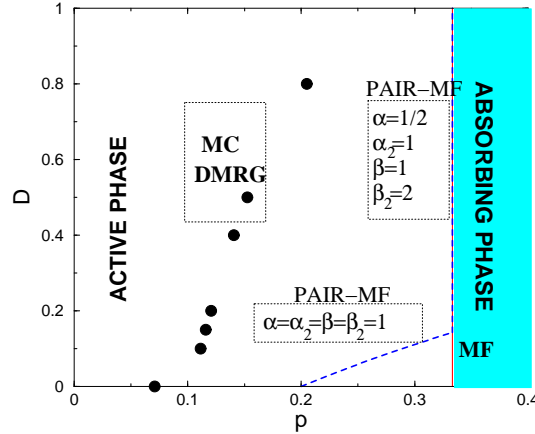


Figure 5.4: Schematic phase diagram of the 1d PCPD model. Circles correspond to simulation and DMRG results, solid line to mean-field, dashed line to pair-approximation.

In the entire inactive phase the decay is characterized by the exponents:

$$\alpha = 1, \quad \alpha_2 = 2. \quad (5.30)$$

The DMRG [225] method and simulations of the 1d PCPD model [226] resulted in agreeing $p_c(D)$ values but for the critical exponents no clear picture was found. They could not clarify if the two distinct universality suggested by the pair mean-field approximations was really observable in the 1d PCPD model. It is still a debated question if one new class, two new classes or continuously changing exponents occur in 1d. Since the model has two (non-symmetric) absorbing states (besides the completely empty one there is an other in which a single particle diffuses) and some exponents were found to be close to those of PC class ($Z = 1.6 - 1.87$, $\beta/\nu_\perp = 0.47 - 0.51$) [225] suspected that the transition (at least for low- D values) is PC type. However the lack of Z_2 symmetry, parity conservation and further numerical data [226, 224] seems to exclude this possibility. Note that the MF correlation length exponents are also different from those of the PC class. Simulations and CAM calculations for the 1d $n = 1$ AF model [224] (with synchronous update) corroborated the two new universality class prospect (see Fig.5.5 and Table 5.1). The order parameter exponent (β) was found to be very far away from both of the DP and PC class values [224]. The two distinct class behavior may be explained on the basis of competing diffusion strengths of particles and pairs (i.e. for large D -s the explicit

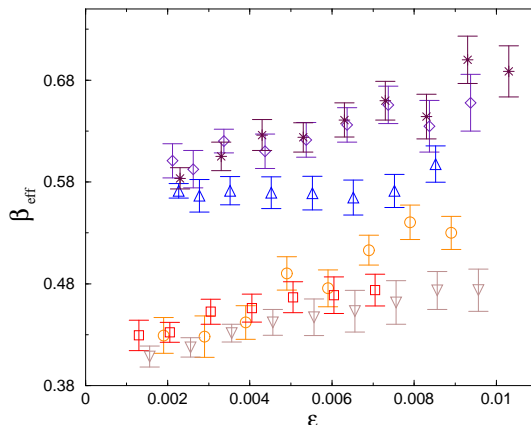


Figure 5.5: Order parameter exponent results of the AF model for $D = 0.9$ (circles), $D = 0.5$ (squares), $D = 0.2$ (diamonds), $D = 0.1$ (triangles), $D = 0.05$ (stars). The simulations were performed on a ring of $L = 24000$ sites such that averaging was done following the steady state is reached for 1000 samples [224].

diffusion of lonely particles is stronger). Similar behavior was observed in case of 1d models with coupled (conserved) diffusive field (see Sect. 5.7). The spreading exponent η seems to change continuously by varying D . Whether this is true asymptotically or the effect of some huge correction to scaling is still not clear. The simulations of [224] confirmed that it is irrelevant whether the particles production is spatially symmetric: $A\emptyset A \rightarrow AAA$ or spatially asymmetric: $AA\emptyset \rightarrow AAA$, $\emptyset AA \rightarrow AAA$.

On the other hand recent simulations and higher level GMF approximations for a 2d AF model ($n = 2$) suggest [338] that the peculiarities of the pair approximation are not real; for $N > 2$ cluster approximations the low- D region scaling disappears.

5.5.2 The annihilation-coagulation (AC) model

If we replace the annihilation process $2A \rightarrow \emptyset$ by coagulation $2A \rightarrow A$ in (5.17) we get the annihilation-coagulation model (AC). GMF approximations and simulations of this model resulted in similar phase diagram than that of the PCPD model albeit without any sign of two distinct regions. In agreement with this CAM approximations and simulations for the 1d model found the same kind of continuous transition independently from D ,

D	0.05	0.1	0.2	0.5	0.9
p_c	0.25078	0.24889	0.24802	0.27955	0.4324
β_{CAM}	-	0.58(6)	0.58(2)	0.42(4)	-
β	0.57(2)	0.58(1)	0.58(1)	0.40(2)	0.39(2)
α	0.273(2)	0.275(4)	0.268(2)	0.21(1)	0.20(1)
η	0.10(2)	-	0.14(1)	0.23(2)	0.48(1)
δl	0.004(6)	-	0.004(6)	0.008(9)	0.01(1)

Table 5.1: Summary of results for 1d, $n = 1$ AF model. The non-universal critical parameter p_c of the parallel model is shown here.

with exponents in agreement with those of the PCPD in the low- D region [227]. Again the spatial symmetry of particle production was found to be irrelevant. An exact solution was found by Henkel and Hinrichsen [229] for the special case of the 1d AC model when the diffusion rate is equal to the coagulation rate, corresponding to the inactive phase according to which the particle decay is like of ARW: $\rho \propto t^{-1/2}$.

5.5.3 Cyclically coupled spreading with pair annihilation

A cyclically coupled two-component reaction-diffusion system was introduced by Hinrichsen [228]



which mimics the PCPD model (Sect.5.5.1) by mapping pairs to A -s and single particles to B -s. This model is a coupled DP+ARW system. Its 1+1 d critical space-time evolution pattern looks very similar to that of the PCPD model. It seems to be a special behavior of this class how the space-time behavior looks like: it is built up from compact domains with a cloud of lonely particles wandering and interacting with them. Furthermore this model also has two non-symmetric absorbing states: a completely empty one and an other with a single wandering B . By fixing the annihilation and diffusion rates of B -s ($r = D = 1$) the model exhibits continuous phase transition by varying the production rate of A -s and the $A \rightarrow B$ transmutation rate. The simulations in 1d showed that $\rho_A \propto \rho_B$ for large times and resulted in the following critical exponent estimates

$$\alpha = 0.21(2), \quad \beta = 0.38(6), \quad \beta' = 0.27(3), \quad Z = 1.75(5), \quad \nu_{||} = 1.8(1), \quad (5.32)$$

satisfying the generalized hyperscaling relation (4.74). These exponents are similar to those of PCPD model in the high diffusion region (see Table 5.1) that is reasonable since $D = 1$ is fixed here.

5.5.4 The parity conserving AF model

Recently Park et al. [230] investigated a parity conserving representative ($n = 2$) of the 1d AF model (5.17). By performing simulations for low- D -s they found critical exponents that are in the range of values determined for the corresponding PCPD class. They claim that the conservation law does not affect the critical behavior and that the binary nature of the offspring production is a necessary condition for this class (see however Sect. 5.5.3 where there is no such condition).

The two dimensional version of the parity conserving AF model was investigated by GMF and simulation techniques [338]. While the $N = 1, 2$ GMF approximations showed similar behavior as in case of the PCPD model (Sect. 5.5.1) (including the two class prediction for $N = 2$) the $N = 3, 4$ approximations do not show D dependence of the critical behavior: $\beta = 1, \beta_2 = 2$ was obtained for $D > 0$. For $D = 0$ GMF approximations give $\beta = \beta_2 = 1$ in agreement with DP mean-field type of behavior (see Table 5.2). Large scale simulations of the particle density confirmed mean-field

D	$N = 2$			$N = 3$			$N = 4$		
	p_c	β	β_2	p_c	β	β_2	p_c	β	β_2
0.75	0.5	1	2	0.4597	1	2	0.4146	1	2
0.5	0.5	1	2	0.4	1	2	0.3456	1	2
0.25	0.5	1	2	0.3333	1	2	0.2973	1	2
0.1	0.4074	1	1	0.2975	1	2	0.2771	1	2
0.01	0.3401	1	1	0.2782	1	2	0.2759	1	2
0.00	0.3333	1	1	0.1464	1	1	0.1711	1	1

Table 5.2: Summary of $N = 2, 3, 4$ approximation results of the $n = 2$ AF process

scaling behavior (5.22) with logarithmic corrections. This is interpreted as numerical evidence supporting that the upper critical dimension in this model is $d_c = 2$. The pair density scales in a similar way but with an additional logarithmic factor to the order parameter. This kind of strongly coupled behavior at criticality and above has been observed in case of the PCP model too (see Sect. 5.4.1). At the $D = 0$ endpoint of the transition

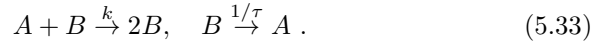
line 2+1 d class DP criticality (see Sect. 4.1) was found for ρ_2 and for $\rho - \rho(p_c)$. In the inactive phase for $\rho(t)$ the two-dimensional ARW class (see Sect.4.3.1) behavior, while for pairs $\rho_2 \propto t^{-2}$ decay appears. Again like in 1d the parity conservation seems to be irrelevant.

5.6 BARWe with coupled non-diffusive field class

A parity conserving version of the PCP model (Sect. 5.4.1) in 1d was introduced by Marques and Mendes [231] in which pairs follow BARW2 process, while lonely particles are frozen. This model has infinitely many absorbing states. Simulations showed that while the critical behavior of pairs in case of uncorrelated, random initial pair distribution belongs to the PC class (Sect. 4.4.2), the spreading exponents satisfy hyperscaling (4.74) and change continuously by varying the initial particle density. These results are similar to those of the PCP model and again long-memory effects in case of correlated, seed initial conditions are responsible for the non-universal behavior. This was confirmed by studying an 1d interacting monomer-monomer model [232] by simulations.

5.7 DP with diffusive conserved slave field classes

One can deduce from the BARW1 spreading process (Sect.4.1.3) a two-component, reaction-diffusion model (DCF) [233, 234] that exhibits total particle density conservation as follows:



By varying the initial particle density ($\rho = \rho_A(0) + \rho_B(0)$) continuous phase transition occurs. General field theoretical investigation has been done by Wijland et al [234] (for the equal diffusion case: $D_A = D_B$ by Kree et al [233]). The mean-field exponents that are valid above $d_c = 4$ are shown in Table 5.3. The rescaled action of this model is

$$\begin{aligned} S[\varphi, \bar{\varphi}, \psi, \bar{\psi}] = & \int d^d x dt \left[\bar{\varphi}(\partial_t - \Delta)\varphi + \bar{\psi}(\partial_t + \lambda(\sigma - \Delta))\psi \right. \\ & + \mu\bar{\varphi}\Delta\psi + g\psi\bar{\psi}(\psi - \bar{\psi}) + u\psi\bar{\psi}(\varphi + \bar{\varphi}) \\ & + v_1(\psi\bar{\psi})^2 + v_2\psi\bar{\psi}(\psi\bar{\varphi} - \bar{\psi}\varphi) + v_3\varphi\bar{\varphi}\psi\bar{\psi} \\ & \left. - \rho_B(0)\delta(t)\bar{\psi} \right] \quad (5.34) \end{aligned}$$

where ψ and ϕ are auxiliary fields, defined such that their average values coincide with the average density of B particles and the total density of particles respectively and the coupling constants are related to the original parameters of the master equation by

$$\begin{aligned} \mu &= 1 - D_B/D_A & g &= k\sqrt{\bar{\rho}}/D_A & u &= -k\sqrt{\bar{\rho}}/D_A \\ v_1 = v_2 = -v_3 &= k/D_A & \lambda\sigma &= k(\rho_c^{\text{mf}} - \bar{\rho})/D_A & \lambda &= D_B/D_A \\ \rho_B(0) &= \rho_B(0)/\sqrt{\bar{\rho}} \end{aligned} \tag{5.35}$$

If one omits from the action Eq. (5.34) the initial time term proportional to $\rho_B(0)$, then the remainder is, for $\mu = 0$ (i. e. $D_A = D_B$), invariant under the time reversal symmetry

$$\begin{aligned} \psi(x, t) &\rightarrow -\bar{\psi}(x, -t) \\ \bar{\psi}(x, t) &\rightarrow -\psi(x, -t) \\ \varphi(x, t) &\rightarrow \bar{\varphi}(x, -t) \\ \bar{\varphi}(x, t) &\rightarrow \varphi(x, -t) \end{aligned} \tag{5.36}$$

Its epsilon expansion solution [233] and simulation results [235, 236] are summarized in Table 5.3. Interestingly RG predicts $Z = 2$ in all orders of perturbation theory.

d	β	Z	ν_{\perp}
1	0.44(1)		2.1(1)
$4 - \epsilon$	$1 - \epsilon/32$	2	$\frac{1}{2} + \epsilon/8$

Table 5.3: Summary of results for DCF classes for $D_A = D_B$

The breaking of this symmetry for $\mu \neq 0$, that is, when the diffusion constants D_A and D_B are different causes different critical behavior for this system. For $D_A < D_B$ RG [234] predicts new classes with $Z = 2$, $\beta = 1$, $\nu_{\perp} = 2/d$, but simulations in 1d [236] show different behavior (see Table 5.4). For non-poissonian initial particle density distributions the critical initial slip exponent η varies continuously with the width of the distribution of the conserved density. The $D_A = 0$ extreme case is discussed in Section 5.8.

For $D_A > D_B$ no stable fixed point solution was found by RG hence [234] conjectured first order transition for which signatures were found in 2d by simulations [237]. However ϵ expansion may break down in case of the occurrence of an other critical dimension $d'_c < d_c = 4$ for which simulations in 1d [236] provided numerical support (see Table 5.5).

d	β	Z	ν_{\perp}
1	0.33(2)		2
$4 - \epsilon$	1	2	$2/d$

Table 5.4: Summary of results for DCF classes for $D_A < D_B$

d	β	Z	ν_{\perp}
1	0.67(1)		2
$4 - \epsilon$	0		

Table 5.5: Summary of results for DCF classes for $D_A > D_B$

5.8 DP with frozen conserved slave field classes

If the conserved field coupled to BARW1 process eq. (5.33) is non-diffusive non-DP universality class (NDCF) behavior is reported [208, 210]. The corresponding action can be derived from (5.34) in the $D_A = 0$ limit:

$$\begin{aligned}
S = \int d^d x dt & \left[\bar{\varphi}(\partial_t + r - D\nabla^2)\varphi + \bar{\psi}(\partial_t - \lambda\nabla^2)\psi \right. \\
& + g\bar{\psi}\bar{\psi}(\psi - \bar{\psi}) + u\bar{\psi}\bar{\psi}(\varphi + \bar{\varphi}) + v_1(\psi\bar{\psi})^2 \\
& \left. + v_2\bar{\psi}\bar{\psi}(\psi\bar{\varphi} - \bar{\psi}\varphi) + v_3\bar{\varphi}\bar{\varphi}\psi\bar{\psi} \right] \quad (5.37)
\end{aligned}$$

By neglecting irrelevant terms (5.37) is invariant under the shift transformation

$$\psi \rightarrow \psi + \delta, \quad r \rightarrow r - v_2\delta \quad (5.38)$$

where δ is any constant. The field theoretical analysis of this action has run into difficulties [210]. The main examples for the NDCF classes are the conserved threshold transfer process (CTTR) and the conserved reaction-diffusion model [208, 210]. Furthermore the models described by the NDCF classes embrace a large group of stochastic sandpile models [211] in particular fixed-energy Manna models [212, 213]. The upper critical dimension $d_c = 4$ was confirmed by simulations [218].

It was also shown [214] that these classes describe the depinning transition of **quenched Edwards-Wilkinson** (see Sect. 6.3) or linear interface models (LIM) [216, 154] owing to the fact that quenched disorder can be mapped onto long-range temporal correlations in the activity field [217].

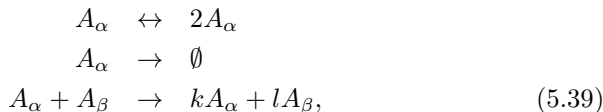
However this mapping could not be done on the level of Langevin equations of the representatives of NDCF and LIM models and in 1d this equivalence may break down [214, 215]. The critical exponents determined by simulations [208, 210, 219, 220] and GMF+CAM method in 1d [221] are summarized in Table 5.6. Similarly to the PCP these models exhibit infinitely many absorbing states, therefore non-universal spreading exponents are expected (in Table 5.6 the exponent η corresponding to natural initial conditions is shown).

d	α	β	γ	Z	$\nu_{ }$	σ	η
1	0.16(4)	0.41(1)		1.5(1)	2.5		
2	0.49(1)	0.64(1)	1.59(3)	1.55(4)	1.29(8)	2.22(3)	0.29(5)
3	0.76(2)	0.84(2)	1.23(4)	1.80(5)	1.10(8)	2.0(4)	0.16(5)
4	1	1	1	2	1	2	0

Table 5.6: Summary of results for NDCF classes

5.9 Coupled N-component DP classes

In [352, 320] Janssen introduced and analyzed by field theoretical RG method (up to two loop order) the quadratically coupled, N-species generalization of the DP process (MDP) of the form:



where k, l may take the values $(0, 1)$. He has shown that the multi-critical behavior is always described by the Reggeon field theory (DP class), but this is instable and leads to unidirectionally coupled DP systems (see Fig.5.6).

He has also shown that by this model the linearly, unidirectionally coupled DP (UCDP) (see Sect.6.7) case can be described. The universality class behavior of UCDP is discussed in Sect.6.7.

In one dimension, if BARWo type of processes are coupled (which alone exhibit DP class transition (see Sect. 4.1.3) **hard-core interactions** can modify the phase transition universality (see Sect. 5.11.1).

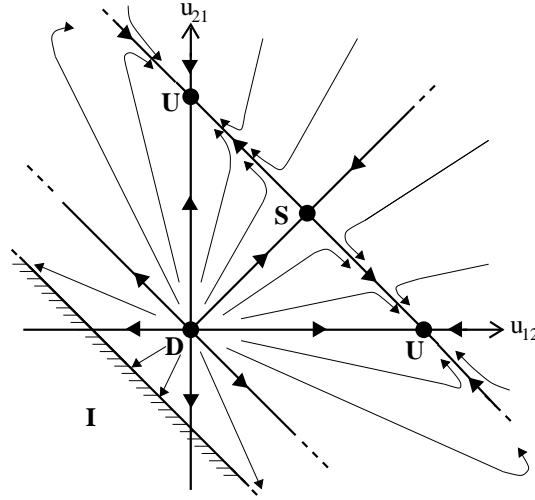


Figure 5.6: Flow of the interspecies couplings in the two-component, MDP model under renormalization. D means decoupled, S symmetric, U unidirectional fixed points [320].

5.10 Coupled N-component BARW2 classes

Bosonic, N component BARW systems with two offsprings (N-BARW2), of the form

$$A_\alpha \rightarrow 3A_\alpha \quad (5.40)$$

$$A_\alpha \rightarrow A_\alpha + 2A_\beta \quad (5.41)$$

$$2A_\alpha \rightarrow \emptyset \quad (5.42)$$

were introduced and investigated by Cardy and Täuber [193] via field theoretical RG method. These models exhibit parity conservation of each species and permutation symmetry on N types (generalization for $O(N)$ symmetry is violated by the annihilation term). The $A \rightarrow 3A$ processes turns out to be irrelevant, because like pairs annihilate immediately. Models with (5.41) branching terms exhibit continuous phase transitions at **zero branching rate**. The universality class is expected to be independent from N and coincides with that of the $N \rightarrow \infty$ (N-BARW2) model that could be solved exactly. The critical dimension is $d_c = 2$ and for $d \leq 2$ the exponents are

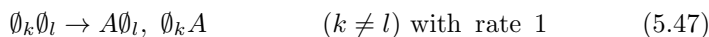
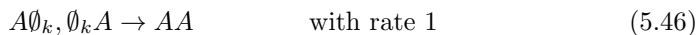
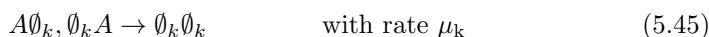
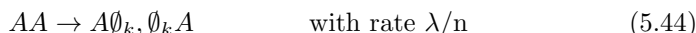
$$\beta = 1, \quad Z = 2, \quad \alpha = d/2, \quad \nu_{\parallel} = 2/d, \quad \nu_{\perp} = 1/d, \quad (5.43)$$

while at $d = d_c = 2$ logarithmic correction to the density decay is expected. Simulations on a $d = 2$ (fermionic) lattice model confirmed these results [201].

In one dimension it turns out that **hard-core interactions** can be relevant and different universal behavior emerges for fermionic models (see Sect. 5.11). The bosonic description of fermionic models in one dimension works (at least for static exponents) in case of *pairwise initial conditions* (see Sect. 5.2) when different types of particles don't make up blockades for each other. Such situation happens when these particles are generated as domain walls of $N+1$ component systems exhibiting S_{N+1} symmetric absorbing states (see Sects. 5.10.1, 5.10.2).

5.10.1 Generalized contact processes with $n > 2$ absorbing state in 1d

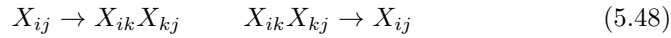
The generalized contact process (GCP) was introduced by Hinrichsen [199] with the main purpose to show an example for PC class universality class transition in case of Z_2 symmetric absorbing states. The more general case with $n > 2$ permutation symmetric absorbing states was investigated using DMRG method by Hooyberghs et al [203]. In the one dimensional model, where each lattice site can be occupied by at most one particle (A) or can be in any of n inactive states ($\emptyset_1, \emptyset_2 \dots \emptyset_n$). The reactions are:



The original contact process (Sect. 4.1.1), corresponds to the $n = 1$ case, in which the reaction (5.47) is obviously absent. The reaction (5.47) in the case $n \geq 2$ ensures that configurations as $(\emptyset_i \emptyset_i \dots \emptyset_i \emptyset_i \emptyset_j \emptyset_j \dots \emptyset_j \emptyset_j)$, with $i \neq j$ are not absorbing. Such configurations do evolve in time until the different domains coarsen and one of the n absorbing states $(\emptyset_1 \emptyset_1 \dots \emptyset_1)$, $(\emptyset_2 \emptyset_2 \dots \emptyset_2)$, \dots $(\emptyset_n \emptyset_n \dots \emptyset_n)$ is reached. For the GCP with $n = 2$, it was found by simulations [199] and DMRG [203] that the transition falls in the PC class if $\mu_1 = \mu_2$, while if the symmetry between the two absorbing states was broken ($\mu_1 \neq \mu_2$) a DP transition was recovered.

The DMRG study for $n = 3$ and $n = 4$ showed that, the model is in the active phase in the whole parameter space and the critical point is shifted to the limit of one infinite reaction rate. In this limit the dynamics of

the model can be mapped onto that of a zero temperature n -state Potts model (see also the simulation results of Lipowski and Droz [85]). It was conjectured by [203] the model is in the same N-BARW2 universality class for all $n \geq 3$. By calling a domain wall between \emptyset_i and \emptyset_j as X_{ij} one can follow the dynamics of such variables. In the limit $\lambda \rightarrow \infty$ X_{ij} coincides a the particle A , or in the limit $\mu \rightarrow \infty$ where X_{ij} coincides with the bond variable $\emptyset_i\emptyset_j$. For finite values of these parameters one can still apply this reasoning at a coarse-grained level. In this case X_{ij} is not a sharp domain wall, but an object with a fluctuating thickness. For $n = 2$ it was shown in Section 4.4.4 that such domain wall variables follow BARW2 dynamics (4.92). For $n > 2$ one can show that besides the N-BARW2 reactions (5.40),(5.41) (involving two types of particles maximum), the reaction types involving three different domains ($i \neq j$, $i \neq k$ and $j \neq k$):



occur with increasing importance as $n \rightarrow \infty$. These reactions break the parity conservation of the N-BARW2 process, therefore the numerical findings in [203] for $n = 3, 4$ indicate that they are probably **irrelevant** there. Owing to the fact that the X_{ij} variables are domain walls they appear in pairwise manner, hence **hard-core exclusion** effects are ineffective for the statistical critical behavior. The effect of pairwise initial conditions for dynamical exponents see Section 5.2.

For $n = 3$ upon breaking the global S_3 symmetry to a lower one, one gets a transition either in the directed percolation (Sect.4.1, or in the parity conserving class (Sect.4.4), depending on the choice of parameters [203]. Simulations indicate [359] that for this model local symmetry breaking may also generate PC class transition.

5.10.2 The NEKIMA model

By breaking the symmetry of the spin updates in the NEKIM model [358] (Sect.4.4.3) phase transitions with non-PC class behavior emerge. The following changes to the Glauber spin-slip rates (4.77) with $\Gamma = 1$, $\tilde{\delta} = 0$ were introduced:

$$w(-;++) = 0, \quad (5.49)$$

$$w(+;+-) = w(+;-+) = p_+ < 1/2, \quad (5.50)$$

while the spin-exchange part remains the same. In the terminology of domain walls as particles the following reaction-diffusion picture arises. Owing to the symmetry breaking there are two kinds of domain walls $-+ \equiv A$ and $+ - \equiv B$, which can only occur alternately (...B..A..B..A..B...A...)

owing to the spin background. Upon meeting $AB \rightarrow \emptyset$ happens, while in the opposite sequence, BA , the two domain-walls are repulsive due to (5.49). The spin exchange leads to $A \leftrightarrow ABA$ and $B \leftrightarrow BAB$ type of kink reactions, which together with the diffusion of A -s and B -s leads to a kind of two-component, coupled branching and annihilating random walk. There are two control parameters in this model: p_{ex} that regulates the kink production-annihilation and p_+ that is responsible for the local symmetry breaking (5.50). By varying these the phase diagram shown on Fig. 5.7 occurs. Simulations show that for $p_{ex} \rightarrow 0$, $p_+ < 0.5$ an absorbing

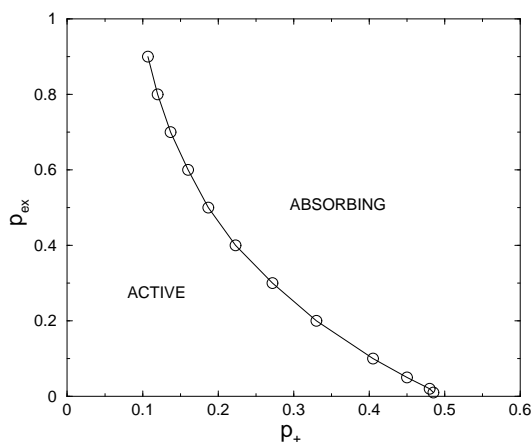


Figure 5.7: Phase diagram of the NEKIMA model for $\tilde{\delta} = 0$, $\Gamma = 1$ [358].

phase emerges with N-BARW2 class exponents (owing to the pairwise order of kinks hard-core effects can not play a role), while the transition on the $p_{ex} > 0$ line belongs to the 1+1 d DP class. Since the $AB \rightarrow \emptyset$ reaction breaks the parity conservation of species (but preserves the global parity conservation) the necessary conditions for N-BARW2 class can be eased. On the other hand the occurrence of the DP transition introduces a new, zero branching rate condition for N-BARW2 universal behavior. This study and the results for GCP (Sect.5.10.1) emphasize that the conditions for N-BARW2 class should be further investigated.

5.11 Hard-core 2-BARW2 classes in 1d

The effect of particle exclusion (i.e. $AB \not\leftrightarrow BA$) in 2-BARW2 models (Sect.5.10) was investigated in [201, 238]. For $d = 2$ the bosonic field theo-

retical predictions of [193] were confirmed [201] (mean-field class transition with logarithmic corrections). In one dimension however two types of phase transitions were identified at zero branching rate ($\sigma = 0$) depending on the arrangement of offsprings relative to the parent in process (5.41). Namely if the parent separates the offsprings (2-BARW2s):



the steady state density is higher than in the case when they are created on the same site (2-BARW2a):



for a given branching rate, because in the former case they are unable to annihilate with each other. This results in different order parameter exponents for the symmetric (2-BARW2s) and the asymmetric (2-BARW2a) cases

$$\beta_s = 1/2, \quad \beta_a = 2. \quad (5.53)$$

This is in contrast to the widespread beliefs that bosonic field theory (where $AB \leftrightarrow BA$ is allowed) can well describe these systems because (in that case the critical behavior is different (Sect. 5.43)). This has led Kwon et al. [238] to the conjecture that in one-dimensional reaction-diffusion systems a series of new universality classes should appear if particle exclusion is present. Note however, that since the transition is at $\sigma = 0$ in both cases the on-critical exponents do not depend on how particles are created and they can be identified with those described in Sect.(5.2). In [201] a set of critical exponents satisfying scaling relations have been determined for this two new classes shown in Table 5.7.

exponent	N-BARW2	N-BARW2s	N-BARW2a
$\nu_{ }$	2	2.0(1) 0.915(2)	8.0(4) 3.66(2)
Z	2	4.0(2) 1.82(2)*	4.0(2) 1.82(2)*
α	1/2	0.25(1) 0.55(1)*	0.25(1) 0.55(1)*
β	1	0.50(1) 1.00(1)	2.0(1) 1.00(1)

Table 5.7: Summary of critical exponents in one dimension for N-BARW2 like models. The N-BARW2 data are quoted from [193]. Data divided by " | " correspond to random vs. pairwise initial condition cases [203, 329, 358]. Exponents denoted by * exhibit slight initial density dependence.

5.11.1 Hard-core 2-BARWo models in 1d

Hard-core interactions in the two-component, one-offspring production model (2-BARW1) were investigated in [239]. Without interaction between different species one would expect DP class transition. By introducing the $AB \not\leftrightarrow BA$ blocking to the two-component model:



a DP class transition at $\sigma = 0.81107$ was located. On the other hand if we couple the two sub-systems by production:



a continuous phase transition emerges at $\sigma = 0$ rate – therefore the on-critical exponents are the same as those described in Sect. (5.2) – and the order parameter exponent was found to be $\beta = 1/2$. This assures that this transition belongs to the same class as the 2-BARW2s model (see Sect.5.11). The parity conservation law that is relevant in case of one component BARW systems (PC versus DP class) is irrelevant here. This finding reduces the expectations suggested by [238] for a whole new series of universality classes in 1d systems with exclusions. In fact the blockades introduced by exclusions generate robust classes. In [239] a hypothesis was set up that **in coupled branching and annihilating random walk systems of N-types of excluding particles for continuous transitions at $\sigma = 0$ two universality classes exist, those of 2-BARW2s and 2-BARW2a models**, depending on whether the reactants can immediately annihilate (i.e. when similar particles are not separated by other type(s) of particle(s)) or not. Recent investigations in similar models [240, 335] are in agreement with this hypothesis.

5.11.2 Coupled binary spreading processes

Two-component versions of the PCPD model (Sect. 5.5.1) with particle exclusion in 1d were introduced and investigated by simulations in [202] with the aim to test if the hypothesis for N-BARW systems set up in [239] (Sect.5.11.1) can be applied for such models. The following models with the same diffusion and annihilation terms ($AA \rightarrow \emptyset$, $BB \rightarrow \emptyset$) as in (Sect.5.2)

and different production processes were investigated.

1) Production and annihilation random walk model (2-PARW):



2) Symmetric production and annihilation random walk model (2-PARWS):



These two models exhibit active steady states for $\sigma > 0$ with a continuous phase transition at $\sigma_c = 0$. Therefore the exponents at the critical point are those of the 2-component ARW model with exclusion (Sect. 5.2). Together with the exponent $\beta = 2$ result for both cases this indicates that they belong to the N-BARW2a class. This also means that the hypothesis set up for N-BARW systems [239] (Sect.5.11.1) may be extended.

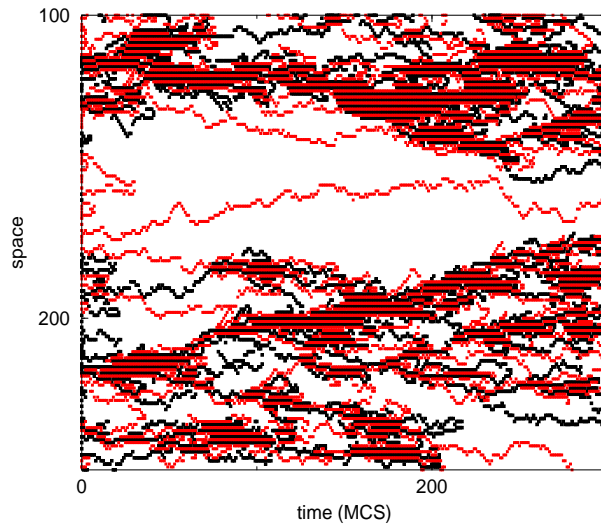


Figure 5.8: Space-time evolution of the 2-PARWAS model at the critical point [202]. Black dots correspond to A particles, others to B -s.

3) Asymmetric production and annihilation random walk model (2-PARWA):



This model does not have an active steady state. The AA and BB pairs annihilate themselves on contact, while if an A and B particle meet an $AB \rightarrow ABB \rightarrow A$ process reduces out blockades and the densities decay with the $\rho \propto t^{-1/2}$ law for $\sigma > 0$. For $\sigma = 0$ the blockades persist, and in case of random initial state $\rho \propto t^{-1/4}$ decay (see Sect. 5.2) can be observed here.

4) Asymmetric production and annihilation random walk model with spatially symmetric creation (2-PARWAS):



In this case AB blockades proliferate by production events. As the consequence of this an active steady state appears for $\sigma > 0.3253(1)$ with a continuous phase transition. The space-time evolution from random initial state shows (Fig.5.8) that compact domains of alternating $..ABAB..$ sequences separated by lonely wandering particles are formed. This is very similar to what was seen in case of one-component binary spreading processes [228]: compact domains within a cloud of lonely random walkers, except that now domains are built up from alternating sequences only. This means that $..AAAA..$ and $..BBBB..$ domains decay for this annihilation rate and particle blocking is responsible for the compact clusters. In the language of coupled DP + ARW model [228] the pairs following DP process are the AB pairs now, which cannot decay spontaneously but through an annihilation process: $AB + BA \rightarrow \emptyset$. They interact with two types of particles executing annihilating random walk with exclusion. The simulations resulted in the critical exponent estimates: $\beta = 0.37(2)$, $\alpha = 0.19(1)$ and $Z = 1.81(2)$ which agree fairly well with those of the PCPD model in the high diffusion rate region [224].

Chapter 6

Interface growth model classes

Interface growth model classes are strongly related to the universality classes discussed so far. The interface models can either be defined by continuum equations or by lattice models of solid-on-solid (SOS) or restricted solid-on-solid (RSOS) types. In the latter case the height variables h_i of adjacent sites are restricted

$$|h_i - h_{i+1}| \leq 1 \quad . \quad (6.1)$$

The morphology of a growing interface is usually characterized by its width

$$W(L, t) = \left[\frac{1}{L} \sum_i h_i^2(t) - \left(\frac{1}{L} \sum_i h_i(t) \right)^2 \right]^{1/2} . \quad (6.2)$$

In the absence of any characteristic length growth processes are expected to show power-law behavior of the correlation functions in space and height and the *Family-Vicsek* scaling [153] form

$$W(L, t) = t^{\tilde{\alpha}/Z} f(L/\xi_{||}(t)), \quad (6.3)$$

describes the surface, where the scaling function $f(u)$ behaves as

$$f(u) \sim \begin{cases} u^{\tilde{\alpha}} & \text{if } u \ll 1 \\ \text{const.} & \text{if } u \gg 1 \end{cases} . \quad (6.4)$$

Here $\tilde{\alpha}$ is the roughness exponent and characterizes the stationary regime in which correlation length $\xi_{||}(t)$ has reached a value larger than the system size L . The ratio $\tilde{\beta} = \tilde{\alpha}/Z$ is called as the growth exponent and characterizes the short time behavior of the surface. Similarly to equilibrium critical

phenomena, these exponents do not depend on microscopic details of the system under investigation. This has made possible to divide growth processes into universality classes according to the values of these characteristic exponents [154, 155]. The (6.3) scaling form of W^2 is invariant under Λ the rescaling

$$x \rightarrow \Lambda x, \quad t \rightarrow \Lambda^Z t, \quad h(x, t) \rightarrow \Lambda^{-\tilde{\alpha}} h(x, t) \quad (6.5)$$

Recently **anomalous roughening** has been observed in many growth models and experiments. In these cases the measurable $\tilde{\alpha}_{loc}$ roughness exponent is different from $\tilde{\alpha}$ and may satisfy different scaling law [155, 157, 158, 159, 160, 161, 70, 163, 164, 165, 166, 167].

Surfaces in $d + 1$ dimensional systems can be **mapped** onto a time step of a d dimensional particle reaction-diffusion or spin models. Example for the 1d Kawasaki spin model corresponding to the $K \leftrightarrow 3K + RW$ reaction-diffusion processes the mapping onto the 1d surface can be done shown on Fig. 6.1.

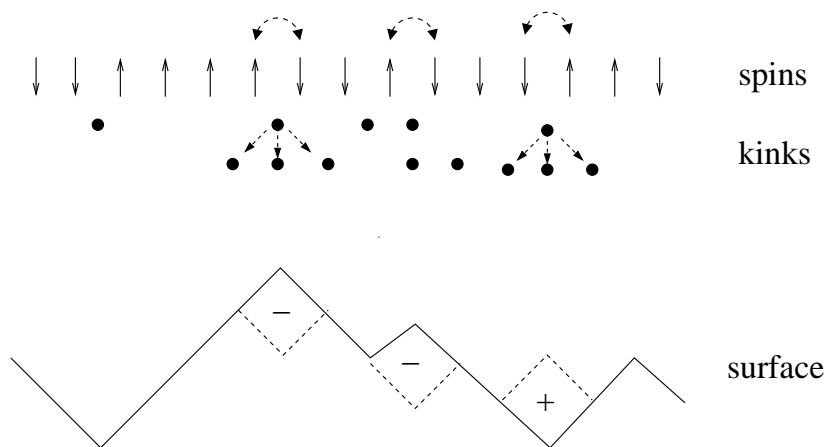


Figure 6.1: Mapping between spins, kinks and surfaces

This means that to a unique $\{s_j\}$ spin configuration at time t corresponds a spatial profile $\{h_i(t)\}$ by cumulating the spin values

$$h_i(t) = \sum_{j=1}^i s_j \quad (6.6)$$

In 1d the surface can also be considered as a random walker with fluctuation

$$\Delta x \propto t^{1/Z_w} \quad (6.7)$$

hence the roughness exponent is related to the dynamical exponent Z_w as

$$\tilde{\alpha} = 1/Z_w . \quad (6.8)$$

The $\tilde{\alpha} = 1/2$ corresponds to uncorrelated (or finite correlation length) random walks. If $\tilde{\alpha} > 1/2$ the surface exhibits correlations, while if $\tilde{\alpha} < 1/2$ the displacements in the profile are anti-correlated. Since the surfaces may exhibit drifts the fluctuations around the mean is measured defining the local roughness (Hurst) exponent. Using this surface mapping Sales et al. [168] have characterized the different classes of Wolfram's 1d CA-s [274].

One can show that by coarse graining the 1d Kawasaki dynamics

$$w_i = \frac{1}{4\tau} [1 - \sigma_i \sigma_{i+1} + \lambda(\sigma_{i+1} - \sigma_i)] \quad (6.9)$$

a mapping can be done onto the KPZ equation (6.19), and the surface dynamics for $\lambda \neq 0$ (corresponding to anisotropic case) is in the KPZ class (Sect.6.4) while for $\lambda = 0$ it is in the Edward Wilkinson class (Sect. 6.2).

While these classes are related to simple random walk with $Z_w = 1/\tilde{\alpha} = 2$ the question arises what surfaces are related to other kind of random walks (example Levy-flights or correlated random walks etc ...). Recently it was shown that globally constrained random walks (i.e. when a walker needs to visit each site an even number of times) can be mapped onto surfaces with dimer-type of dynamics [170] with $Z_w = 3 = 1/\tilde{\alpha}$.

By studying correspondence between lattice models with absorbing states and models of pinned interfaces in random media Dickman and Munoz [169] established the scaling relation

$$\tilde{\beta} = 1 - \beta/\nu_{||} \quad (6.10)$$

that was confirmed numerically for $d = 1, 2, 3, 4$ contact processes (Sect. 4.1.1). The local roughness exponent was found to be smaller than the global value indicating anomalous surface growth in DP class models.

In interface models different types of transitions may take place. **Roughening transitions** may occur between smooth phase characterized by finite width W (in an infinite system) and rough phase where the width

and diverges in an infinite system (but saturates in finite ones) by varying some control parameters (ϵ). Near the transition point the spatial ($\xi_{||}$) and growth direction correlations (ξ_{\perp}) diverge as

$$\xi_{||} \propto \epsilon^{\nu_{||}} \quad (6.11)$$

$$\xi_{\perp} \propto \epsilon^{\nu_{\perp}} \quad (6.12)$$

(note that in RD systems $\xi_{||}$ denote temporal correlation length). In the smooth phase the heights $h_i(t)$ are correlated below ξ_{\perp} . While in equilibrium models roughening transitions exist in $d > 1$ dimensions only in nonequilibrium models this may happen in $d = 1$ as well.

An other surface transition is the **depinning transition** where as the consequence of changing control parameters (usually an external force F) the surface starts propagating with speed v and evolves in a rough state. Close to the transition v is expected to scale as

$$v \propto (F - F_c)^{\tilde{\theta}} \quad (6.13)$$

where $\tilde{\theta}$ is the velocity exponent and again the correlation exponents diverge. Known depinning transitions (in random media) are related to absorbing phase transitions with conserved quantities (see Sects. 6.3, 6.5).

In the rough phase a so-called **faceting phase transition** may also take place where up-down symmetrical facets appear. In this case the surface scaling behavior changes (see Section 6.8).

6.1 The random deposition class

The random deposition is the simplest surface growth process that involves uncorrelated adsorption of particles on top of each other. Therefore columns grow independently, linearly without bounds. This means that the roughness exponent $\tilde{\alpha}$ (and correspondingly Z) is not defined. The width of the surface grows as $W \propto t^{1/2}$ hence $\tilde{\beta} = 1/2$ in all dimensions. An example for such behavior is shown in a dimer growth model in Sect. 6.8.1.

6.2 Edwards-Wilkinson (EW) classes

If we postulate the following translation and reflection symmetries

$$\mathbf{x} \rightarrow \mathbf{x} + \Delta\mathbf{x} \quad \mathbf{t} \rightarrow \mathbf{t} + \Delta\mathbf{t} \quad \mathbf{h} \rightarrow \mathbf{h} + \Delta\mathbf{h} \quad \mathbf{x} \rightarrow -\mathbf{x} \quad \mathbf{h} \rightarrow -\mathbf{h} \quad (6.14)$$

we are led to the Edwards-Wilkinson (EW) equation [171]

$$\partial_t h(\mathbf{x}, t) = v + \sigma \nabla^2 h(\mathbf{x}, t) + \zeta(\mathbf{x}, t), \quad (6.15)$$

which is the simplest stochastic differential equation that describes a surface growth with these symmetries. Here v denotes the mean growth velocity, σ the surface tension and ζ the zero-average Gaussian noise field with variance

$$\langle \zeta(\mathbf{x}, t) \zeta(\mathbf{x}', t') \rangle = 2D \delta^{d-1}(\mathbf{x} - \mathbf{x}') (t - t') \quad (6.16)$$

This equation is linear and exactly solvable and the critical exponents of EW classes are

$$\tilde{\beta} = \left(\frac{1}{2} - \frac{d}{4} \right), \quad Z = 2 \quad (6.17)$$

6.3 Quenched EW classes

In random media linear interface growth is described by the so called quenched Edwards-Wilkinson equation

$$\partial_t h(\mathbf{x}, t) = \sigma \nabla^2 h(\mathbf{x}, t) + F + \eta(\mathbf{x}, h(\mathbf{x}, t)), \quad (6.18)$$

where F is a constant, external driving term and $\eta(\mathbf{x}, h(\mathbf{x}, t))$ is the quenched noise. The corresponding linear interface models (LIM) exhibit a depinning transition at F_c . The universal behavior of these models were investigated in [173, 174, 172] and it was shown to be equivalent with NDCF classes (Sect. 5.8). Analytical studies [174] predict $\tilde{\alpha} = (4 - d)/3$ and $Z = 2 - (2/9)(4 - d)$.

6.4 Kardar-Parisi-Zhang (KPZ) classes

If we drop the $h \rightarrow -h$ symmetry from (6.14) we can add a term to the (6.15) equation that is the most relevant term in renormalization sense breaking the up-down symmetry:

$$\partial_t h(\mathbf{x}, t) = v + \sigma \nabla^2 h(\mathbf{x}, t) + \lambda (\nabla h(\mathbf{x}, t))^2 + \zeta(\mathbf{x}, t) \quad (6.19)$$

that is the Kardar-Parisi-Zhang (KPZ) equation [175]. Here again v denotes the mean growth velocity, σ the surface tension and ζ the zero-average Gaussian noise field with variance

$$\langle \zeta(\mathbf{x}, t) \zeta(\mathbf{x}', t') \rangle = 2D \delta^{d-1}(\mathbf{x} - \mathbf{x}') (t - t') \quad (6.20)$$

This is non-linear, but exhibits a tilting symmetry as the result of the Galilean invariance of (6.19):

$$h \rightarrow h' + \epsilon \mathbf{x}, \quad \mathbf{x} \rightarrow \mathbf{x}' - \lambda \epsilon t, \quad t \rightarrow t' \quad (6.21)$$

where ϵ is an infinitesimal angle. As the consequence the scaling relation

$$\tilde{\alpha} + Z = 2 \quad (6.22)$$

holds in any dimensions. In one dimension the critical exponents are known exactly whereas for $d > 1$ dimensions numerical estimates exist [154] (see Table 6.1). The upper critical dimension of this model is debated. Mode

d	$\tilde{\alpha}$	$\tilde{\beta}$	Z
1	1/2	1/3	3/2
2	0.38	0.24	1.58
3	0.30	0.18	1.66

Table 6.1: Scaling exponents of KPZ from [154]

coupling theories and various phenomenological field theoretical schemes [176, 177] settle to $d_c = 4$. Contrary to analytical approaches numerical solution of the KPZ equation [178], simulations [179, 180], and the results of real-space renormalization group calculations [181] provide no evidence for a finite d_c . Furthermore, the only numerical study [182] of the mode-coupling equations gives no indication for the existence of a finite d_c either. Recent simulations of the universal scaling function associated with the steady-state width distribution also indicate that the upper critical dimension is at infinity [183].

6.4.1 Multiplicative noise systems

Grinstein et al. [360] introduced and studied systems via the Langevin equation

$$\partial_t n(x, t) = D \nabla^2 n(x, t) - r n(x, t) - u n(x, t)^2 + n(x, t) \eta(x, t), \quad (6.23)$$

exhibiting real multiplicative noise (MN) :

$$\langle \eta(x, t) \rangle = 0, \quad \langle \eta(x, t) \eta(x', t') \rangle = 2\nu \delta^d(x - x') \delta(t - t'), \quad (6.24)$$

that is proportional to the field (n). Since for DP class the noise is square root proportional to the field; for ARW and PC systems the noise is imaginary one may expect distinct universal behavior for such systems. Howard

and Täuber [223] on the other hand argued on field theoretical basis that such 'naive' Langevin equations fail to accurately describe systems controlled by particle pair reaction processes, where the noise is in fact 'imaginary' and one should derive proper Langevin equation by starting from master equation of particles. Therefore they investigated the simplest RD systems where both real and imaginary noise is present and compete:

- (a) $2A \rightarrow \emptyset$, $2A \rightarrow 2B$, $2B \rightarrow 2A$, and $2B \rightarrow \emptyset$
- (b) $2A \rightarrow \emptyset$ and $2A \rightarrow (n+2)A$ (see Sect. 5.5)

by setting up the action first – derived from the master equation of particles. In neither case were they able to recover the MN critical behavior reported in [360]. Therefore they suspected that there might not be real RD system possessing the MN behavior.

On the other hand [360] have established connection of MN systems via the Cole-Hopf transformation: $n(x, t) = e^{h(x, t)}$ to the KPZ theory. They have shown in 1d that the phase diagram and the critical exponents Z , ν_{\perp} and β of the two systems agree within numerical accuracy. They have also found diverging susceptibility (with continuously changing exponent as the function of r) for the entire range of r .

6.5 Quenched KPZ classes

In random media nonlinear interface growth is described by the so called **quenched KPZ equation** [154],

$$\partial_t h(\mathbf{x}, t) = \sigma \nabla^2 h(\mathbf{x}, t) + \lambda (\nabla h(\mathbf{x}, t))^2 + F + \eta(\mathbf{x}, h(\mathbf{x}, t)) \quad (6.25)$$

where F is a constant, external driving term and $\eta(\mathbf{x}, h(\mathbf{x}, t))$ is the quenched noise (do not fluctuate in time). Its universal behavior was investigated in [184, 185] and predicted $\tilde{\alpha} \simeq 0.63$ in one dimension, $\tilde{\alpha} \simeq 0.48$ in two dimensions and $\tilde{\alpha} \simeq 0.38$ in three dimensions. It was shown numerically that in 1d this class is described by 1+1 d directed percolation depinning [186]. In higher dimensions however it is related to percolating directed surfaces [187].

6.6 Other continuum growth classes

For continuum growth models exhibiting the symmetries

$$\mathbf{x} \rightarrow \mathbf{x} + \Delta \mathbf{x} \quad \mathbf{t} \rightarrow \mathbf{t} + \Delta \mathbf{t} \quad \mathbf{h} \rightarrow \mathbf{h} + \Delta \mathbf{h} \quad \mathbf{x} \rightarrow -\mathbf{x} \quad (6.26)$$

the possible general Langevin equations with relevant terms are classified as follows [154].

- The deterministic part describes conservative or nonconservative process (i.e. the integral over the entire system is zero or not). Conservative terms are $\nabla^2 h$, $\nabla^4 h$ and $\nabla^2(\nabla h)^2$. The only relevant nonconservative terms is the $(\nabla h)^2$.
- The system is linear or not.
- The noise term is conservative (i.e. the result of some surface diffusion) with correlator

$$\langle \zeta_d(\mathbf{x}, t) \zeta_d(\mathbf{x}', t') \rangle = (-2D_d \nabla^2 + D'_d \nabla^4) \delta(\mathbf{x} - \mathbf{x}') \delta(t - t') \quad (6.27)$$

or nonconservative like in eq.(6.16) (as the result of adsorption, desorption mechanisms).

Analysing the surface growth properties of such systems besides the EW and KPZ classes five other universality classes were identified (see Table 6.2).

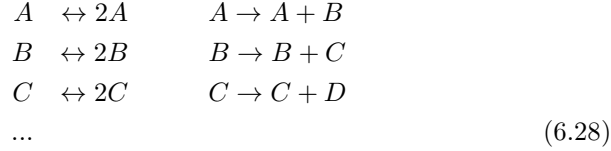
Langevin equation	$\tilde{\alpha}$	$\tilde{\beta}$	Z
$\partial_t h = -K \nabla^4 h + \zeta$	$\frac{4-d}{2}$	$\frac{4-d}{8}$	4
$\partial_t h = \nu \nabla^2 h + \zeta_d$	$\frac{-d}{2}$	$\frac{-d}{4}$	2
$\partial_t h = -K \nabla^4 h + \zeta_d$	$\frac{2-d}{2}$	$\frac{2-d}{8}$	4
$\partial_t h = -K \nabla^4 h + \lambda_1 \nabla^2 (\nabla h)^2 + \zeta$	$\frac{4-d}{3}$	$\frac{4-d}{8+d}$	$\frac{8+d}{3}$
$\partial_t h = -K \nabla^4 h + \lambda_1 \nabla^2 (\nabla h)^2 + \zeta_d$	$\frac{2-d}{3}$	$d \leq 1$	$\frac{10+d}{3}$
		$\frac{2-d}{10+d}$	
		$d > 1$	
	$\frac{2-d}{2}$	$\frac{2-d}{8}$	4

Table 6.2: Summary of continuum growth classes discussed in this section following ref. [154].

6.7 Unidirectionally coupled DP classes

As it was mentioned in Section 5.9 in case of coupled, multi-species DP processes (MDP) field theoretical RG analysis [352] predict DP criticality with an unstable symmetrical fixed point, such that sub-systems with unidirectionally coupled DP behavior emerge. This was shown to be valid for

linearly coupled MDP-s too. Unidirectionally coupled DP systems of the form (UCDP)



were investigated by Täuber et al [361, 362] with the motivation that such models were found to describe interface growth models, where adsorption-desorption are allowed at terraces and edges (see Sect.6.7.1). The simplest set of Langevin equations for such systems was set up by Alon et al. [363]:

$$\partial_t \phi_k(\mathbf{x}, t) = \sigma \phi_k(\mathbf{x}, t) - \lambda \phi_k^2(\mathbf{x}, t) + D \nabla^2 \phi_k(\mathbf{x}, t) + \mu \phi_{k-1}(\mathbf{x}, t) + \zeta_k(\mathbf{x}, t), \tag{6.29}$$

where ζ_k are independent multiplicative noise fields for level k with correlations

$$\langle \zeta_k(\mathbf{x}, t) \rangle = 0, \quad \langle \zeta_k(\mathbf{x}, t) \zeta_l(\mathbf{x}', t') \rangle = 2\Gamma \phi_k(\mathbf{x}, t) \delta_{k,l} \delta^d(\mathbf{x} - \mathbf{x}') \delta(t - t'), \tag{6.30}$$

for $k > 0$, while for the lowest level ($k = 0$) $\phi_{-1} \equiv 0$ is fixed. The parameter σ controls the offspring production, μ is the coupling and λ is the coagulation rate. As one can see the $k = 0$ equation is just the Langevin equation of RFT (4.4). The **mean-field** solution of these equations that is valid above $d_c = 4$ result in critical exponents for the level k :

$$\beta_{MF}^{(k)} = 2^{-k}. \tag{6.31}$$

and $\nu_{\perp}^{MF} = 1/2$ and $\nu_{\parallel}^{MF} = 1$ independently of k . For $d < d_c$ field theoretical RG analysis of the action for $k < K$ levels

$$\begin{aligned}
S = \sum_{k=0}^{K-1} \int d^d x dt \left\{ \tilde{\phi}_k(\mathbf{x}, t) \left(\tau \partial_t - D \nabla^2 - \sigma \right) \phi_k(\mathbf{x}, t) - \mu \tilde{\phi}_k \phi_{k-1} \right. \\
\left. + \frac{\Gamma}{2} \tilde{\phi}_k(\mathbf{x}, t) \left(\phi_k(\mathbf{x}, t) - \tilde{\phi}_k(\mathbf{x}, t) \right) \phi_k(\mathbf{x}, t) \right\}, \tag{6.32}
\end{aligned}$$

was performed in [361, 362]. The RG treatment run into several difficulties. Infrared-divergent diagrams were encountered [365] and the coupling constant μ was shown to be a relevant quantity (that means it diverges under RG transformations). Goldschmidt et al. [362] argued that this is the reason why scaling seems to break down in simulations for large times

	$d = 1$	$d = 2$	$d = 3$	$d = 4 - \epsilon$
β_1	0.280(5)	0.57(2)	0.80(4)	$1 - \epsilon/6 + O(\epsilon^2)$
β_2	0.132(15)	0.32(3)	0.40(3)	$1/2 - \epsilon/8 + O(\epsilon^2)$
β_3	0.045(10)	0.15(3)	0.17(2)	$1/4 - O(\epsilon)$
δ_1	0.157(4)	0.46(2)	0.73(5)	$1 - \epsilon/4 + O(\epsilon^2)$
δ_2	0.075(10)	0.26(3)	0.35(5)	$1/2 - \epsilon/6 + O(\epsilon^2)$
δ_3	0.03(1)	0.13(3)	0.15(3)	$1/4 - O(\epsilon)$
η_1	0.312(6)	0.20(2)	0.10(3)	$\epsilon/12 + O(\epsilon^2)$
η_2	0.39(2)	0.39(3)	0.43(5)	$1/2 + O(\epsilon^2)$
η_3	0.47(2)	0.56(4)	0.75(10)	$3/4 - O(\epsilon)$
$2/Z_1$	1.26(1)	1.10(2)	1.03(2)	$1 + \epsilon/24 + O(\epsilon^2)$
$2/Z_2$	1.25(3)	1.12(3)	1.04(2)	
$2/Z_3$	1.23(3)	1.10(3)	1.03(2)	
$\nu_{\perp,1}$	1.12(4)	0.70(4)	0.57(4)	$1/2 + \epsilon/16 + O(\epsilon^2)$
$\nu_{\perp,2}$	1.11(15)	0.69(15)	0.59(8)	
$\nu_{\perp,3}$	0.95(25)	0.65(15)	0.62(9)	
$\nu_{\parallel,1}$	1.78(6)	1.24(6)	1.10(8)	$1 + \epsilon/12 + O(\epsilon^2)$
$\nu_{\parallel,2}$	1.76(25)	1.23(17)	1.14(15)	
$\nu_{\parallel,3}$	1.50(40)	1.15(30)	1.21(15)	

Table 6.3: Critical exponents of UCDP [362].

(in lattice realization μ is limited). The exponents of the one-loop calculations for the first few levels, corresponding to the interactive fixed line as well as results of lattice simulations are shown in Table 6.3. These scaling exponents can be observed for intermediate times but it is not clear if in the asymptotically long time they drift to the decoupled values or not.

6.7.1 Monomer adsorption-desorption at terraces models

Alon et al. defined SOS and RSOS models [363, 364] that can be mapped onto UCDP (Sect.6.7). In this models adsorption an desorption processes may take place at terraces and edges. For each update a site i is chosen at random and an atom is adsorbed

$$h_i \rightarrow h_i + 1 \quad \text{with probability } q \quad (6.33)$$

or desorbed at the edge of a plateau

$$\begin{aligned} h_i &\rightarrow \min(h_i, h_{i+1}) \text{ with probability } (1-q)/2, \\ h_i &\rightarrow \min(h_i, h_{i-1}) \text{ with probability } (1-q)/2. \end{aligned} \quad (6.34)$$

Identifying empty sites at a given layer as A particles, the adsorption process can be interpreted as the decay of A particles ($A \rightarrow \emptyset$), while the desorption process corresponds to A particle production ($A \rightarrow 2A$). These processes generate reactions on subsequent layers hence they are coupled. The simulations in 1d have shown that this coupling is relevant in the upward direction only hence the model is equivalent to the UCDP process. Defining the order parameters on the k -th layer as

$$n_k = \frac{1}{N} \sum_i \sum_{j=0}^k \delta_{h_i, j}, \quad (6.35)$$

where h_i is the height at site i , they are expected to scale as

$$n_k \sim (q_c - q)^{\beta^{(k)}}. \quad k = 1, 2, 3, \dots \quad (6.36)$$

By varying the growth rate (q) these models exhibit a roughening transition at $q_c = 0.189$ (for RSOS) and at $q_c = 0.233(1)$ (for SOS) from a non-moving, smooth phase to a moving, rough phase in one spatial dimension. The β^k (and other exponents) take those of the 1d UCDP class (see Table 6.3).

The scaling behavior of the interface width is characterized by many different length scales. At criticality it increases as

$$W(t) \propto (\ln t)^\gamma \quad (6.37)$$

until it saturates at

$$W_{sat} \propto (\ln N)^\kappa, \quad (6.38)$$

where $\kappa \simeq 0.43$ for RSOS and $\kappa \simeq 0.24$ for SOS cases.

6.7.2 Polynuclear growth models

Polynuclear growth models (PNG) are realizations of unidirectionally coupled DP processes (Sect.6.7). In these models depinning transition takes place [366, 367, 368]. The PNG model investigated by Kertész and Wolf [366] is defined by the following **parallel** update dynamic rules. In the first half time step atoms ‘nucleate’ stochastically at the surface by

$$h_i(t + 1/2) = \begin{cases} h_i(t) + 1 & \text{with prob. } p, \\ h_i(t) & \text{with prob. } 1 - p. \end{cases} \quad (6.39)$$

In the second half time step the islands grow deterministically in lateral direction by one step.

$$h_i(t+1) = \max_{j \in \langle i \rangle} [h_i(t+1/2), h_j(t+1/2)] , \quad (6.40)$$

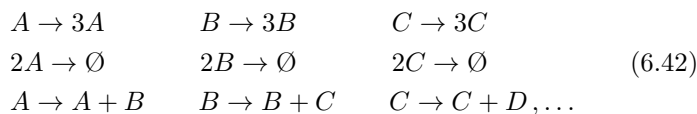
where j runs over the nearest neighbors of site i . For p large enough, the interface is smooth and propagates with velocity 1. Below a critical threshold, the density of active sites at the maximal height $h_i(t) = t$ vanishes, and the growth velocity is smaller than 1. Identifying the sites with $h_i = t$ as A particles, those with $h_i \geq t-1$ as B particles etc., the dynamical processes resemble the rules of coupled DP. The corresponding order parameters are defined by

$$\rho_k = \frac{1}{N} \sum_i \sum_{h=0}^{k-1} \delta_{h_i, t-h} . \quad (6.41)$$

Thus PNG models may be interpreted as a realization of coupled DP in a *co-moving* frame.

6.8 Unidirectionally coupled PC classes

Similarly to the UCDP case (see Sect.6.7) surface growth processes stimulated the introduction of unidirectionally coupled BARW2 (Sect.4.4.2) models [369, 347]:



generalizing the concept of UCDP. The mean field approximation of the reaction scheme (6.42) looks as

$$\begin{aligned} \partial_t n_A &= \sigma n_A - \lambda n_A^2, \\ \partial_t n_B &= \sigma n_B - \lambda n_B^2 + \mu n_A, \\ \partial_t n_C &= \sigma n_C - \lambda n_C^2 + \mu n_B, \dots \end{aligned} \quad (6.43)$$

where n_A, n_B, n_C correspond to the densities n_0, n_1, n_2 in the growth models. σ and λ are the rates for offspring production and pair annihilation respectively. The coefficient μ is an effective coupling constant between different particle species. Since these equations are coupled in only one direction, they can be solved by iteration. Obviously, the mean-field critical

point is $\sigma_c = 0$. For small values of σ the stationary particle densities in the active state are given by

$$n_A = \frac{\sigma}{\lambda}, \quad n_B \simeq \frac{\mu}{\lambda} \left(\frac{\sigma}{\mu} \right)^{1/2}, \quad n_C \simeq \frac{\mu}{\lambda} \left(\frac{\sigma}{\mu} \right)^{1/4}, \quad (6.44)$$

corresponding to the mean field critical exponents

$$\beta_A^{MF} = 1, \quad \beta_B^{MF} = 1/2, \quad \beta_C^{MF} = 1/4, \dots \quad (6.45)$$

These exponents should be valid for $d > d_c = 2$. Solving the asymptotic temporal behavior one finds $\nu_{\parallel} = 1$, implying that $\delta_k^{MF} = 2^{-k}$.

The effective (unshifted) action of unidirectionally coupled BARW2's should be given by

$$\begin{aligned} S[\psi_0, \psi_1, \psi_2, \dots, \bar{\psi}_0, \bar{\psi}_1, \bar{\psi}_2, \dots] = \\ \int d^d x dt \sum_{k=0}^{\infty} \left\{ \bar{\psi}_k (\partial_t - D\nabla^2) \psi_k - \lambda (1 - \bar{\psi}_k^2) \psi_k^2 + \right. \\ \left. + \sigma (1 - \bar{\psi}_k^2) \bar{\psi}_k \psi_k + \mu (1 - \bar{\psi}_k) \bar{\psi}_{k-1} \psi_{k-1} \right\} \end{aligned} \quad (6.46)$$

where $\psi_{-1} = \bar{\psi}_{-1} \equiv 0$. Here the fields ψ_k and $\bar{\psi}_k$ represent the configurations of the system at level k . Since even the RG analysis of the one component BARW2 model suffered serious problems [193] the solution of the theory of (6.46) seems to be hopeless. Furthermore one expects similar IR diagram problems and diverging coupling strengths as in case of UCDP that might be responsible for violations of scaling in the long time limit.

Simulations in a 1d, 3-component model (6.42) with instantaneous couplings resulted in decay exponents for the order parameter defined as (6.35):

$$\delta_A = 0.280(5), \quad \delta_B = 0.190(7), \quad \delta_C = 0.120(10), \quad (6.47)$$

For further critical exponents see Sect.6.8.1.

It would be interesting to investigate parity-conserving growth processes in higher dimensions. Since the upper critical dimension d'_c is less than 2, one expects the roughening transition – if still existing – to be described by mean-field exponents. In higher dimensions, n -mers might appear in different shapes and orientations.

6.8.1 Dimer adsorption-desorption at terraces models

Similarly to the monomer case (Sect.6.7.1) dimer adsorption-desorption models were defined [369, 347, 370]. With the restriction that desorption

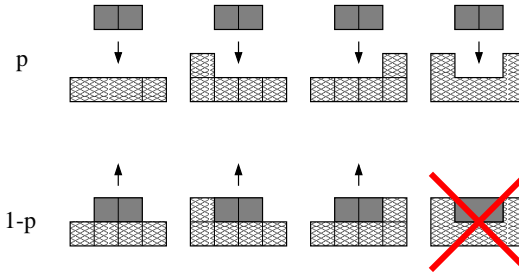


Figure 6.2: Dimers are adsorbed with probability p and desorbed at the edges of terraces with probability $1 - p$. Evaporation from the middle of plateaus is not allowed [347].

may only take place at the edges of a plateau the models can be mapped onto the unidirectionally coupled BARW2 (Sect.6.8). The dynamical rules in 1d are defined on Fig. 6.2. The mapping onto unidirectionally coupled BARW2 can be seen on Fig.6.3.

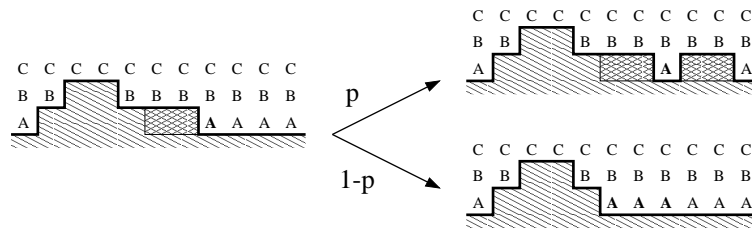


Figure 6.3: Extended particle interpretation. Dimers are adsorbed ($2A \rightarrow \emptyset$) and desorbed ($A \rightarrow 3A$) at the bottom layer. Similar processes take place at higher levels [347].

Such dimer models can be defined in arbitrary spatial dimensions, in [347] four one dimensional variants were investigated.

- 1) Variant A is a restricted solid-on-solid (RSOS) model evolving by random sequential updates.
- 2) Variant B is a solid-on-solid (SOS) model evolving by random sequential updates.
- 3) Variant C is a restricted solid-on-solid (RSOS) model evolving by paral-

lel updates.

4) Variant D is a solid-on-solid (SOS) model evolving by parallel updates.

Variants C and D resulted in the same universal behavior unlike PNG (Sect.6.7.2) and PC-PNG (Sect.6.8.2), where only parallel update rules allow roughening transitions. By varying the adsorption rate p the phase diagram shown on Fig.6.4 emerges for RSOS and SOS cases. If p is very

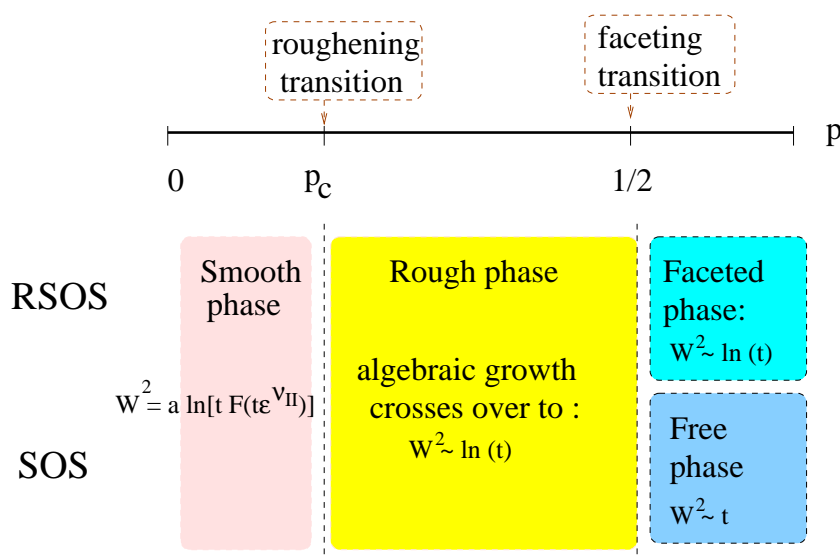


Figure 6.4: Phase diagram of 1d dimer models.

small, only a few dimers are adsorbed at the surface, staying there for a short time before they evaporate back into the gas phase. Thus, the interface is anchored to the actual bottom layer and does not propagate. In this smooth phase the interface with growths logarithmically until it saturates to a finite value (even for $L \rightarrow \infty$).

As p increases, a growing number of dimers covers the surface and large islands of several layers stacked on top of each other are formed. Approaching a certain critical threshold p_c the mean size of the islands diverges and the interface evolves into a rough state (i.e $W \rightarrow \infty$) with the finite-size scaling form

$$W^2(L, t) \simeq a \ln \left[t G(t/L^Z) \right]. \quad (6.48)$$

The order parameter defined on the k -th layer as (6.35) exhibits unidirec-

tionally coupled BARWe critical behavior. The transition rates and exponents are summarized in Table 6.4.

variant	A	B	C	D
restriction	yes	no	yes	no
updates	random	random	parallel	parallel
p_c	0.3167(2)	0.292(1)	0.3407(1)	0.302(1)
a	0.172(5)	0.23(1)	0.162(4)	0.19(1)
Z	1.75(5)	1.75(5)	1.74(3)	1.77(5)
δ_0	0.28(2)	0.29(2)	0.275(10)	0.29(2)
δ_1	0.22(2)	0.21(2)	0.205(15)	0.21(2)
δ_2	0.14(2)	0.14(3)	0.13(2)	0.14(2)
$\tilde{\alpha}$	1.2(1)	undefined	1.25(5)	undefined
$\tilde{\beta}$	0.34(1)	0.50(1)	0.330(5)	0.49(1)

Table 6.4: Numerical estimates for the four variants of the dimer model at the roughening transition $p = p_c$ (upper part) and at the transition $p = 0.5$ (lower part).

Above p_c one may expect the interface to detach from the bottom layer in the same way as the interface of monomer models starts to propagate in the supercritical phase. However, since dimers are adsorbed at neighboring lattice sites, solitary unoccupied sites may emerge. These pinning centers prevent the interface from moving and lead to the formation of ‘droplets’. Due to interface fluctuations, the pinning centers can slowly diffuse to the left and to the right. When two of them meet at the same place, they annihilate and a larger droplet is formed. Thus, although the interface remains pinned, its roughness increases continuously. The width initially increases algebraically until it slowly crosses over to a logarithmic increase $W(t) \sim \sqrt{a \ln t}$.

The restricted as well as the unrestricted variants undergo a second phase transition at $p = 0.5$ [370] where the width increases *algebraically* with time as $W \sim t^{\tilde{\beta}}$. In the RSOS case ordinary *Family-Vicsek* scaling (6.3) occurs with the exponents given in Table 6.4. The dynamic exponent is $Z = \tilde{\alpha}/\tilde{\beta} \simeq 3$. This value stays the same if one allows dimer digging at the faceting transition but other surface exponents $\tilde{\alpha} \simeq 0.29(4)$ and $\tilde{\beta} \simeq 0.111(2)$ will be different [370]. An explanation of the latter exponents is given in [170] based on mapping to globally constrained random walks. In the SOS cases (variants B,D) large spikes are formed, the surface roughens

much faster with a growth exponent of $\tilde{\beta} \simeq 0.5$. The interface evolves into configurations with large columns of dimers separated by pinning centers. These spikes can grow or shrink almost independently. As the columns are spatially decoupled, the width does not saturate in finite systems, i.e., the dynamic exponents $\tilde{\alpha}$ and Z have no physical meaning.

For $p > 0.5$ the restricted models A and C evolve into faceted configurations. The width first increases algebraically until the pinning centers become relevant and the system crosses over to a logarithmic increase of the width. Therefore, the faceted phase may be considered as a rough phase. The unrestricted models B and D, however, evolve into spiky interface configurations. The spikes are separated and grow independently by deposition of dimers. Therefore, W^2 increases *linearly* with time, defining the *free* phase of the unrestricted models.

In the simulations mentioned by now the interface was grown from flat initial conditions. It turns out that starting with **random initial conditions** $h_i = 0, 1$ the densities n_k turn out to decay much slower. For restricted variants an algebraic decay of n_0 with an exponent

$$\delta_0 \simeq 0.13 \tag{6.49}$$

was observed. Similarly, the critical properties of the faceting transition at $p = 0.5$ are affected by random initial conditions. The non-universal behavior for random initial conditions is related to an *additional* parity conservation law. The dynamic rules not only conserve parity of the particle number but also conserve parity of the droplet size. Starting with a flat interface the lateral size of droplets is always even, allowing them to evaporate entirely. However, for a random initial configuration, droplets of odd size may be formed which have to recombine in pairs before they can evaporate, slowing down the dynamics of the system. In the language of BARW2 processes the additional parity conservation law is due to the absence of nearest-neighbor diffusion. Particles can only move by a combination of offspring production and annihilation, i.e., by steps of *two* lattice sites. Therefore, particles at even and odd lattice sites have to be distinguished. Only particles of different parity can annihilate. Starting with a fully occupied lattice all particles have alternating parity throughout the whole temporal evolution, leading to the usual critical behavior at the PC transition. For random initial conditions, however, particles of equal parity cannot annihilate, slowing down the decay of the particle density. Similar sector decomposition has been observed in diffusion of k -mer models [348].

6.8.2 Parity conserving polynuclear growth

In analogy with PNG models (Sect.6.7.2) parity conserving PNG models were introduced in [347]. The model is defined on a one-dimensional lattice with periodic boundary conditions and evolves by sub-lattice-parallel updates. In the first half time step pairs of sites $(i, i + 1)$ with even i are updated. If $h_i(t) \neq h_{i+1}(t)$, the heights are incremented by one step

$$\begin{aligned} h_i(t + 1/2) &= h_i(t) + 1 , \\ h_{i+1}(t + 1/2) &= h_{i+1}(t) + 1 . \end{aligned} \tag{6.50}$$

If, however, the two heights are equal, they are updated by the probabilistic rule

$$\begin{aligned} h_i(t + 1/2) &= h_{i+1}(t + 1/2) = \\ &= \begin{cases} m(t) + 1 & \text{with prob. } p \\ m(t) & \text{with prob. } 1 - p \end{cases} , \end{aligned} \tag{6.51}$$

where $m(t) = \max[h_{i-1}(t), h_i(t), h_{i+1}(t), h_{i+2}(t)]$. In the second half time step the same update rule is applied to odd pairs of sites. Clearly, this model generalizes the PNG model and conserves parity at each height level in a co-moving frame. The conservation law leads to the formation of pinning centers moving at maximal velocity. Simulations showed that the critical behavior at the threshold $p_c = 0.5697(3)$ are the same as those of the unidirectionally BARW2 class in 1d.

Chapter 7

Summary

In summary dynamical extensions of classical equilibrium classes were introduced in the first part of this review. New exponents, concepts, subclasses, mixing dynamics and some unresolved problems were discussed. The common behavior of these models was the fluctuating ordered state. In the second part genuine nonequilibrium dynamical classes of reaction-diffusion systems and interface growth models were overviewed. These were related

CLASS ID	features	degree of knowledge	Section
DP	time reversal symm.	RG to ϵ^2 , series exp.	4.1
DyP	long memory	RG, simulations	4.2
VM	Z_2 symmetry	RG, exactly sol.	4.3
PCP	coupled frozen field	RG, simulations	5.4
PC	BARW2 conservation	RG, simulations	4.4.2
PC	Z_2 symmetry	simulations	4.4.3
N-BARW2	N-comp. BARW2 cons.	RG, simu., DMRG	5.10
NDCF	global conservation	RG, simulations	5.8
BP	DP coupled to ARW	simulations	5.5
DCF	global conservation	RG, simulations	5.7
N-BARW2s	symm. NBARW + excl.	simulations, MF	5.11
N-BARW2a	asym. NBARW + excl.	simulations, MF	5.11

Table 7.1: Summary of known absorbing state universality classes in homogeneous isotropic systems.

to phase transitions to absorbing states of weakly fluctuating ordered states. The class behavior is usually determined by the spatial dimensions, symmetries, boundary conditions and inhomogeneities like in case of equilibrium

models but in low dimensions hard-core exclusion was found to be a relevant factor too, splitting up criticality to fermionic and bosonic models. The symmetries are not so evident as in case of equilibrium models, they are expressed in terms of the relations of fields and response fields most precisely. Furthermore in recently discovered binary spreading systems (BP) no special symmetry seems to be responsible for novel critical behavior. Perhaps a field theoretical analysis of coupled DP+ARW system could shed some light on this problem. The parity conservation in hard-core and in binary spreading models seems to be irrelevant. In Table 7.1 I summarized the most well known families of absorbing phase transition classes of homogeneous, spatially isotropic systems. Those which are below the horizontal line exhibit *fluctuating absorbing states*. The necessary and sufficient conditions for these classes are usually unknown precisely. Finally in Table 7.2 I collected the mean-field exponents and upper critical dimensions of some of the most common absorbing-state model classes.

CLASS ID	β	β'	Z	ν_{\perp}	α	δ	η	d_c
DP	1	1	2	1/2	1	1	0	4
DyP	1	1	2	1/2	1	1	0	6
VM	0	1	2	1/2	0	1	0	2
PC	1	0	2	1/2	1	0	-1/2	2
BR& $kA \rightarrow \emptyset$	$1/(k-1)$	0	2	1/2	$1/(k-1)$	0	0	$2/(k-1)$
BP	1	0	2	1	1/2	0	0	2
NDCF	1	1	2	1/2	1	1	0	4
NBARW2	1	0	2	1/2	1	0	0	2

Table 7.2: Mean-field classes of known, homogeneous absorbing-state transitions

7.1 Frequently used abbreviations

ABC	active boundary condition
ARW	annihilating random walk ($AA \rightarrow \emptyset$)
AC	annihilation-coagulation process
AF	annihilation-fission process
BARW	branching and annihilation random walk
BARWe	even-offspring branching and annihilation random walk
BARWo	odd-offspring branching and annihilation random walk
BARW2	two-offspring branching and annihilation random walk
BP	binary production
CA	cellular automaton
CAM	coherent anomaly method
CP	contact process
CDP	compact directed percolation
DCF	diffusive conserved field
DDS	driven diffusive system
DK	Domany-Kinzel cellular automaton
DP	directed percolation
DS	damage spreading
DyP	dynamical percolation
EW	Edwards-Wilkinson
DMRG	density matrix renormalization group
GCP	generalized contact process
GEP	generalized epidemic process
GDK	generalized Domany-Kinzel cellular automaton
GMF	generalized mean-field approximation
IBC	inactive boundary condition
IP	isotropic percolation
KPZ	Kardar-Parisi-Zhang
LIM	linear interface model
MC	Monte Carlo
MDP	multi-component directed percolation
MF	mean-field approximation
N-BARW	N-component branching and annihilation random walk
N-BARW2	even-offspring, N-component branching and annihilation random walk
NDCF	nondiffusive conserved field
NEKIM	nonequilibrium Ising model
NEKIMA	nonequilibrium Ising model with locally broken symmetry
PC	parity conserving
PCP	pair contact process
PCP	pair contact process with particle diffusion
RBC	reflecting boundary condition
RD	reaction-diffusion
RDLG	randomly driven lattice gas
RG	renormalization group
RFT	Reggeon field theory
RSOS	restricted solid on solid model
RW	random walk
SCA	stochastic cellular automaton
SOS	solid on solid model
TTP	threshold transfer process
UCDF	unimodal conserved field

Bibliography

- [1] E. V. Albano, J. Phys. A **27**, L881 (1994).
- [2] T. Liggett, Interacting particle systems (Springer-Verlag, Berlin, 1985)
- [3] J. R. Stat. Soc B **39**, 283 (1977).
- [4] R. Ziff, E. Gulari, Y. Barshad, Phys. Rev. Lett. **56**, 2553 (1986).
- [5] S. Havlin, D. ben-Avraham, Adv. Phys. **36**, 695 (1987).
- [6] J.-P. Bouchaud, A. Georges, Phys. Rep. **195**, 127 (1990).
- [7] For references see : J. Marro and R. Dickman, *Nonequilibrium phase transitions in lattice models*, Cambridge University Press, Cambridge, 1999.
- [8] P. Grassberger, *Directed percolation: results and open problems*, preprint WUB 96-2 (1996)
- [9] H. Hinrichsen, Adv. Phys. **49**, 815 (2000).
- [10] H. Hinrichsen, cond-mat/0006212.
- [11] R. J. Glauber, J. Math. Phys. **4**, 191 (1963).
- [12] N. Menyhárd and G. Odor, J. Phys. A **31**, 6771 (1998).
- [13] H. K. Janssen and B. Schmittman, Z. Phys. B **64**, 503 (1986).
- [14] B. Derrida, Phys. Rep. **301**, 65 (1998).
- [15] R. Dickman and T. Tomé, Phys. Rev A **44**, 4833 (1991).
- [16] T. Tomé and M.J. de Oliveira, Phys. Rev. A **40**, 6643 (1989).
- [17] A. Szolnoki, Phys. Rev. E **62**, 7466 (2000).

- [18] A. Lipowski and M. Lopata, Phys. Rev. **60**, 1516 (1999); A. Lipowski, Phys. Rev. **60**, R6255 (1999);
- [19] H. Hinrichsen, Phys. Rev. E **63**, 16109 (2001).
- [20] G. Ódor, N. Boccara, G. Szabó, Phys. Rev. E **48**, 3168 (1993).
- [21] N. Menyhárd and G. Ódor, J. Phys. A. **28**, 4505 (1995).
- [22] G. Ódor and A. Szolnoki, Phys. Rev. E **53**, 2231 (1996).
- [23] L. D. Landau and E. M. Lifshitz, *Statistical mechanics*, (Pergamon, London, 1981)
- [24] N. D. Mermin and H. Wagner, Phys. Rev. Lett. **17**, 1133 (1996).
- [25] B. I. Halperin and P. C. Hohenberg, Rev. Mod. Phys. **49**, 435 (1977).
- [26] K. Binder and D. Stauffer, Phys. Rev. Lett **33**, 1006 (1974).
- [27] J. Marro, J. Lebowitz and M. H. Kalos, Phys. Rev. Lett **43**, 282 (1979).
- [28] H. K. Janssen, B. Schaub and B. Schmittman, Z. Phys. **73**, 539 (1989).
- [29] D. A. Huse, Phys. Rev. B **40**, 304 (1989).
- [30] B. Derrida, A. J. Bray and C. Godrèche, J. Phys. A **27**, L357 (1994).
- [31] S. N. Majumdar, A. J. Bray, S. J. Cornell and C. Sire, Phys. Rev. Lett. **77**, 3704 (1996).
- [32] N. Menyhárd and G. Ódor, J. Phys. A **30**, 8515 (1997).
- [33] S. A. Kauffman, J. Theor. Biol. **22**, 437 (1969).
- [34] M. Creutz, Ann. Phys. **167**, 62 (1986).
- [35] H. Stanley, D. Stauffer, J. Kertész and H. Herrmann, Phys. Rev. Lett. **59**, 2326 (1986).
- [36] B. Derrida and G. Weisbuch, Europhys. Lett. **4**, 657 (1987)
- [37] P. Grassberger, Physica A **214**, 547 (1995).
- [38] A. M. Mariz, H. J. Herrmann and L. de Arcangelis, J. Stat. Phys. **59** 1043 (1990).
- [39] N. Jan and L. de Arcangelis, Ann. Rev. Comp. Phys. **1**, 1 (ed. D. Stauffer, World Scientific, Singapore 1994).

- [40] P. Grassberger, J. Phys. A **28** L67, (1995)
- [41] H. Hinrichsen, S. Weitz and E. Domany, J. Stat. Phys. **88**, 617 (1997).
- [42] P. Grassberger, J. Stat. Phys. **79**, 13, (1995).
- [43] U. Gropengiesser, Physica A **207**, 492 (1994).
- [44] F. Wang and M. Suzuki, Physica A **223**, 34 (1996).
- [45] T. Vojta, J. Phys. A **31**, 6595 (1998).
- [46] H. Hinrichsen, E. Domany and D. Stauffer, J. Stat. Phys. **91**, 807-814 (1998).
- [47] H. Hinrichsen and E. Domany, Phys. Rev. **E 56**, 94 (1997).
- [48] E. Ising, Z. Phys. **31**, 253 (1925).
- [49] L. Onsager, Phys. Rev. **65**, 117 (1944).
- [50] For a review see M. Henkel, *Conformal Invariance and Critical Phenomena*, Springer 1999.
- [51] M. Suzuki, Prog. Theor. Phys. **46**, 1337 (1971).
- [52] E. Frdakin and L. Susskind, Phys. Rev. D **17**, 2637 (1978).
- [53] I. J. Alonso and M. A. Munoz, Eur. Phys. Lett. **56**, 485 (2001).
- [54] K. Kawasaki, Phys. Rev. **145**, 224 (1966).
- [55] W. Zwerger, Phys. Lett. A **84**, 269 (1981).
- [56] S. J. Cornell K. Kaski and R. B. Stinchcomb, Phys. Rev. B **44**, 12263 (1991).
- [57] B. Zheng, Int. J. Mod. Phys. **12** 1419 (1998).
- [58] D. Stauffer, Int. J. Mod. Phys. C **7**, 753 (1996).
- [59] B. Zheng, Phys. Lett. A **277**, 257 (2000); *ibid.* A **282** 132 (2001).
- [60] A. Jaster, J. Mainville, L. Schuelke, B. Zheng, J. Phys. A: Math. Gen. **32**, 1395 (1999).
- [61] S. Tang and D. P. Landau, Phys. Rev. B **36**, 567 (1987).

- [62] Z. Rácz, in *Nonequilibrium Statistical Mechanics in one Dimension*, Ed. by V. Privman (Cambridge University Press, 1996) *Kinetic Ising models with competing dynamics: Mappings, correlations, steady states and phase transitions*.
- [63] Grinstein G, Jayaprakash C, and Yu He, Phys. Rev. Lett. **55**, 2527 (1985),
- [64] K. E. Bassler and B. Schmittman, Phys. Rev. Lett. **73**, 3343 (1994).
- [65] U. C. Täuber and Z. Rácz, Phys. Rev. E **55**, 4120 (1997).
- [66] B. Schmittman and R. K. P. Zia, *Phase transitions and Critical Phenomena*, eds. C. Domb and J. L. Lebowitz (Academic Press, New York 1996).
- [67] B. Schmittman and R. K. P. Zia, Phys. Rev. Lett. **66**, 357 (1991).
- [68] B. Schmittman, Europhys. Lett. **24**, 109 (1993).
- [69] K. E. Bassler and Z. Rácz, Phys. Rev. Lett. **73**, 1320 (1994); Phys. Rev. E **52**, R9 (1995).
- [70] M. J. Oliveira, J. Stat. Phys. **66**, 273 (1992).
- [71] C. H. Bennett, G. Grinstein, Phys. Rev. Lett. **55**, 657 (1985).
- [72] J. M. González-Miranda, P. L. Garrido, J. Marro and J. Lebowitz, Phys. Rev. Lett. **59**, 1934 (1987).
- [73] H. W. J. Blöte, J. R. Heringa, A. Hoogland and R. K. P. Zia, J. Phys. A **23**, 3799 (1990).
- [74] M. J. Oliveira, J. F. F. Mendes, M. A. Santos, J. Phys. A **26**, 2317 (1993).
- [75] M. C. Marques, J. Phys. A **22**, 4493 (1989).
- [76] M. C. Marques, Phys. Lett. A **145**, 379 (1990).
- [77] T. Tomé, M. J. Oliveira and M. A. Santos, J. Phys. A **24**, 3677 (1991),
- [78] H. W. J. Blöte, J. R. Heringa, A. Hoogland and R. K. P. Zia, Int. J. Mod. Phys. B **5**, 685 (1990).
- [79] P. Tamayo, F. J. Alexander and R. Gupta, Phys. Rev. E **50**, 3474 (1995)

- [80] P. L. Garrido , J. Marro and J. M. Gonzalez-Miranda, Phys. Rev. A **40**, 5802 (1989).
- [81] M. A. Santos and S. Teixeira, J. Stat. Phys. **78**, 963 (1995)
- [82] J. M. Drouffe and C. Godréche, J. Phys. A **32**, 249 (1999).
- [83] I. Dornic, H. Chaté and H. Hinrichsen, Phys. Rev. Lett. 045701 (2001).
- [84] A. Achahbar, J. J. Alonoso and M. Munoz, Phys. Rev. E **54**, 4838 (1996).
- [85] A. Lipowski and M. Droz, Phys. Rev. E **65**, 056114 (2002)
- [86] J. Zhuo, S. Redner and H. Park, J. Phys A **26**, 4197 (1993).
- [87] K. E. Bassler and D. A. Browne, Phys. Rev. E **55**, 5225 (1997).
- [88] K. S. Brown, K. E. Bassler and D. A. Browne, Phys. Rev. E **56**, 3953 (1997).
- [89] K. E. Bassler, Dana A. Browne, J. Phys. A **31**, 6309 (1998).
- [90] H. Park, Mann Ho Kim, and H. Park, Phys. Rev. E **52**, 5664 (1995).
- [91] S. Kwon and H. Park, Phys. Rev. E **52**, 5955 (1995).
- [92] E. Praestraad et al. Europhys. Lett **25** 447 (1994); E. Praestraad, B. Schmittmann and R. K. P. Zia, cond-mat/0010053.
- [93] P. L. Garrido, J. L. Lebowitz, C. Maes and H. Spohn, Phys. Rev. A **42**, 1954 (1990).
- [94] K. Binder, Z. Phys. B **43**, 119 (1981).
- [95] A. Achahbar, Pedro L. Garrido, J. Marro, Miguel A. Munoz, Phys. Rev. Lett. **87**, 195702 (2001).
- [96] J. L. Vallés, J. Marro, J. Stat. Phys. **49**, 89 (1987).
- [97] K.-t. Leung, Phys. Rev. Lett. **66**, 453 (1991).
- [98] R.K.P. Zia, L.B.Shaw and B. Schmittman, Physica A **279**, 60 (2000).
- [99] M. Droz, Z. Rácz and T. Tartaglia, Phys. Rev A **41**, 6621 (1990).
- [100] A. J. Bray, K. Humayun, and T. J. Newman, Phys. Rev. **B 43**, 3699 (1991).

- [101] B. Bergersen and Z. Rácz, Phys. Rev. Lett. **67**, 3047 (1991).
- [102] R. B. Potts, Proc. Camb. Phil. Soc. **48**, 106 (1952).
- [103] F. Y. Wu, Rev. Mod. Phys. **54**, 235 (1982).
- [104] C. M. Fortuin and P. W. Kasteleyn, Physica **57**, 536 (1972).
- [105] S. F. Edwards and P. W. Anderson, J. Phys. F **5**, 965 (1975).
- [106] R. J. Baxter, *Exactly Solved Models in Statistical Mechanics*, Academic, London, 1982.
- [107] R. de Silva, N. A. Alves and J. R. D. de Felicio, Physics Lett. A **298**, 325 (2002).
- [108] B. Derrida, V. Hakim and V. Pasquier, Phys. Rev. Lett. **75**, 751 (1995).
- [109] G. I. Menon and P. Ray, J. Phys. A **34**, L735 (2001).
- [110] A. J. Bray, B. Derrida and C. Godreche, Euro. Phys. Lett. **27**, 175 (1994).
- [111] A. Gopinathan, cond-mat/0111068.
- [112] Z. Glumac and K. Uzelac, Phys. Rev. E **58** 4372 (1998).
- [113] A. Brunstein and T. Tomé, Physica A **257**, 334 (1998).
- [114] A. Crisanti and P. Grassberger, J. Phys. A **27**, 6955 (1994).
- [115] G. Szabó and T. Czárán, Phys. Rev. E **50**, 061904 (2001).
- [116] L. da Silva, F. A. Tamarit and A. C. N. Magalhães, J. Phys. A **30**, 2329 (1997).
- [117] J. M. Kosterlitz and D. J. Thouless, J. Phys. C **6**, 1181 (1973).
- [118] C. Itzykson and J. M. Drouffe, *Statistical Field Theory*, Camb. U. Press, Cambridge 1989.
- [119] R. Guida and J. Zinn-Justin, cond-mat/9803240.
- [120] T. H. Berlin and M. Kac, Phys. Rev. **86**, 821 (1952); H. E. Stanley, Phys. Rev. **176**, 718 (1968).
- [121] A. Pelissetto, E. Vicari, cond-mat/0012164.

- [122] H. P. Ying, B. Zheng, Y. Yu and S. Trimper, Phys. Rev. E **63**, R35101 (2001)
- [123] K. E. Bassler and Z. Rácz, Phys. Rev. Lett. **73**, 1320 (1994).
- [124] S. G. Gorishny, S. A. Larin and F.V. Tkachov, Phys. Lett. **101A**, 120 (1984).
- [125] J. Berges, N. Tetradis, C. Wetterich, hep-ph/0005122, to appear in Physics Reports
- [126] M. Hasenbuch, cond-mat/0010463.
- [127] K. Oerding, S. J. Cornell and A.J.Bray, Phys. Rev. E **56**, R25 (1997).
- [128] U. C. Täuber, J. E. Santos and Z. Rácz, cond-mat/9807207.
- [129] D. Stauffer and A. Aharony, *Introduction to percolation theory*, Taylor & Francis, London (1994).
- [130] A. Bunde and S. Havlin, *Fractals and disordered systems*, eds. A. Bunde and S. Havlin, Springer Verlag, Heidelberg 1991.
- [131] J. Benzonzi and J. L. Cardy, J. Phys. A **17**, 179 (1984).
- [132] G. Grimmett, *Percolation* Springer-Verlag 1999.
- [133] A. Coniglio and W. Klein, J. Phys. A **13**, 2775 (1980).
- [134] P. Bialas et al., Nucl. Phys. B **583**, 368 (2000).
- [135] S. Fortunato, H. Satz, Nucl. Phys. B **598**, 601 (2001); S. Fortunato, cond-mat/0204366.
- [136] P. Blanchard et al., J. Phys. A **33** 8603 (2000).
- [137] P. Grassberger, in *Fractals in physics*, eds. L. Pietronero and E. Tosatti (Elsevier, 1986).
- [138] M. C. Marques and A. L. Ferreira, J. Phys. A **27**, 3389 (1994).
- [139] H. K. Janssen, K. Oerding, F. van Wijland and H. Hilhorst, Eur. Phys. J. B **7**, 137 (1999).
- [140] H. Hinrichsen and M. Howard, Eur. Phys. J. B **7**, 635 (1999).
- [141] G. Zumofen and J. Klafter, Phys. Rev. E **50**, 5119 (1994).
- [142] K. Oerding, J. Phys. A **29**, 7051 (1996).

- [143] M. W. Deem and J.-M. Park, Phys. Rev. E **57**, 2681 (1998); *ibid.* 3618.
- [144] H. Hinrichsen and G. Ódor, Phys. Rev. E **58**, 311 (1998).
- [145] A. B. Harris, J. Phys. C **7**, 1671 (1974).
- [146] A. J. Noest, Phys. Rev. Lett. **57**, 90 (1986); A. J. Noest, Phys. Rev. B **38**, 2715 (1988).
- [147] H. K. Janssen, Phys. Rev. E **55**, 6253 (1997).
- [148] A. G. Moreira and R. Dickman, Phys. Rev. E **54**, R3090 (1996).
- [149] I. Webman, D. ben Avraham, A. Cohen, and S. Havlin, Phil. Mag. B **77**, 1401 (1998).
- [150] R. Cafiero, A. Gabrielli, and M. A. Muñoz, Phys. Rev. E **57**, 5060 (1998).
- [151] J. Hooyberghs, F. Iglói and C. Vanderzande, cond-mat/0203610.
- [152] Phys. Rev. Lett. **77**, 4988 (1996).
- [153] F. Family and T. Vicsek, J. Phys. A **18**, L75 (1985).
- [154] A.-L. Barabási and H. E. Stanley, *Fractal Concepts in Surface Growth*, Cambridge University Press, Cambridge, (1995)
- [155] J. Krug, Adv. Phys. **46**, 139 (1997).
- [156] J. Krug, Phys. Rev. Lett. **72**, 2907 (1994).
- [157] M. Schroeder, *et. al.*, Europhys. Lett. **24**, 563 (1993).
- [158] J.M. López and M.A. Rodríguez, Phys. Rev. E **54**, R2189 (1996).
- [159] S. Das Sarma, *et. al.*, Phys. Rev. E **53**, 359 (1996).
- [160] C. Dasgupta, S. Das Sarma and J.M. Kim, Phys. Rev. E **54**, R4552 (1996).
- [161] J.M. López and M.A. Rodríguez, J. Phys. I **7**, 1191 (1997).
- [162] M. Castro, *et. al.* Phys. Rev. E **57**, R2491 (1998).
- [163] H.-Yang, G.-C. Wang and T.-M. Lu, Phys. Rev. Lett. **73**, 2348 (1994).
- [164] J.H. Jeffries, J.-K. Zuo and M.M. Craig, Phys. Rev. Lett. **76**, 4931 (1996).

- [165] J.M. López and J. Schmittbuhl, Phys. Rev E **57**, 6405 (1998).
- [166] S. Morel *et. al.*, Phys. Rev. E **58**, 6999 (1998).
- [167] A. Bru *et. al.* Phys. Rev. Lett. , 1998
- [168] J. A. Sales, M. L. MArtins and J. G. Moreira, Physica A **245**, 461 (1997).
- [169] R. Dickman and M. A. Munoz, Phys. Rev. E **62**, 7631 (2000).
- [170] J. D. Noh, H. Park, D. Kim and M. den Nijs, Phys. Rev. E **64**, 046131 (2001).
- [171] S. F. Edwards and D. R. Wilkinson, Proc. R. Soc. **381**, 17 (1982).
- [172] H. Kim, K. Park and I. Kim, Phys. Rev. E **65**,017104 (2001).
- [173] T. Nattermann, S. Stepanow, L-H. Tang and H. Leschhorn, J. Phys. II **2**, 1483 (1992); H. Leschhorn T. Nattermann, S. Stepanow and L-H. Tang, Ann. Phys. **7**, 1 (1997).
- [174] O. Narayan and D. S. Fisher, Phys. Rev. B **48**, 7030 (1993).
- [175] M. Kardar, G. Parisi and Y.C. Zhang, Phys. Rev. Lett. **56**, 889 (1986).
- [176] T. Halpin-Healy, Phys. Rev. A **42**, 711 (1990).
- [177] M. Lässig, Nucl. Phys. B **559**, (1995); M. Lässig and H. Kinzelbach, Phys. Rev. Lett **78**, 906 (1997).
- [178] K. Moser, D. E. Wolf and J. Kertész, Physica A **178**, 215 (1991).
- [179] J.M. Kim and J.M. Kosterlitz, Phys. Rev. Lett. **62**, 2289 (1989); D.E. Wolf and J. Kertész, Europhys. Lett. **4**, 651 (1987); L.H. Tang, B.M. Forrest, and D.E. Wolf, Phys. Rev. A**45**, 7162 (1992); T. Ala-Nissila, T. Hjelt, J.M. Kosterlitz, and O. Venäläinen, J. Stat. Phys. **72**, 207 (1993).
- [180] E. Marinari, A. Pagnani, and G. Parisi, J. Phys. A**33**, 8181 (2000).
- [181] C. Castellano, M. Marsili, and L. Pietronero, Phys. Rev. Lett. **80**, 3527 (1998); C. Castellano, A. Gabrielli, M. Marsili, M.A. Munoz, and L. Pietronero, Phys. Rev. E**58**, R5209 (1998); C. Castellano, M. Marsili, M.A. Munoz, and L. Pietronero, Phys. Rev. E**59**, 6460 (1999).
- [182] Y. Tu, Phys. Rev. Lett. **73**, 3109 (1994).

- [183] E. Marinari, A. Pagnani G. Parisi and Z. Rácz, Phys. Rev. E **65**, 026136 (2002).
- [184] H. Leschorn, Phys. Rev E **54**, 1313 (1996).
- [185] S. V. Buldrev, S. Havlin and H. E. Stanley, Physica A **200**, 200 (1993)
- [186] L. Tang and H. Leschhorn, Phys. Rev. A **45**, R8309 (1992).
- [187] A. L. Barabási, G. Grinstein and M. A. Munoz, Phys. Rev. Lett **76**, 1481 (1996).
- [188] W. Kinzel, in *Percolation Structures and Processes*, ed. G. Deutscher, R. Zallen, and J. Adler, Ann. Isr. Phys. Soc. **5** (Hilger, Bristol, 1983).
- [189] H. K. Janssen, Z. Phys. B **42**, 151 (1981); P. Grassberger, Z. Phys. B **47**, 365 (1982); G. Grinstein, Z-W. Lai and D. A. Browne, Phys. Rev A **40**, 4820 (1989).
- [190] H. Hinrichsen, Braz. J. Phys. **30**, 69-82 (2000).
- [191] H. Takayasu and A. Yu. Tretyakov, Phys. Rev. Lett. **68**, 3060, (1992).
- [192] I. Jensen, Phys. Rev. E **50**, 3623 (1994).
- [193] J. L. Cardy and U. C. Täuber, Phys. Rev. Lett. **77**, 4780 (1996); J. L. Cardy and U. C. Täuber, J. Stat. Phys. **90**, 1 (1998).
- [194] P. Grassberger, F. Krause and T. von der Twer, J. Phys. A:Math.Gen., **17**, L105 (1984).
- [195] N. Menyhárd, J.Phys.A **27**, 6139 (1994).
- [196] N. Menyhárd and G. Ódor, J.Phys.A **29**, 7739 (1996).
- [197] M. H. Kim and H. Park, Phys. Rev. Lett. **73**, 2579, (1994).
- [198] K. E. Bassler and D. A. Browne, Phys. Rev. Lett. **77**, 4094 (1996).
- [199] H. Hinrichsen, Phys. Rev. E **55**, 219 (1997).
- [200] I. Jensen, J. Phys. A, **30**, 8471 (1997).
- [201] G. Ódor, Phys. Rev. E **63**, 021113 (2001).
- [202] G. Ódor, Phys. Rev E **65** 026121 (2002).
- [203] J. Hooyberghs, E. Carlon and C. Vanderzande, Phys. Rev. E **64**, 036124 (2001).

- [204] J. W. Essam, J. Phys. A **22**, 4927 (1989).
- [205] E. Domany , W. Kinzel, Phys. Rev. Lett. **53**, 311 (1984).
- [206] J. W. Essam and D. TanlaKishani, J. Phys. A **A 27**, 3743 (1994).
- [207] J. W. Essam and A. J. Guttmann, J. Phys. A **28**, 3591 (1995).
- [208] M. Rossi, R. Pastor-Satorras and A. Vespagnani, Phys. Rev. Lett. **85**, 1803 (2000).
- [209] M. A. Munoz, R. Dickman, A. Vespagnani and S. Zapperi, Phys. Rev. **59**, 6175 (1999).
- [210] R. Pastor-Satorras and A. Vespagnani, Phys. Rev. E **62**, 5875 (2000).
- [211] H. J. Jensen, *Self-Organized Criticality*, Cambridge Univ. Press, Cambridge England 1998.
- [212] S. S. Manna, J. Phys. A **24**, L363 (1991), D. Dhar, Physica A **263**, 4 (1999).
- [213] R. Dickman, A. Vespignani and S. Zapperi, Phys. Rev. E **57**, 5095 (1998).
- [214] M. Alava and M. A. Munoz, Phys. Rev. E **65**, 026145 (2001).
- [215] R. Dickman, M. Alava, M. A. Munoz, J. Peltola, A. Vespignani, S. Zapperi, Phys. Rev. E **64** 056104 (2001).
- [216] T. Halpin-Healy and Y.-C. Zhang, Phys. Rep. **254**, 215 (1995).
- [217] M. Marsili, J. Stat. Phys. **77**, 733 (1994).
- [218] S. Lübeck and A. Hucht, J. Phys. A **35**, 4853 (2002).
- [219] S. Lübeck, Phys. Rev. E **64** 016123 (2001); Phys. Rev. E **65** 046150 (2002);
- [220] R. Dickman, T. Tomé and M. J. de Oliveira, cond-mat/0203565.
- [221] R. Dickman, cond-mat/0204608.
- [222] P. Grassberger, Z. Phys. B **47**, 365 (1982).
- [223] M. J. Howard and U. C. Täuber, J. Phys. **A 30**, 7721 (1997).
- [224] G. Ódor , Phys. Rev. E **62**, R3027 (2000).

- [225] E. Carlon, M. Henkel and U. Schollwöck, Phys. Rev. E **63**, 036101-1 (2001).
- [226] H. Hinrichsen, Phys. Rev. E **63**, 036102-1 (2001).
- [227] G. Ódor, Phys. Rev. E **63**, 067104 (2001).
- [228] H. Hinrichsen, Physica A **291**, 275 (2001).
- [229] M. Henkel and H. Hinrichsen, J. Phys. A **34**, 1561 (2001).
- [230] K. Park, H. Hinrichsen, and In-mook Kim, Phys. Rev. E **63**, 065103(R) (2001).
- [231] M.C. Marques and J.F.Mendes, Eur. Phys. B **12**, 123 (1999).
- [232] H. S. Park and H. Park, J. of Korean Phys. Soc. **38**, 494 (2001).
- [233] R. Kree, B. Schaub and B. Schmitmann, Phys. Rev. A **39**, 2214 (1989).
- [234] F. van Wijland, K. Oerding and H. J. Hilhorst, Physica A **251**, 179 (1998).
- [235] J. E. de Freitas, L. S. Lucena, L. R. da Silva and H. J. Hilhorst, Phys. Rev. E **61**, 6330 (2000).
- [236] U. L. Fulco, D. N. Messias and M. L. Lyra, Phys. Rev. E **63**, 066118 (2001).
- [237] K. Oerding, F. van Wijland, J.P. Leroy and H. J. Hilhorst, J. Stat. Phys. **99**, 1365 (2000).
- [238] S. Kwon, J. Lee and H. Park, Phys. Rev. Lett. **85**, 1682 (2000).
- [239] G. Ódor, Phys. Rev. E **63**, 056108 (2001).
- [240] H. S. Park and H. Park, J. of Korean Phys. Soc. **38**, 494 (2001).
- [241] S. Park, D. Kim and J. Park, Phys. Rev. E **62**, 7642 (2000).
- [242] F. Wijland, Phys. Rev. E **63**, 022101 (2001)
- [243] P. L. Krapivsky and E. Ben-Naim, Phys. Rev. E **56**, 3788 (1997).
- [244] D. ben-Avraham, M. A. Burschka and C.R. Doring, J. Stat. Phys. **60**, 695 (1990).

- [245] S. R. Broadbent and J. M. Hammersley, Proc. Camb. Phil. Soc. **53**, 629 (1957).
- [246] I. Jensen and R. Dickman, Phys. Rev. E **48**, 1710 (1993).
- [247] J. F. F. Mendes, R. Dickman, M. Henkel and M. C. Marques, J. Phys. **A 27**, 3019 (1994).
- [248] H. Park and H. Park, Physica A **221**, 97 (1995).
- [249] K. B. Lauritsen, P. Fröjd, and M. Howard, Phys. Rev. Lett. **81**, (1998).
- [250] P. Fröjd, M. Howard, K. B. Lauritsen, Int. J. Mod. Phys. B **15**, 1761 (2001).
- [251] N. Menyhárd and G. Ódor, J. Phys. A. **29**, 7739 (1996).
- [252] G. Ódor, A. Krikelis, G. Vesztergombi and F. Rohrbach: Proceedings of the 7-th Euromicro workshop on parallel and distributed process Funchal (Portugal) Feb. 3-5 1999, IEEE Computer society press, Los Alamitos, ed.: B. Werner; e-print: physics/9909054
- [253] G. Ódor and N. Menyhárd, Phys. Rev. E **57**, 5168 (1998).
- [254] H. K. Janssen, Z. Phys. B **23**, 377 (1976).
- [255] J. L. Cardy and R. L. Sugar, J. Phys. A **13**, L423 (1980).
- [256] H. D. I. Abarbanel, J. B. Bronzan, R. L. Sugar and A. R. White, Phys. Rep. **21**, 119 (1975); R. Brower, M. A. Furman and M. Moshe, Phys. Lett. B **76**, 213 (1978).
- [257] P. Grassberger and A. de la Torre, Ann. Phys. **122**, 373 (1979).
- [258] M. A. Munoz, G. Grinstein and Y. Tu, Phys. Rev. E **56**, (1997) 5101.
- [259] E. Ben-Naim and P. L. Krapivsky, J. Phys. A **27**, L481 (1994).
- [260] G. Ódor, Phys. Rev. E **51**, 6261 (1995).
- [261] H. Hinrichsen and H. M. Koduvely, Eur. Phys. J. B **5**, 257 (1998).
- [262] K. Oerding and F. van Wijland, J. Phys. A **31**, 7011 (1998).
- [263] I. Jensen, J. Phys. A **32**, 5233 (1999).
- [264] C. A. Voigt and R. M. Ziff, Phys. Rev. E **56**, R6241 (1997).

- [265] I. Jensen, Phys. Rev. E **45**, R563 (1992).
- [266] J. B. Bronzan and J. W. Dash, Phys. Lett. B **51**, 496 (1974).
- [267] P. Grassberger, J. Phys. A **22**, 3673 (1989).
- [268] P. Grassberger, J. Phys. A **25**, 5867 (1992).
- [269] R. Dickman and I. Jensen, Phys. Rev. Lett. **67**, 2391 (1991).
- [270] K. De'Bell and J. W. Essam, J. Phys. A **16**, 385 (1983). J. W. Essam, A. Guttmann and K. De'Bell, *ibid.* **21**, 3815 (1988). I. Jensen and R. Dickman, J. Stat. Phys. **71**, 89 (1993); I. Jensen, Phys. Rev. Lett. **77**, 4988 (1996); I. Jensen and R. Dickman, J. Phys. A **26**, L151 (1993). I. Jensen and A. J. Guttmann, *ibid.* **28**, 4813 (1995). I. Jensen and A. J. Guttmann, Nucl. Phys. B **47**, 835 (1996).
- [271] T. E. Harris, *Ann. Prob.* **2**, 969 (1974); P. Grassberger and A. de la Torre, *Ann. Phys. (NY)* **122**, 373 (1979).
- [272] R. Dickman and J. K. de Silva, Phys. Rev. E **58**, 4266 (1998).
- [273] N. Boccara and M. Roger, in *Instabilities and Nonequilibrium Structures IV*, edited by E. Tirapegui and W. Zeller (Kluwer Academic, Dordrecht, 1993), p. 109.
- [274] S. Wolfram, Rev. Mod. Phys. **55**, 601 (1983).
- [275] G. Ódor et al, CERN-OPEN-97-034.
- [276] G. Szabó and G. Ódor, Phys. Rev. E **49**, 2764 (1994).
- [277] K. Eloranta and E. Nummelin, J. Stat. Phys. **69**, 1131 (1992).
- [278] R. Bidaux, N. Boccara, H. Chate, Phys. Rev. A **39**, 3094 (1989).
- [279] I. Jensen, Phys. Rev. A **43**, 3187 (1991).
- [280] Y. Hieida, J. Phys. Soc. Jpn. **67**, 369 (1998); E. Carlon, M. Henkel, and U. Schollwöck, Euro. Phys. J. B **12**, 99 (1999);
- [281] E. Frey, U. C. Täuber and F. Schwabl, Phys. Rev. E **49**, 5058 (1993).
- [282] P. Fröjdh and M. den Nijs, Phys. Rev. Lett. **78**, 1850 (1997).
- [283] V. Brunel, K. Oerding and F. van Wijland, J. Phys. A **33**, 1085 (2000).

- [284] O. Deloubrière and F. van Wijland, *Phys. Rev. E* **65**, 046104 (2002).
- [285] G. Ódor and N. Menyhárd, cond-mat/0109399, *Physica D* **168**, 305 (2002).
- [286] I. Jensen, *Phys. Rev. E* **47**, R1 (1993).
- [287] F. Iglói, I. Peschel, and L. Turban, *Adv. Phys.* **42**, 683 (1993).
- [288] J. L. Cardy, *J. Phys. A* **16**, 3617 (1983).
- [289] J. W. Essam, A. J. Guttmann, I. Jensen and D. TanlaKishani, *J. Phys. A* **29** 1619 (1996).
- [290] K. B. Lauritsen, K. Sneppen K, M. Markošová and M. H. Jensen M H, *Physica A* **247**, 1 (1997).
- [291] H. K. Janssen, B. Schaub and B. Schmittmann, *Z. Phys. B* **72**, 111 (1988).
- [292] I. Jensen, *J. Phys. A* **32**, 6055 (1999).
- [293] P. Fröjdh, M. Howard, and K. B. Lauritsen, *J. Phys. A* **31**, 2311 (1998).
- [294] M. Howard, P. Fröjdh, and K. B. Lauritsen, *Phys. Rev. E* **61**, 167 (2000).
- [295] E. V. Albano, *Phys. Rev. E* **55**, 7144 (1997).
- [296] C. Kaiser and L. Turban, *J. Phys. A* **27**, L579 (1994); C. Kaiser and L. Turban, *J. Phys. A* **28**, 351 (1995).
- [297] P. Grassberger, H. Chaté and G. Rousseau, *Phys. Rev. E* **55**, 2488 (1997).
- [298] D. Mollison, *J. R. Stat. Soc. B* **39**, 238 (1977).
- [299] P. Grassberger, *Math. Biosci.* **63**, 157 (1982).
- [300] J. L. Cardy, *J. Phys. A* **16**, L709 (1983).
- [301] J. L. Cardy and P. Grassberger, *J. Phys. A* **18**, L267 (1985).
- [302] H. K. Janssen, *Z. Phys. B* **58**, 311 (1985).
- [303] M. A. Munoz, R. Dickman, G. Grinstein and R. Livi, *Phys. Rev. Lett.* **76**, 451 (1996).

- [304] M. A. Munoz, G. Grinstein and R. Dickman, J. Stat. Phys. **91**, 541 (1998).
- [305] G. Ódor, J. F. Mendes, M. A. Santos and M. C. Marques, Phys. Rev. E **58**, 7020 (1998).
- [306] M. C. Marques, M. A. Santos and J. F. Mendes, Phys. Rev. E **65**, 016111 (2001).
- [307] M. A. Munoz, C. A. da S. Santos and M. A. Santos, cond-mat/0202244.
- [308] R. Dickman and J. Kamphorst Leal da Silva, Phys. Rev. E **58**, 4266 (1998).
- [309] R. Dickman, cond-mat/9909347
- [310] R. Dickman, W. R. M. Rabelo and G. Ódor, Phys. Rev. E **65** 016118 (2001).
- [311] J. Kamphorst Leal da Silva and R. Dickman, Phys. Rev. E **60** 5126 (1999).
- [312] M. A. Munoz, R. Dickman, A. Vespignani and S. Zapperi, Phys. Rev. E **59**, 6175 (1999).
- [313] H. Drossel and F. Schwabl, Physica A **199**, 183 (1993).
- [314] T. Antal, M. Droz, A. Lipowski and G. Ódor, Phys. Rev. E **64** 036118 (2001).
- [315] P. Grassberger, J. Phys. A **25**, 5867 (1992).
- [316] R. Dickman and A. Yu. Tretyakov, Phys. Rev. E **52**, 3218 (1995).
- [317] R. Durrett, *Lecture Notes on Particle Systems and Percolation*, (Wadsworth, Pacific Grove, CA 1988).
- [318] M. Scheucher and H. Spohn, J. Stat. Phys. **53**, 279 (1988).
- [319] P. L. Krapivsky, Phys. Rev. A **45**, 1067 (1992); L. Frachebourg and P. L. Krapivsky, Phys. Rev. E **53**, R 3009 (1996).
- [320] H. K. Janssen, J. Stat. Phys. **103** 801 (2001).
- [321] V. Privman, *Nonequilibrium Statistical Mechanics in one Dimension* Cambridge University Press, 1996.

- [322] B. P. Lee, *J. Phys. A* **27**, 2633 (1994).
- [323] Z. Rácz, *Phys. Rev. Lett.* **55**, 1707 (1985).
- [324] A. A. Lushnikov, *Phys. Lett. A* **120**, 135 (1987)
- [325] L. Peliti, *J. Phys. A: Math. Gen.* **19**, L365 (1986).
- [326] A. A. Ovchinnikov and Ya. B. Zel'dovich, *Chem. Phys.* **28**, 215 (1978); S. F. Burlatskii and A. A. Ovchinnikov, *Russ. J. Phys. Chem.* **52**, 1635 (1978); D. Toussaint and F. Wilczek, *J. Chem. Phys.* **78**, 2642 (1983); K. Kang and S. Redner, *Phys. Rev. A* **32**, 435 (1985); M. Bramson and J. Lebowitz, *Phys. Rev. Lett.* **61**, 2397 (1988).
- [327] B. P. Lee and J. Cardy, *J. Stat. Phys.* **?**, 971 (1995).
- [328] S. J. O'Donoghue and A. J. Bray, *Phys. Rev. E* **64**, 041105 (2001).
- [329] G. Ódor and N. Menyhárd, *Phys. Rev. E.* **61**, 6404 (2000)
- [330] R. Dickman and D. ben-Avraham, *Phys. Rev. E* **64**, 020102 (2001).
- [331] P. L. Krapivsky and S. Redner, private communication.
- [332] S. N. Majumdar, D. S. Dean and P. Grassberger, *Phys. Rev. Lett.* **86**, 2301 (2001).
- [333] I. Jensen and R. Dickman, *Phys. Rev. E* **48**, 1710 (1993); I. Jensen, *Phys. Rev. Lett.* **70**, 1465 (1993).
- [334] U.C. Täuber, M.J. Howard, and H. Hinrichsen, *Phys. Rev. Lett.* **80**, 2165 (1998);
- [335] A. Lipowski and M. Droz, *Phys. Rev. E* **64**, 031107 (2001).
- [336] N. Imui, A. Y. Tretyakov and H. Takayasu, *J. Phys. A* **28**, 1145 (1995).
- [337] K. Park, H. Hinrichsen and I. Kim, *Phys. Rev. E* **63**, 065103(R) (2001).
- [338] G. Ódor, M.A. Santos, M.C. Marques, *Phys. Rev. E* **65**, 056113 (2002).
- [339] U. Täuber, private communication.
- [340] G. Ódor, *Phys. Rev. E* **63**, 056108 (2001).
- [341] H. Park and H. Park, *Physica A* **221**, 97 (1995).

- [342] W. Hwang, S. Kwon, H. Park, H. Park, Phys. Rev. E **57**, 6438 (1998).
- [343] W. Hwang and H. Park, Phys. Rev. E **59**, 4683 (1999).
- [344] N. Menyhárd and G. Ódor, Brazilian J. of Physics, **30**, 113 (2000).
- [345] K. Mussawisade, J. E. Santos and G. M. Schütz, J. Phys. A **31**, 4381 (1998).
- [346] A. Sudbury, Ann. Prob. **18**, 581 (1990).
- [347] H. Hinrichsen and G. Ódor, Phys. Rev. E **60**, 3842 (1999).
- [348] M. Barma, M. D. Grynberg and R. B. Stinchcomb, Phys. Rev. Lett. **70**, 1033 (1993); M. Barma and D. Dhar, *ibid.* **73**, 2135 (1994).
- [349] P. Grassberger, J. Phys. A **22** L1103, (1989).
- [350] D. Zhong and D. ben Avraham, Phys. Lett. A **209**, 333 (1999).
- [351] A. Lipowski, J. Phys. A **29**, L355, (1996).
- [352] H. K. Janssen, Phys. Rev. Lett. **78**, 2890 (1997).
- [353] D. ben Avraham, F. Leyvraz and S. Redner, Phys. Rev. E **50**, 1843 (1994).
- [354] I. Jensen, J. Phys. A **26**, 3921 (1993).
- [355] A. DeMasi, P. A. Ferrari, J. L. and Lebowitz, Phys. Rev. Lett. **55**, 1947 (1985); J. Stat. Phys. **44**, 589 (1986).
- [356] J. S. Wang and J. L. Lebowitz, J. Stat. Phys. **51**, 893 (1988).
- [357] M. Droz, Z. Rácz and J. Schmidt, Phys. Rev. A **39**, 2141 (1989).
- [358] N. Menyhárd and G. Ódor, Phys. Rev. E **66**, 016127 (2002); cond-mat/0203419.
- [359] A. Lipowski and M. Droz, cond-mat/0110404, Phys. Rev. E **66**, 016106 (2002).
- [360] Grinstein G., Muñoz M.A., and Tu Y., Phys. Rev. Lett. **76**, 4376 (1986); Tu Y., Grinstein G., and Muñoz M.A. Phys. Rev. Lett. **78**, 274 (1997).
- [361] U. C. Täuber, M. J. Howard, and H. Hinrichsen, Phys. Rev. Lett. **80**, 2165 (1998).

- [362] Y. Y. Goldschmidt, H. Hinrichsen, M. Howard, and U. C. Täuber, *Phys. Rev. E* **59**, 6381 (1999).
- [363] U. Alon, M. Evans, H. Hinrichsen, and D. Mukamel, *Phys. Rev. E* **57**, 4997 (1998).
- [364] U. Alon, M. Evans, H. Hinrichsen, and D. Mukamel, *Phys. Rev. Lett* **76**, 2746 (1996).
- [365] Y. Y. Goldschmidt, *Phys. Rev. Lett.* **81**, 2178 (1998).
- [366] J. Kertész and D. E. Wolf, *Phys. Rev. Lett.* **62**, 2571 (1989).
- [367] C. Lehner, N. Rajewsky, D. Wolf, and J. Kertész, *Physica A* **164**, 81 (1990).
- [368] A. Toom, *J. Stat. Phys.* **74**, 91 (1994); A. Toom, *J. Stat. Phys.* **74**, 111 (1994).
- [369] H. Hinrichsen and G. Ódor, *Phys. Rev. Lett.* **82**, 1205 (1999).
- [370] J. D. Noh, H. Park, M. den Nijs, *Phys. Rev. Lett.* **84**, 3891 (2000)